LASER DOPPLER ANEMOMETER STUDY OF THE FLOWFIELD IN A CENTERBODY DIFFUSION BURNER

By

LARRY ALAN ROE

A DISSERTATION PRESENTED TO THE GRADUATE SCHOOL
OF THE UNIVERSITY OF FLORIDA IN
PARTIAL FULFILLMENT OF THE REQUIREMENTS
FOR THE DEGREE OF DOCTOR OF PHILOSOPHY

UNIVERSITY OF FLORIDA

1987

Dedicated to my wife and companion, Cathy,
without whose love and support my effort
would not have succeeded.

ACKNOWLEDGMENT

The research on which this document is based was funded in part by the U. S. Air Force, Air Force Engineering and Services Center, Tyndall AFB, Florida, and in part by the College of Engineering of the University of Florida. The aid and assistance of these agencies and their representatives are greatly appreciated.

TABLE OF CONTENTS

Abstract of Dissertation Presented to the
Graduate School of the University of Florida
in Partial Fulfillment of the Requirements for the
Degree of Doctor of Philosophy

INVESTIGATION OF THE FLOWFIELD IN A CENTERBODY DIFFUSION BURNER USING A LASER DOPPLER ANEMOMETER

By

Larry Alan Roe

August 1987

Chairman: C. L. Proctor, II
Major Department: Mechanical Engineering

A two-color, two-component, laser Doppler anemometer was used to evaluate the flowfield in a centerbody, turbulent diffusion burner exhausting into free air. Fuel composition and flow rates were varied over a wide range. Results are presented in the forms of vector plots, velocity tables, velocity probability density functions, turbulence profiles, and shear stress profiles. Comparisons between reacting and nonreacting cases showed the reaction to increase the axial and radial extent of the separation region, increase the axial turbulent fluctuations, and increase the shear stress. Increases in fuel flow beyond a very lean flame did not significantly affect the velocity parameters. Time-weighted mean velocities and fluctuations did not significantly differ from particle averages.

CHAPTER I
INTRODUCTION

Combustion plays a key role in transportation, electrical generation, waste disposal, and manufacturing. Proper understanding of the physical processes involved is essential to maximize efficiency and reduce emissions in these applications. Combustion technology is still largely empirical in nature due to the combination of complex flow fields with internal energy generation coupled with chemical reactions which are by themselves not accurately quantified.

Separated, turbulent flow is encountered in most practical combustion systems. Additionally, these devices are predominantly of the nonpremixed type, where the fuel and oxidizer enter the reaction region separately. Many laboratory studies of reacting flows have been conducted on laminar flames, premixed turbulent flames, or nonpremixed flames in nonseparated flow fields. While these tests are essential for providing information on the chemical processes involved, they provide no insight into the mixing processes that control the combustion in the nonpremixed burners which form the bulk of practical combustion systems.

Attempts to model separated, reacting flows using commonly employed closure models have not been particularly successful, and are never expected to be truly predictive as

they are credible only when applied to flows similar to those used to evaluate the parameters (Tishkoff, 1983). Larsen and Buchhave (1985, p. 4) state that "velocity fields are needed to verify computational capability for problems of complex steady laminar Newtonian flows . . . fully turbulent flows of practical interest remain mathematically intractable in all detail . . . only the average behaviour, in terms of mean velocity fields and turbulent stresses, are needed in most cases." A serious lack of data and failure of existing modeling techniques have also been cited by Bill et al. (1981), Krishnamurthy (1981), Jones and Whitelaw (1985), and Mongia et al. (1986). As a result, the Air Force Office of Scientific Research and other sponsoring agencies have indicated a need for flow mapping and the acquisition of time-resolved data in realistic environments. This study is an attempt to contribute to that effort.

For the information produced by a research effort to be of the greatest value, the specific experimental apparatus should be such that the results are not device specific, or, if this is not practical, are applicable to other experimental and practical devices in common usage. The burner used for this study provides an intermediate model between simple, flat-flame type burners and actual gas turbine combustors. It is the same apparatus used in a study by Proctor et al. (1985), and is very similar to devices used by Roquemore et al. (1980), Lightman et al. (1980), and other researchers (Krishnamurthy 1981, Lightman

and Magill 1981, Switzer et al. 1986), and is identical to the burner used for soot evaluations by Proctor et al. (1987). It exhausts into free air directly downstream of the centerbody, providing virtually unlimited optical access to the entire flowfield. The configuration is such that the processes of interest to the sponsoring agency are modeled generally enough to provide the widest possible application to practical turbine combustors.

Obtaining real-time flow data in a high temperature, separated flow field requires sophisticated instrumentation. Laser Doppler velocimetry (LDV, or LDA for laser Doppler anemometry) is indicated for its ability to sample velocity at high data rates over very small regions of the flow, with no probe induced disturbances. LDV response is also relatively insensitive to flow direction, an absolute requirement in regions where flow reversals occur intermittently. There are significant difficulties in both the application of this technique and the analysis of the resulting data. Sensitive optical alignments, the utilization of large amounts of nonmature electronic instrumentation, and software and hardware interfacing problems between the various system components make the very acquisition of data far from trivial. Even when the data have been successfully collected, the interpretation can be difficult, due largely to the fact that the data are discrete rather than continuous, leading to a wide variety of possible problems in the statistical analysis of the

information. If the experiments are performed carefully, however, many of these potential problems can be minimized or eliminated.

A major part of this experimental effort was conducted in parallel with soot sampling studies conducted at Tyndall AFB. Soot formation in gas turbine engines is a major concern as it is indicative of incomplete combustion, increases the radiative thermal load on burner liners and turbine components, and increases the visible and infrared signatures of military aircraft. The processes leading to soot formation and destruction are not well understood, and soot concentration data acquired in realistic environments can only be interpreted with a knowledge of the flowfield of the apparatus.

The pages to follow will provide a progressive dissertation describing the investigation of the turbulent reacting flowfield in the separated wake of a centerbody combustor. Chapter II will give an introduction to the concepts of the laser anemometer and the complexities involved in the acquisition and analysis of LDA data. This will be followed in Chapter III by a review of the literature showing that, with proper experimental and analytical treatment, this instrumentation system can be applied to provide meaningful results even in the difficult environment of a separated reacting flow, and that the investigation of this type flowfield is a prime candidate for investigation due to a need for quantified information

for design and analysis studies coupled with a shortage of this very information. The specific research program will be outlined in Chapter IV, demonstrating that the specific instrumentation system constructed for this investigation, the subject experimental burner, and the test conditions chosen are appropriate to the task. Chapter V will describe the pertinent aspects of the software developed for data acquisition and analysis, with the specifics of the implementation included in Appendix A.

Experimental results and discussion of these data will be ascribed to Chapter VI. The mean flow patterns of primary interest for the associated soot investigations are presented. The limits of the instrumentation system to this type study are also identified and discussed as a guide to future experimenters. Turbulence levels, Reynolds stresses, correlation coefficients, and velocity probability density functions necessary for the development and evaluation of future modeling techniques are quantified and shown to be generally inconsistent with past modeling treatments. Specific conclusions and recommendations for future areas of investigation are offered in Chapter VII.

In summary, this research effort provides the experimental data essential for near-term combustor design and far-term development of predictive tools. It requires the construction of sophisticated optical and electronic systems, the origination and development of software

necessary for the interpretation of the results, proof of the system in a difficult environment, and the acquisition, reduction, and analysis of the appropriate data.

CHAPTER II
CONCEPTS OF LASER DOPPLER VELOCIMETRY (LDV)

Although many different forms of laser velocimetry systems have been proposed and tested since the earliest work of Yeh and Cummins (1964), the most common is known as the differential Doppler, fringe, or dual beam velocimeter. This approach is in almost exclusive use presently, is the favored system for future research, and was used in this study. Consequently, the bulk of this discussion centers on the differential Doppler velocimeter. A good overall introduction to laser velocimetry systems in general is given by Stevenson (1977).

All laser anemometers work by collecting and analyzing the light scattered or reflected from particulate matter in the flowfield. In the case of differential Doppler velocimeters, the scattered light is from two separate incident beams which intersect to form an effective measuring region known as the probe volume. A very simple configuration is shown in Figure 1. Here a beam from a laser of suitable power and wavelength is split into two equal-intensity, parallel beams which are brought to a common focus by a single lens. The scattered light is collected by a lens and focused onto an appropriate photodetector, whose output is electronically characterized

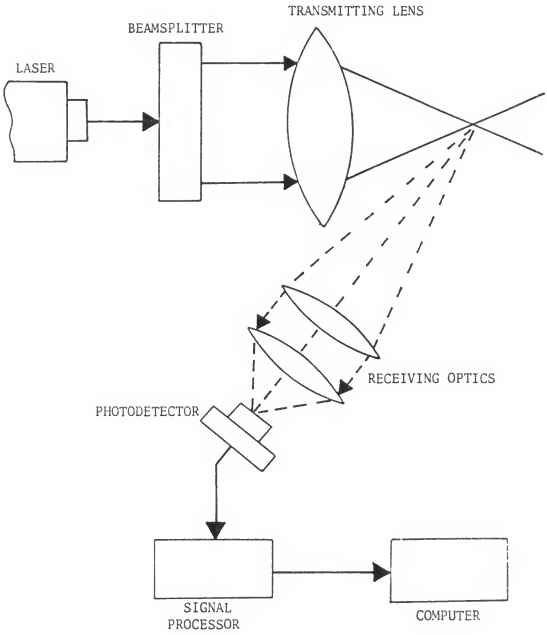

Figure 1. Simple, single-component LDV system.

in a signal processor. Strictly, the scattered light from the two incident beams mixes at the photodetector to yield an output frequency equal to the differential of the frequencies of the two scattered light signals. A common and more readily visualized description is known as the fringe model.

In the fringe model, the probe volume at the intersection of the two incident beams contains a set of interference fringes as shown in Figure 2. Here, two coherent beams having equal wavelengths and planar wavefronts intersect at an angle k. A series of planar interference fringes with spacing d forms at the intersection. As a particle traverses this field, the scattered light will vary in intensity as the particle passes through the constructive and destructive interference zones. The velocity component of the particle in the plane of the incident beams is then a direct function of this frequency. If more than one simultaneous component of velocity is required, other beams must be added to the probe volume.

The scattered light may be collected in any direction relative to the incident beams. Collection 180 degrees away from the incident (forward scatter) gives the highest intensity and the best theoretical signal-to-noise ratio. This installation can be difficult to align properly, however, and requires two optical paths to the region of interest. Collection in the back-scatter direction is

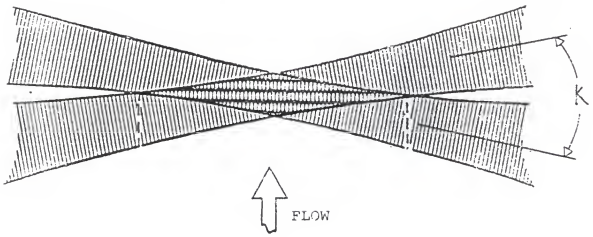

Cross-sectional view

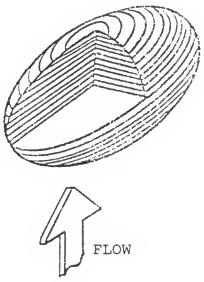

Three-dimensional view

Figure 2. Fringe model.

usually more convenient from the standpoint of equipment logistics and allows the incident beam transmitting lens to double as a receiving lens for the scattered light. This generally allows easier optical alignment. The signals in this direction are of lower intensity, however, and the signal-to-noise ratios are typically lower than in the forward direction. Collection may also be at any other location with the required optical access, but alignment difficulties and poor signal quality usually preclude this.

Figure 3 shows a typical photomultiplier output signal. In addition to the high frequency contribution from the particulate fringe crossings, there is a low frequency component to the signal due to the Gaussian nature of the incident beams. (The beams have higher intensity at the center.) This low frequency component, usually referred to as the pedestal, is filtered electronically in most applications to yield the more easily treated signal shown. Analysis can then proceed using any of a variety of signal processors, with counters being the most commonly utilized and frequency trackers and spectrum analyzers used less frequently. Counters are essentially frequency meters with special provisions for the handling of intermittent signals that arrive in short bursts. Amplification, data validation, and filtering capability is also generally provided.

One serious drawback with the system as described is directional ambiguity. Since the processor output is

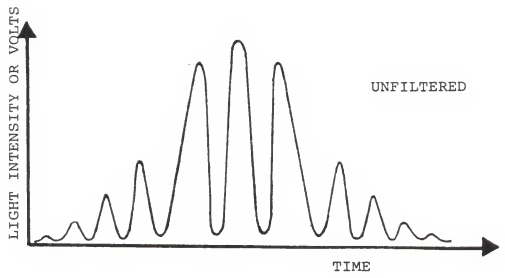

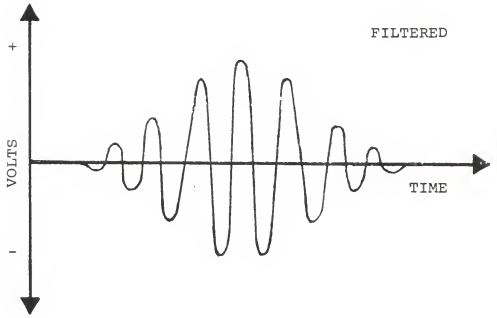

Figure 3. Typical Doppler signal caused by particle traversing probe volume.

actually a fringe crossing frequency, it is impossible to distinguish between particles with identical speeds but opposite velocity vectors. Additionally, a stationary particle would yield no signal at all and particles with very low velocity components in the measured direction would generally not cross enough fringes to produce reliable data. These difficulties can be largely eliminated by the implementation of frequency shifting. By introducing suitable optical elements into the incident beam paths, the beams can be made to have different wavelengths. This effectively creates a moving fringe pattern, with the fringes sweeping across the probe volume at the difference frequency between the two incident beams. Figure 4 depicts the relationships between frequency and velocity for both unshifted and frequency-shifted LDV systems.

Another aspect of the overall instrumentation system that requires careful consideration is the selection and distribution of the seeding material. Obviously, the particles must be small enough to follow the flow properly but large enough to be visible to the receiving optics. When used in reacting systems, the particles must be survivable. These constraints usually result in the selection of ceramic particles (usually aluminum oxide) in the size range of 0.1 to 1.0 micron. The seed is generally introduced into the flow stream with a fluidized bed or cyclone device, with some precautions taken to minimize particle agglomeration. Seeding density affects the data

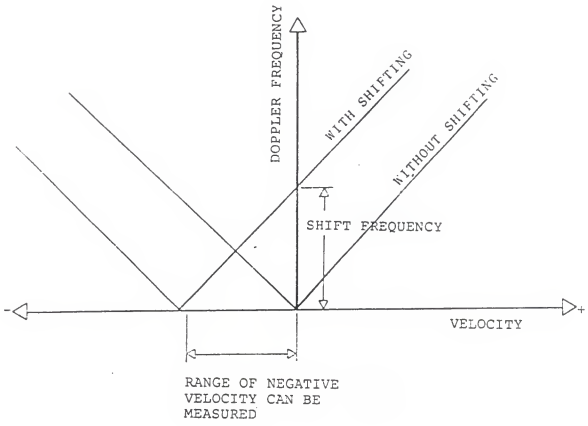

Figure 4. Effect of frequency shifting.

rate, which in turn influences the frequency resolution of the turbulence in the flow, the statistical interpretation of the data, and even the correct calculation of mean velocity. Many of the early theoretical analyses of LDV assumed spatially uniform seeding to derive statistical relations and corrections for discrete sampling. In practice, however, uniformity is never approached and attempts to obtain truly uniform seeding in the flow system have been largely abandoned, although a reasonably uniform distribution is still considered desirable.

The final interpretation of LDV data is still a matter of question. The root of the problem is that in virtually all systems, the data arrive intermittently rather than continuously. As a result, the data are particulate, rather than time, correlated. The calculation of time averages, then, requires some type of correction for this fact. The exact form of this correction has been the subject of much discussion. In addition, the particulate arrivals are not generally random but can be correlated with the fluid mechanics of the flow, since particles in high speed regions of the flow would be expected to arrive at the probe volume more frequently than particles in lower velocity regions. This would bias average velocity calculations to the high side if particle averages were used. The preponderance of biasing studies discussed in Chapter III concern this velocity biasing problem. There are also possible directional biases introduced due to the fringe crossing

phenomena discussed previously, gradient broadening because of velocity changes within the small (but still finite) probe volume and processor biasing caused by uneven frequency response in the electronics. The LDV community has not resolved these questions entirely, but recommendations have been made for minimizing the possible errors introduced and reporting the results in a uniform manner.

CHAPTER III
LITERATURE REVIEW

A literature review of pertinent topics was conducted to establish a technology baseline for this investigation and to help identify appropriate experimental and analytical methods. Primary sources were the proceedings of various combustion and turbulence symposia, technical journals such as Combustion and Flame and the Journal of Fluid Mechanics, and AIAA and ASME papers. Although there is of necessity a substantial amount of overlap, the results of this review are divided into two categories; LDV technology, and relevant flowfield investigations.

LDV Technology

Laser Doppler velocimetry has been under development since the mid 1960s. Major investigative areas have included seeding requirements, data rates, frequency shifting, and bias errors.

In the pioneering work of Durst et al. (1972), a simple LDV system was used to obtain velocity statistics in a turbulent, premixed Bunsen burner flame. Non-Gaussian turbulence and bimodal velocity probability density distributions were observed.

Baker, Hutchinson, and Whitelaw (1973) used a single-component, frequency-shifted LDV system to measure mean

velocity and average turbulence intensity distributions in the recirculation region of a concentric tube type burner operating on natural gas, expanding on an earlier work using an unshifted system (Baker, Bourke, and Whitelaw, 1973). A counter processor was used, with no biasing corrections. Turbulent velocities were found to vary by a maximum of 35 percent throughout the flow field, even in the reacting regions.

In a benchmark study, McLaughlin and Tiederman (1973) conducted an analytical evaluation of biasing corrections in turbulent flow and referred to observed discrepancies between hot wire and LDV experimental results. They concluded that time weighting of the samples is necessary and that higher bias can be expected with nonuniform seeding. A one-dimensional weighting based on only one component of the particle instantaneous velocity vector was deemed adequate in many flow situations.

Whiffen and Meadows (1974) developed a specialized, two-component LDV system for evaluation of turbulence spectra in a jet at frequencies up to 20 khz. They examined seeding requirements, processing parameters, and data validation and concluded that a velocity time history could not be reconstructed from single particle data, using their specialized processing system. Smith and Meadows (1974) used this system to derive power spectrum information through correlation analysis. The procedure was validated by comparing results to a known acoustic input and to hot wire

data. Sensitivity studies showed that data inaccuracies produced larger errors at lower frequencies. Mayo (1974) conducted an analytical evaluation of the limitations of the procedures used. Effects of various systematic and flow induced errors were estimated.

Boutier (1974) measured velocity profiles and turbulence in a separated flow using a single-component LDV and a spectrum analyzer. Results were compared to pitot tube and hot wire data, but are difficult to relate to more recent studies as no frequency shifting was employed.

Durst (1974) reported an observation that LDV data from complex flows (such as the a region where a flame front moves back and forth across the probe volume) requires special attention due to differences in particle concentrations. These variations would bias the results obtained from using the particle averaging technique employed in these evaluations. The concept of using a time weighting based on the intermittency of the flow was introduced.

In a published discussion session at the Second International Workshop on Laser Velocimetry, George, Asher, Mayo, and Fingerson considered the effects of data rate with counter based data processors (Thompson and Stevenson, 1974). The conclusion at that time was that (for the statistical analyses under consideration) high data rates are not desirable since the points will not be statistically independent unless they are in separate turbulent eddies.

In another discussion session, Meyers, Murphy, and Yanta debated the origin of data points in a boundary layer with higher velocities than the local mean. The possibilities of particle collisions and counter error were both deemed valid.

Barnett and Bentley (1974) conducted an analytical study of statistical bias, concluding that the bias is related to particle density and presenting numerical corrections to apply to the data. It was also concluded that biasing is related to the turbulence intensity. Substantial disagreements were expressed in a related discussion section with Asher, Barnett, Mayo, and Tiederman participating and the biasing question was still not resolved. Barnett concluded that all the analytical studies to that time were based on such simple models that they were probably not realistic and recommended an experimental resolution.

Tiederman (1977) helped provide this information and expanded on earlier sampling bias studies by measuring the velocity profiles in both unseparated and separated regions of a wind tunnel, using a two-component LDV. Weighting of the individual particle velocities was done using both single and two-component corrections. Results were then compared to unweighted (particle average) velocities. In the unseparated regions, the differences were small, but in the separated flow region there were substantial differences. The two-component model (the more rigorous)

was much more closely matched by the unweighted data than by the one-component weighted data.

Edwards (1978) evaluated particle bias errors analytically and concluded that for individual realization detectors such as the counters used for the present study, the velocity bias is independent of seeding density, in contrast to the previously discussed results of Barnett and Bentley (1974). It was also concluded that for counter type processors under saturated conditions (high particle density), the biasing error will disappear.

Giel and Barnett (1978) conducted an experimental evaluation of biasing errors under what were felt to be worst-case conditions in a low velocity, highly turbulent jet flow. A counter was used at a data rate of approximately 4 khz, limited by the seeding density. While it was determined that seeding nonuniformity increases bias, low data rates reduce bias, and time delay in the processor reduces bias, no significant bias was found in any case investigated. As a result, automatically correcting for velocity bias was not recommended.

Bogard and Tiederman (1978) evaluated sampling bias in an experimental study of naturally and artificially seeded flows in a turbulent channel viscous sublayer. The photodetector signal was recorded on magnetic tape so that different processing parameters could be evaluated. Counters were utilized. Particle size distribution, differences in light intensity due to particle velocity, and

particle arrival rate were all found to have no effect on the results. Data rates on the order of 1 khz were obtained due to low seeding densities.

Whiffen, Lau, and Smith (1978) discussed observations from several theoretical and experimental investigations of turbulence using LDV techniques. Counters were concluded to produce erroneously high turbulence levels due to signal-to-noise ratio and digital resolution limitations. This was based on observed differences between autocorrelation distributions as measured with laser and hot-wire anemometers, although the calculation of autocorrelations from discrete, randomly sampled information was not addressed. The processors used were designed and constructed by the experimenters, and the applicability of their conclusions to different electronic systems is questionable.

In a panel discussion at the conclusion of the Third International Workshop on Laser Velocimetry (Thompson and Stevenson, 1978), several participants made comments relative to the current work. Hans Pfeifer opined that the bias problem had not yet been solved and doubted that a universally applicable solution would be found. Paul Dimotakis reported a changing viewpoint on turbulence, with a current view that turbulence is about 80 percent composed of large structures. These structures would be very difficult to identify with point measurements unless they are periodic, as in the case of a cylinder in crossflow, in

spite of all the statistical correlations and moments. (Pfeifer agreed.) Ronald Adrian cited cases where refractive index variations in nonisothermal flows gave erroneous turbulence levels. Others stated that they observed only a decrease in data rate due to the effects of refractive index changes on the beam crossing and probe volume visibility to the receiving optics, with no effect on measured parameters. It was agreed that any problem that might exist was reduced using back-scatter collection.

Stevenson et al. (1982) examined many of the results of previous biasing studies and conducted experiments in a separated, nonreacting flow at various seeding densities and turbulence levels. Their shifted, single-component system used the same type counter processor as used for the radial velocity component in the current work. It was found that if the data points were recorded at equal time intervals (rate controlled by a fixed processor response time), then the data average is a true, unbiased, time average. Bias occurs, however, if the rate is controlled by the particle arrivals, as the arrival rate is correlated with velocity. The bias was concluded to depend on turbulence level, seeding density, and processor sampling rate. The McLaughlin-Tiederman single-component bias correction was deemed valid for turbulence levels less than 20 percent and velocities greater than 0.1 m/s, provided no compensating effects occurred in the sampling process. Weighting of the

particle velocities using the time between data points (TBD) was not evaluated due to equipment limitations.

Polyakov and Shindin (1983) measured turbulence parameters in a heated pipe flow and compared the LDV results to simultaneously recorded hot-wire data. The processor internally corrected for bias using a weighting function of the McLaughlin-Tiederman type. A spectral analysis of the LDV data was attempted, although the method used was not disclosed. It was concluded that LDV gives erroneous data in the high frequency part of the spectrum (above 1 khz) due to noise and/or loss of resolution.

Chen and Lightman (1985) examined bias due to particle arrival statistics, using axial velocity data from the U. S. Air Force Wright Aeronautical Laboratories (AFWAL) centerbody combustor. A successful correction scheme based on probability density functions (PDFs) for the interarrival time (or TBD) was presented.

The separated flow region behind a step was studied by Adams and Eaton (1985). A major aspect of this work was an evaluation of the biasing errors present using a shifted, single-component system. For the turbulence levels encountered (less than 20 percent), the maximum velocity bias was found to be four percent. Time averaging corrections were concluded to yield unbiased results. It was cautioned that any correction scheme used must be able to tolerate occasional unbiased particle statistics which may occur due to sampling procedures or signal-to-noise

ratio effects. The McLaughlin-Tiederman type corrections would yield erroneous results for these cases. The authors also observed a bimodal velocity probability distribution in an area where this was not expected. Unsuccessful attempts to eliminate this pattern by changing both data collection and analysis techniques led the researchers to conclude that some type of error inherent to LDV systems was causing a data dropout near zero velocity, but no convincing explanation was offered.

An unpublished panel discussion on biasing errors was conducted at the conclusion of the International Symposium on Laser Anemometry held during the ASME 1985 Winter Annual Meeting. After some discussion, the recommendations of the particle bias committee were summarized by chairman R. V. Edwards:

1. Researchers should thoroughly know and report all pertinent aspects of their system, including seed size distribution and dispersion uniformity, frequency shifts used, filter settings, number of cycles counted, beam waist matching, processor response times, data rates, etc.

2. Flow scales should be reported, although the committee specifically declined to recommend any method for their determination.

3. The McLaughlin-Tiederman 1-D correlation may be used to estimate whether velocity bias will be a

problem in a particular situation, although this technique will overpredict any correction and should not actually be used for data analysis.

4. The data collection rate should be at least twice the highest frequency of interest in the flow to ensure representative sampling.

5. Time between data points (TBD) should be recorded and, if a correction is to be made at all, some type of equal time averaging scheme should be applied for bias corrections. These corrections are to be applied only to mean, single-component parameters, not instantaneous values or cross-correlated results.

6. A list of recommended definitions and nomenclature was proposed to eliminate great confusion in the literature concerning biasing problems.

Although the recommendations of this committee will be followed to the largest practical extent in the proposed program, the biasing problem appears to be unresolved at present, especially in separated or highly turbulent flows. The separated, recirculating flowfields manifested in this apparatus will require careful evaluation of possible data biasing.

In recent years, the technology has advanced sufficiently to allow laser anemometry to be applied to many

research situations, although two-component, time-resolved instrumentation is still in the minority.

Investigations of Turbulent Combustion

Laser velocimetry has been used to determine mean and fluctuating velocity characteristics in combustion systems and to examine structure in well-behaved flow systems. In addition, there have been some attempts to combine these techniques with other instrumentation to obtain correlated information necessary for an improved understanding of mixing/combusting systems.

Durst et al. (1972) used a simple LDV system to obtain velocity statistics in a turbulent, premixed Bunsen burner flame. The turbulence was found to be non-Gaussian, and a bimodal velocity probability density distribution was attributed to "combustion induced periodic fluctuations."

Baker et al. (1974) used a frequency-shifted, single-component LDV system to determine mean velocities and normal stresses in a swirling, coaxial burner. Isothermal and combusting flows were compared; the fuel was natural gas. Signal processing was via a filter bank, oscilloscope, and digital voltmeter system, making the applicability of the results difficult to judge from a modern perspective. Important conclusions were that combustion enlarges the recirculation region substantially, that the turbulence is nonisotropic and non-Gaussian in all cases and that combustion increases the turbulent fluctuations.

Ribeiro and Whitelaw (1975) measured turbulent characteristics in a free jet. Near-Gaussian behavior was observed with no large structure reported.

Chigier and Dvorak (1974) measured average velocity components and turbulence in a premixed, swirling, natural gas flame. A single-component system with frequency shifting and a counter processor was used. Biasing corrections were not applied. Comparisons of reacting and nonreacting flows showed a substantial increase in turbulence in the reacting case, in contradiction to the benchmark work of Durst and Kleine (1973). This work investigated flow in a turbulent premixed flame without recirculation. A spectrum analyzer was used with a single-component, unshifted system. Substantial consideration was given to particle physical characteristics and possible particle effect on combustion processes. Some difficulty in evaluating the results was experienced due to intermittency of the flame front location.

Owen (1975) used a frequency-shifted, one-component LDV to measure mean velocity profiles, turbulence levels, and turbulence probability density distributions in both reacting and nonreacting coaxial jets. Free expansion and confined jets were investigated, with significant separation/recirculation regions in both cases. For the reacting cases, the effects of refractive index changes on the data acquisition were found to be insignificant. Velocity PDFs with significant portions of the distribution

crossing the zero velocity line were interpreted as indicative of large-scale unsteadiness in the flow.

Pope and Whitelaw (1976) compared predictions from a k-e turbulence model and two Reynolds stress models against previous measurements in two-dimensional isothermal wake flows. Combustion applications were the primary topic of interest, but nonreacting flows were evaluated due to a lack of reliable data in reacting flows in general, especially with recirculation. Significant discrepancies were observed between the predictions and experimental results, with the most obvious being a significant underprediction of the length of the recirculation zone.

Ballantyne and Bray (1976) investigated methane jet diffusion flames identified as "laminar to transitional" with time-resolved LDV and quantitative laser schlieren. A cross correlation was attempted with inconclusive results. Low frequency turbulent structure was observed in cases with reaction, but was not clearly defined for cold flows.

Moreau and Boutier (1976) used an unshifted, single-component, counter-based LDV to measure mean velocity and turbulence levels in a premixed methane flame with varying inlet turbulence conditions and no recirculation. In this study, combustion was concluded to increase turbulence, with a larger effect noted in the axial component, and increased inlet turbulence was found to improve combustion efficiency.

Owen et al. (1976) investigated the flow field in a confined, coaxial, turbulent diffusion burner operating on

natural gas. A shifted, single-component system was used; temperatures and molecular species were also measured. Nonreacting data were not presented. From high speed cinematography it was concluded that large-scale motion associated with flow reversals provided a major contribution to measured turbulence levels, was largely responsible for the non-Gaussian nature, and significantly affected mixing due to large-scale inhomogenieties in the flow.

In a later effort, Owen (1977) again used a shifted, single-component LDV to evaluate the flowfield in the initial mixing regions of a swirling, turbulent, diffusion burner operating on liquid fuels. Probability density functions without seeding were obtained to determine droplet velocities, then these were subtracted from the distribution obtained with seeding to determine gas velocities. Time-averaged droplet trajectories were determined and found to be relatively insensitive to fuel type and swirl angle for this particular apparatus. A model for droplet breakdown was proposed.

Fujii et al. (1978) utilized a single channel, shifted LDV with a frequency tracker to investigate the flow field behind a bluff-body stabilizer in nonreacting flow. Axial velocity profiles and mean turbulence parameters were presented, with a downstream centerline stagnation point observed.

Elliman et al. (1978) compared experimental data for velocity and temperature to a k-e turbulence model

prediction as applied to a recirculating reacting flow behind a disk in a duct. Velocity was measured with a spherical, multiport pitot probe, the inadequacies of which led to low confidence in the results comparison. The model significantly underpredicted the observed length of the recirculation zone, with the cause being attributed to a combination of experimental errors and inadequacies in the model.

Owen (1978) made laser velocimeter measurements in a turbulent diffusion burner operating on liquid iso-octane. Both swirling and nonswirling cases were examined and separation was slight due to a small centerbody diameter. A shifted, single-component, counter processed LDV system was used; the issue of biasing corrections was not addressed and time-resolved data was not presented. The fuel droplets were not found to adversely affect the measurements. Data obtained included mean axial and tangential velocity profiles and probability distributions. Ambient pressure and inlet swirl were found to significantly affect the flow field. Large-scale structure was concluded to provide a major contribution to turbulent fluctuations but was not quantified.

Durao and Whitelaw (1978) measured mean axial and radial velocities in the separated flow in the wake of a disk. A frequency-shifted, single-component LDV was utilized, with velocity bias effects assumed to be small. The turbulence was found to be very anisotropic.

Examination of the velocity probability distributions revealed a bimodal pattern which was interpreted as being indicative of a sinusoidal oscillation "superimposed" on the turbulence. This was observed near the outer edge of the annular exit, but not in the disk wake. Evaluation of the turbulence spectra also indicated an absence of predominant frequencies in the wake.

Smith and Giel (1978) used a frequency-shifted, two-component LDV to measure the flow field in a coaxial dump combustor. Hydrogen was introduced through a screen in the outer annular region while a high velocity air stream entered through the central duct. A recirculation region was established between the central core of the flow and the outer duct wall. Comparisons between reacting and nonreacting cases showed that the reaction reduced the axial velocity decay, broadened the radial velocity profile and increased the radial gradient of turbulence intensity. The velocity cross correlation profile was also affected considerably by the presence of reaction. No corrections for velocity bias were applied to the results.

Driscoll and Pelaccio (1978) used an unshifted, single-component system to measure axial velocities in a can type gas turbine research combustor operating on liquid fuel. No flow separation was present. A counter processor was used with no attempt to correct for bias. It was concluded that the presence of combustion did not significantly affect turbulence levels.

Gunther and Wittmer (1980) used a shifted, tracker-based, single-component LDV to measure mean axial and radial velocities and fluctuations in a coannular diffusion burner using methane. No flow recirculations were present. Correlations with local temperatures and degree of ionization were obtained. Observations of the data and flame photographs led to a description of the reaction region as a distribution of flame sheets aligned predominantly in the axial direction. Axial turbulent fluctuations were found to increase in reacting flows, but shear stress was not significantly affected.

Starner and Bilger (1980) measured axial velocity with an unshifted LDV in a coaxial, hydrogen, turbulent diffusion burner. A counter processor was used, but the potential problem of velocity bias in the results was not addressed. Mean velocity and turbulence levels were calculated and correlated with density and mixture fraction at various pressure gradients.

Moreau (1980) investigated a premixed methane/air flow with a single-component, unshifted LDV and generated velocity probability density functions. No separation was present in the flow; a counter processor was used with no biasing corrections. The influence of different jet velocities on the velocity PDFs was examined, with bimodal distributions observed in the regions where mixing between the two jets occurred.

In a program closely related to the current effort, Lightman et al. (1980) used a shifted single-component LDV to measure axial velocities in a centerbody stabilized, propane diffusion flame at the AFWAL facility. A counter processor was used with no biasing correction. Time-averaged mean axial velocities and turbulence were measured on and near the burner centerline and found to match hot-wire data within 10 percent in nonreacting flow. For a nonreacting fuel jet, the main recirculating flowfield was found to be independent of the fuel flow. Heat release was found to increase the recirculation zone length in the axial direction. Velocity vectors, time-resolved data and shear stresses were not presented.

Yanagi and Mimura (1980) used a shifted, single-component LDV with a frequency tracker to provide data for a velocity-temperature correlation in a premixed, Bunsen-type methane flame. Both axial and radial velocities were obtained, with turbulent fluctuations higher in reacting cases. A bimodal velocity PDF in the reacting region was interpreted as indicative of the alternating passage of burned and unburned gases and supportive of the wrinkled flame sheet model.

A single-component, shifted, tracker processed LDV system was used by Yoshida (1980) to measure axial and radial velocities in a premixed Bunsen burner fueled by natural gas. There was no major effect observed on

turbulent fluctuations due to the presence of reaction when comparing data obtained on both sides of the flame front.

Roquemore et al. (1980) conducted a preliminary evaluation of the AFWAL centerbody burner which has a similar configuration to the burner currently under investigation. High speed photography of the propane flame and exhaust gas analyses were studied. A proposed flowfield was shown but no actual velocity measurements were obtained.

Bill et al. (1981) used an unshifted, single-component LDV and frequency tracker to investigate the flow field in a premixed ethylene/air flame with grid-induced turbulence. There was no recirculation present and only axial velocities were measured. The turbulence intensity was found to decrease downstream of the flame holder and a bimodal velocity PDF was observed but not explained. Density was also measured through Rayleigh scattering, but not concurrently with the LDV data, so cross correlations were not presented.

Lightman and Magill (1981) used a shifted, single-component LDV to obtain mean velocities, turbulence intensities, and velocity probability density functions in a centerbody diffusion burner.

Krishnamurthy (1981) used a numerical model with a constant eddy viscosity to predict the isothermal flow field in a centerbody combustor similar to that of the current work. Eddy viscosity was determined via trial and error by matching the solution for the downstream stagnation point to

observed data. Qualitative agreement with the previously reviewed experimental results of Lightman et al. (1980) was obtained but quantitative differences in time-averaged flowfield geometry were substantial. A requirement for more accurate measurements of mean and fluctuating velocities was stressed.

Takagi et al. (1981) evaluated turbulence properties in a hydrogen-air coaxial burner, using a shifted, single-component LDV. Time-averaged information was produced for combusting and noncombusting situations. There were no separations or flow reversals. The presence of a flame was found to retard axial velocity decay, retard radial mixing, reduce turbulent velocities, and increase turbulence macroscale. Turbulence increased with axial distance in the reacting cases, but decreased where no reaction was present. No regular frequency was observed, indicating a random fluctuation.

An unshifted, single-component, tracker system was utilized by Shepherd et al. (1982) to measure axial velocities in a step-stabilized, premixed flame in a duct. Luminosity-conditioned sampling was used to separate the velocity statistics during the alternating passage of reacting and nonreacting portions of the flowfield. The conditioned PDFs were Gaussian in nature but the total velocity distributions were often bimodal. Density was measured concurrently with velocity and cross correlations were successfully analyzed.

Driscoll et al. (1982) measured axial and radial velocities in a turbulent, nonseparated, nonpremixed flame using a shifted, single-component LDV system. The biasing problem was not addressed. Correlated density data were also obtained. The velocity probability distributions were reported to be nearly Gaussian, and there was little difference in the turbulent velocity fluctuations between reacting and nonreacting cases.

Cheng and Ng (1983) used a single-component LDV to measure velocity statistics in premixed turbulent flames at various inlet turbulence levels. The anemometer was unshifted and used a counter; fixed rate sampling was utilized to eliminate velocity biasing. Schlieren photography was used to qualitatively evaluate changes in flame structure due to inlet turbulence variations. The intermittency effect due to convolutions of the flame sheet in this rod-stabilized flame was determined to be the most significant contribution to turbulence and was the cause for bimodal PDFs observed in some locations.

El Banhawy et al. (1983) evaluated the flow in a premixed, ducted burner with a natural gas/air flame stabilized behind a step in the duct wall. A shifted, single-component LDA system was used, with signal processing provided by a spectrum analyzer. Only axial velocities were measured, and mean values were presented for velocity, temperature, and species distribution. Predominant

frequencies were observed in the temperature spectrum and found to correspond to the natural frequency of the duct.

Stevenson et al. (1983) examined a reacting flow in an axisymmetric sudden expansion, using a shifted, single-component, counter-based system. Only axial velocities were measured. The velocity biasing problem was attacked by fixed rate sampling at high seeding levels, so TBD information was not collected. This attack proved effective in nonreacting cases, but the propane-fueled flows produced excessively low data rates and the results were interpreted as being biased. No signal degradation from refractive index variations in the flow was observed. Turbulence levels on the order of 20 percent of the inlet mean flow velocity were measured, with the fluctuations lower in reacting situations. The recirculation zone also diminished in the combusting cases. Generally unsatisfactory agreement with predicted axial velocity profiles was attributed to the k-e model used, with a need expressed for the acquisition of two-component and shear data.

This study was followed up by Durrett et al. (1985), again using a single-component, shifted system to measure mean profiles and turbulence levels in a sudden expansion in a duct. Low speed data acquisition was used to minimize velocity bias, after the method of Stevenson et al. (1982). Both axial and radial components were measured in nonreacting flow. Comparison to a k-e turbulence model showed reasonable agreement on mean velocities downstream of

the expansion but not near the step. Measured values for turbulent kinetic energy were as much as three times higher than those predicted.

Dibble et al. (1984) combined a single-component LDV with Raman scattering to simultaneously obtain axial velocity, species concentration, and temperature information. The hydrogen flame was a turbulent nonpremixed type but did not utilize a bluff body. The LDV aspect of the experiment was not heavily discussed, but some cross-correlation success was obtained.

Bill and Tarabanis (1984) evaluated turbulent, bluff-body stabilized, premixed combustion using a single-component, shifted LDV, in a followup investigation to Bill et al. (1981). Density data were also obtained but were not correlated with velocity. No biasing corrections were made to the counter data and only axial velocities were measured. Combustion was found to increase the magnitude of counterflowing velocities in the recirculating region, lower the turbulent fluctuations, and expand the length of the recirculation zone.

Park and Chen (1984) obtained average velocity statistics in a nonreacting, coannular jet flow using a shifted, single-component LDV. The sampling frequency was held constant at a much lower rate than the particle arrival rate, following the method of Stevenson et al. (1982). Axial mean velocities and turbulence levels were mapped.

Masri and Bilger (1985) evaluated flowfield characteristics in a centerbody diffusion burner using thermocouples and shadowgraphs. They defined a type A flame as one in which the fuel stagnates on the centerline and then flows radially outward along the centerbody face. Their analysis on LPG indicated a maximum jet velocity for this case to be about 30 m/s for an annular velocity of 14 m/s.

Zimmerman (1985) used a two-component LDV configuration similar to that constructed for this work to evaluate the velocity profiles for the concentric air flow around an air-blast gas turbine fuel nozzle under nonreacting conditions. Analyses showed good spatial resolution, and sensitivity to seeding methods only in the high shear region where the jet entrained ambient air. A bimodal velocity probability distribution in this area was convincingly attributed to differing statistics between the two fluid streams, unrelated to turbulent structure.

Leder (1985) compared a k-e model and a constant eddy viscosity model with LDV results for separated flows behind a vertical flat plate acting as a bluff body in a uniform cross-flow. A shifted, single-component, counter system was used, with no correction for velocity bias. Both numerical models greatly overpredicted the length of the recirculation zone and underpredicted the Reynolds stresses by as much as one order of magnitude.

Switzer et al. (1986) measured temperature and velocity in the AFWAL centerbody burner operating on propane under conditions similar to those presently being investigated. A shifted, two-component LDA system was used with counter processors and no time weighting, with only axial velocity data presented. These data were characterized as not sufficiently detailed to describe the separated flowfield in which the reaction occurred, apparently due to data acquisition difficulties. A qualitative agreement was demonstrated between the available velocity information and a predictive code using a k-e turbulence closure.

CHAPTER IV
RESEARCH PROGRAM

Program Goals

The first goal of this effort was to construct an LDV system capable of obtaining real-time, high speed, correlated, two-component data. It was next necessary to write and implement software required for the acquisition, storage, manipulation, and analysis of these data. Limits for the applicability of this instrumentation in reacting environments had to be established.

Once the instrumentation system had been developed, the next goal was to acquire two-component, coincident, time-resolved data in both reacting and nonreacting separated turbulent flowfields.

The final goal was to generate velocity vector plots, velocity probability density functions, and turbulence and shear stress distributions for the separated turbulent diffusion flames typical of the primary combustion zone of gas turbine combustors and other practical combustion systems.

LDV System

The laser Doppler velocimeter constructed for this study is a high power, two-component, four beam

configuration with frequency shifting on both components. It is operated in the back-scatter mode and uses nominal 0.3 micron alumina for seeding. Data are processed with counters, collected with a minicomputer, stored on disk, and analyzed.

The major optical components of the LDV system are shown in Figure 5. The instrumentation system was built from various components over a period of time, and is similar to a TSI, Incorporated, Model 9100-7. The laser is a Lexel Model 95-4, four watt, argon-ion laser, operated in the multiline mode at an output power level of 600 mW. The laser is housed in a separate room from the burner and focusing optics to maintain a clean environment and to control access. The beam is delivered to the LDV transmitting optics via a beam port in the wall separating the two rooms and appropriate mirrors. All optical elements are coated achromats optimized for use at the 514.4nm and 488 nm wavelengths used.

On entering the transmitting optics assembly, the multiline beam enters a dispersion prism color separator where the 514.5 nm green line and the 488 nm blue line are separated from the other lines produced in the laser. In this way, two distinct colors are used for the two components of velocity being measured. After the beamsplitters, one beam of each color pair passes through a Bragg cell which shifts the frequency 40 MHz relative to the other beam to eliminate directional ambiguity and minimize

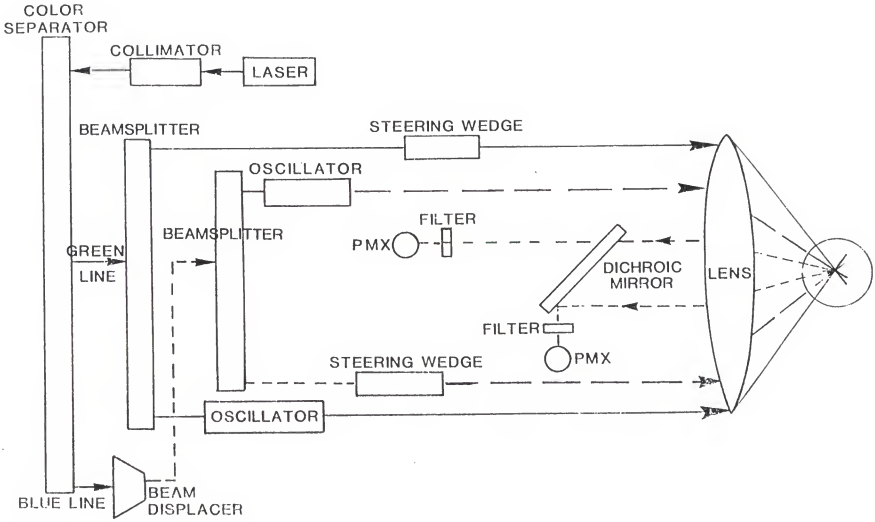

Figure 5. LDV system, major optical components.

angle biasing. A beam stop intercepts the several minor beams produced in the Bragg oscillators. The second beam out of each beamsplitter passes through a steering wedge to aid alignment in the beam crossing region; all four beams then enter a beam expander to widen the separation and increase the intersection angle, thereby minimizing the probe size. The beams then pass through a 152 mm diameter, 480 mm focal length lens and intersect above the burner to form the probe volume. The probe diameter is approximately 0.5 mm and the estimated length is 1.5 mm. Fringe spacings are 1.89 microns for the green pattern and 1.82 microns for the blue.

The light scattered by seed particles passing through the probe volume is collected in the back-scatter direction using the same lens and beam expander as used for the transmitted beams. This technique allows precise alignment of the receiving optics and provides a large collection area. The scattered light then encounters a dichroic mirror which effectively separates the light into the two distinct colors required for identification of the two velocity components. Each color passes through a narrow bandpass filter and is focused onto a photomultiplier tube which produces the electrical signals interpreted by the data processing system.

Figure 6 shows the main elements of the electronic processing system. Each photomultiplier output is amplified, then routed through the Bragg cell power supply

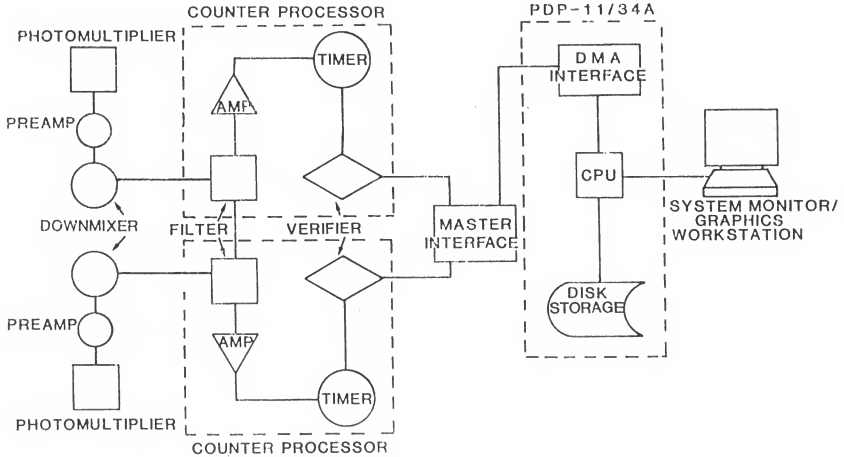

Figure 6. LDV electronics.

where it is downmixed to give a choice of effective shift frequencies at the signal processor input. The radial component uses a TSI 9186 power supply and downmixer while a 9186A is used for the axial component. Effective shift frequencies of 10 MHz were used for both components throughout the test program. Shift directions were chosen to give resulting Doppler frequencies above 10 MHz for axial outflow and radial inflow.

The signals then proceed to signal conditioning modules in the processors. A TSI 1990A counter is used in the axial component and a TSI 1980 counter is used for the radial. In the subsequent amplification and filtering of the signal, frequency components due to optically or electronically generated noise which fall outside the measurement range can be rejected. After the initial calibration testing of the system, the high limit filters were set at 50 MHz for the axial component and 30 MHz for the radial component. Both components were low filtered at one kHz. All data collected fell between 6 and 23 MHz, well within the unfiltered range of the processor systems.

Each processor timer, which is in essence a digital frequency meter, times the period for a fixed number of cycles and has the option of comparing the effective frequencies obtained (for a single Doppler pulse) for both the full cycle count and half that number. For this test program, eight cycles were counted, and data comparison was used at a 7 percent level, meaning a Doppler burst whose

frequency varied more than 7 percent was rejected as a nonvalid reading. Signals surviving the filtering and comparison procedures are treated as valid data and passed to the master interface. Here the data from each processor are timed and checked for coincidence.

To assure that the two velocity components have been measured at approximately the same time, a coincidence window can be defined in the interface. Data must be received from each processor within this time window or they are rejected as noncorrelated information. The coincidence window was set at 1.2 msec for all data presented here. Another feature offered by the master interface is a running time clock that times the period between valid data points. This TBD feature is essential to provide a temporal history of the flow. Coincident frequency data and TBD information are then transmitted to the PDP-11/34A minicomputer via a direct memory access (DMA) data link.

The DMA transfer is effected by an assembly language routine running in the PDP-11/34A and appropriate handshaking signals between the DMA interface (DEC DR11-B)and the TSI 1998J master interface. A fixed number of data points is stored in memory before system control is returned to the main Fortran program which controls data acquisition, reduction, and graphical output. For this series of tests, the number of individual velocity realizations recorded at each spatial location ranged from 512 to 4096. The data acquired through the DMA transfer are

stored on DEC RK05 or RK07 disks to permit thorough examination and to allow for different data reduction techniques to be applied to the same data.

Burner and Peripheral Systems

The burner is a nonpremixed, centerbody type exhausting into free air, as shown in Figure 7. This configuration is representative of the primary reaction zone of gas turbine combustors and other practical devices, guaranteeing applicability of the results. Main burner air enters the plenum through four 2-inch diameter PVC pipes while the air containing the seed particles enters the plenum through a 0.25-inch diameter tube where it mixes with the main combustion air. The fuel is unseeded; earlier investigations with this same burner (Proctor et al. 1985), and the results of Lightman et al. (1980) showed no significant changes in observed flow pattern with the addition of fuel seeding. Fuel nozzle plugging was thus avoided.

The total air flow enters the annular air passage, passes through a flow straightener, and exhausts at the burner exit plane. The outer air passage wall is PVC pipe with a 8.00 cm ID while the aluminum centerbody has a 5.72 cm OD. The fuel mixture passes through a tube in the centerbody and exits through a 1.37 mm diameter conical fuel nozzle designed for oil burner applications.

The burner is mounted on a three-axis traversing table as also shown in Figure 7. Vertical position can be

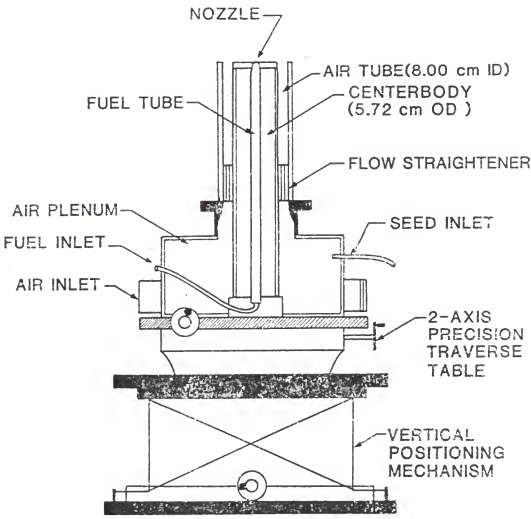

Figure 7. Centerbody burner and table assembly.

determined to the nearest 0.2 mm by visually observing the location of the beam crossing region (probe volume) on a scatter plate attached to the burner. This scatter plate has an accurately scribed grid system on the surface and is referenced to the burner by a pin which is inserted into the fuel nozzle. The horizontal axes are controlled by a precision two-axis traversing table with a potential positioning accuracy of 0.001 mm. However, tolerances in the vertical positioning and support mechanism limit the practical resolution to approximately the nearest 0.5 mm.

The burner supply systems are shown in Figure 8. The main combustion air is provided by a 1-horsepower blower. The inlet to the blower incorporates a throttle plate for flow control and a hot-wire flowmeter to monitor air flow rate. For these tests, the air flow was held constant at a mean annular reference velocity of 14 m/s. The fuel is supplied from regulated bottles or a commercial natural gas line. In either case, the pressure is regulated in the fuel control system and flow is then controlled with a needle valve and measured with a rotameter. Nitrogen supplied from a regulated bottle, metered, and mixed with the fuel after the rotameters is available for diluted fuel studies.

The seeding system operates on compressed air which is dried, metered with a control valve, measured with a rotameter and enters the seeder at two locations. The primary stream enters the base of the seeder and passes through a distribution plate to fluidize the particle bed.

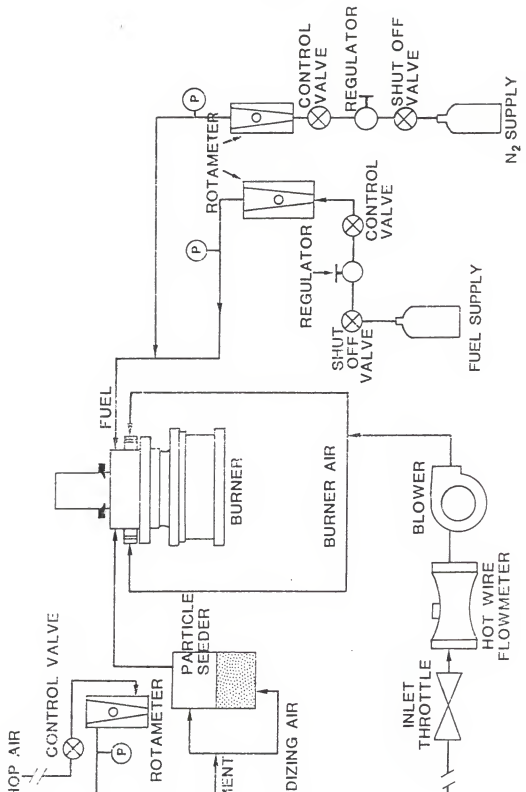

Figure 8. Burner supply systems.

The secondary air stream enters on an upward angle near the bed surface to help entrain the particles in the exit stream. The particle laden air is then carried to the burner plenum for mixing with the main combustion air from the blower. Aluminum oxide particles of nominal 0.3 micron diameter are used for seeding, as recommended and used by several previous researchers (Stevenson 1977, Bill et al. 1981, Cheng and Ng 1983). Extractive sampling of seed material from the burner flowfield was not conducted, so the degree of particle agglomeration is not known.

Testing Conditions

The test format and sequence for the acquisition of data in the reacting regions of the separated flow were chosen to meet all requirements of the contract under which the bulk of this work was conducted, and to provide velocity information throughout the recirculation zone and other regions to be sampled for soot in the associated soot characterization studies.

A coordinate system was chosen with the burner axial direction represented by x and the radial coordinate represented by r. Positions within the flowfield are generally nondimensionalized by the burner radius, R. The axial velocities are U (average), u (instantaneous fluctuation), and u′ (rms average fluctuation). The corresponding velocities in the radial component are V, v, and v′.

The spatial coordinate matrix provided for the acquisition of data at radial locations of r/R=0.0, 0.2, 0.4, 0.6, 0.8, and 1.0, at axial positions of x/R=0.50, 0.75, 1.00, 1.50, 2.00, 3.00, and 4.00. Inspection of preliminary velocity vector plots indicated the desirability of including some additional points near the axial limit of the recirculation pattern. As a result, three data locations at axial coordinate x/R=2.50 were added to provide better visualization of the recirculation pattern when viewing the velocity vector plots, yielding a 45-point spatial matrix.

The testing plan called for the evaluation of both pure and nitrogen-diluted fuels. This provided an opportunity to separate the effects of chemistry, heat release, and fuel jet velocity. The specific fuels and dilutions were chosen after preliminary soot sampling at Tyndall AFB. The pure fuels have virtually identical heating values on a mass basis, so that a test sequence run with different fuels at a fixed air/fuel mass ratio should show no change in heat release rate, but would vary only in the specific fuel chemistry. While this might be expected to yield variations in soot production, no fluid mechanical effects were anticipated.

In subsequent testing for the effects of the soot on LDV data acquisition, natural gas and nitrogen were added to the list of fuels. Areas of investigation included obscuration of the probe volume by particulates between the

measuring region and receiving optics, overloading of the probe volume by excessive numbers of particles, particle luminosity, and the possible intermittency of all these. Data were taken at varying air/fuel ratios at points within the recirculation zone and in the annular flow region both in front of and behind the flame.

Actual laboratory testing procedures were established early in the program. The laser was started and allowed to stabilize for a few minutes. Power was then fixed at 600 mW. LDV associated electronics, including the PDP-11/34A and its peripheral devices, were brought on-line. Bragg cell frequencies were set but the photomultiplier power supplies were not powered up immediately. The laser beam was then attenuated upstream of the prism assembly by a polarization rotator acting in concert with the polarization filter.

The burner centerline was moved to the LDV optical axis by visually observing the location of the beam crossing region (probe volume) on the scatter plate attached to the burner. The coordinates of the translating table were recorded at this centerline position and all radial positions referenced from these. The scatter plate and polarization rotator were then removed, the photomultipliers switched on, a low rate of fuel flow established, and the burner ignited. The fuel flow was increased and burner air applied and adjusted to produce the required annular reference velocity of 14 m/s. The fuel flow rate was

regulated to provide the proper air/fuel ratio for the specific test being performed.

At this point, with all indications appearing normal, air was supplied to the particle seeder and data collection started through software control of the DMA interface via the PDP-11/34A system console. Data collection halted automatically and a message to this effect was printed on the system console when the predetermined amount of data was stored in memory. Seeding was then stopped. If no system errors were encountered, the data were written to disk for later reduction and analysis, and the burner moved to the next radial location. After completion of a radial profile at a fixed axial location, fuel and air flow were stopped, any soot accumulation on the burner face was removed, and the burner table was translated to the next axial position with the probe volume again located on the centerline through use of the scatter plate.

CHAPTER V
DATA ACQUISITION AND ANALYSIS SOFTWARE

The data acquired through the DMA transfer were stored on disk to permit thorough examination and to allow for different analysis techniques to be applied to the same data. For the calculation of average velocities, turbulence levels, and turbulence correlations, individual particle statistics were correctable to time based statistics. The collection of TBD information allowed this to be conveniently done, as a time history of the flow could be generated with a resolution limited only by the data acquisition rate; rates ranged from approximately 20 Hz to 500 Hz in the separated region, and as high as 2 kHz outside the recirculation zone.

Data analysis was conducted using a statistical package with three-sigma filtering and TBD weighting as options, ReGIS graphics routines for velocity probability density functions (PDFs), velocity-time plots, stress-time plots, and TBD-time plots, and an HPGL graphics routine for vector plots. ReGIS output was to either a DEC GIGI graphics terminal or LA-50 dot matrix printer-plotter, while the HPGL vector plots were produced on a Hewlett-Packard 7475A.

Much signal processing actually occurs in the counters. Filter settings, amplification levels, the number of cycles

to be counted in each Doppler burst, data validation tolerance, and the size of the two-component coincidence window are all switch selectable on the processors. The coincidence option and number of cycles counted are transmitted to the computer along with the time required for that number of cycles.

The information from the master interface is passed to the PDP-11 as a series of 16 bit words in a specific sequence, with the sequence depending on the specific options in effect within the processors. These data are stacked in the computer main memory in the order of arrival, with handshaking between the computer DMA interface and processor master interface handled by an assembly language routine which also loads the information. The master interface manufacturer supplied a listing of this routine; it was keyed in, stored on disk, and utilized with no modifications. Another TSI-supplied assembly language routine pulls the data from memory and converts the raw data string to variables accessible by user-written programs.

A sample Fortran program which controls calls to the two assembly routines was supplied by the manufacturer and modified extensively for the specific LDV system configuration being used. The original software package was menu driven, offering a series of options including data acquisition, conversion to velocity files, statistical analyses, histogram plotting, etc. During development, the increasing size of the software caused it to expand beyond

the limited, 32 kbyte memory available in the PDP-11/34A, so the individual subroutines were separated and reconfigured to function as independent main programs. The option to reassociate them into a menu-driven package for installations with more available memory is still open.

Changes to the standard subroutine calls were also required to overcome a hardware malfunction in the processor interface which prevented an accurate transfer of the number of cycles counted in each Doppler burst. The data acquisition program (DMA.FOR) sets the number of data points taken in a single test and also provides an opportunity for the system operator to store burner spatial coordinates, fuel and air flowrates, fuel type, test date, and Bragg cell downmixer shift settings along with the information being passed directly from the processors. The result is a data file on disk containing the test parameters and a series of processor addresses, cycle times, and TBD for a fixed number of velocity realizations. A listing of this program and sample output are included in Appendix A.

The frequency files are then converted into velocity files in the routine MASCON.FOR, also listed in Appendix A. An inspection of the code will reveal that this program reads a list of input file names to be converted, calculates the velocities corresponding to the Doppler frequencies, and stores the new velocity files on disk using another list of file names. There is also an option to output the results to a serial port for printing, viewing on a terminal, or

transfer to another computer. The test setup parameters are passed through to the new file unchanged. The conversion from frequency to velocity requires a knowledge of the fringe spacings, which are different for the two components; these are identified by the processor addresses. Processor addressing is switch selectable in the interfaces, but this program is written for address 0 being assigned to the blue component (system vertical, burner axial) and address 1 assigned to the green (system horizontal, burner radial). In addition to the two components of velocity, there are two possible velocities for each frequency, so that each data point actually has four velocities being calculated. Rather than decide a priori which of the two possible velocity calculations is correct, both are written to the output file for later evaluation. TBDs from the original frequency file are cumulatively added to generate a sequential runtime for each velocity pair and this time after data start is written in addition to TBD. The total runtime for the test is output to the console for reference.

The velocity statistics routine (MASTAT.FOR), like the conversion routine, requires no operator interaction once initiated and is configured to operate unattended from a set of prespecified input velocity data files. An early version calculated mean velocities and fluctuations only, for both possible velocities associated with each Doppler frequency. Testing at a series of different shift frequencies showed that, for the shift directions and conventions chosen in the

frequency-to-velocity conversion package, the value defined as the 'primary' velocity was the correct quantity in all cases, for this particular flow system. The calculation of the 'secondary' value was then eliminated from the statistics routine to allow room for larger data sets and the calculation of turbulence correlations. This expanded version is listed in Appendix A.

The statistics routine reads the burner test parameters from the input velocity data file, and calculates the mean annular air exit velocity for use as a reference velocity for normalization of velocity fluctuations. For the set of velocity files being evaluated, the operator may choose to filter the velocity data to eliminate all points falling outside three standard deviations from the mean and use TBD weighting on the means, deviations, and turbulence correlations. Each input velocity file is read, the velocities and TBDs stored in arrays, and mean velocities calculated, using TBD weighting if selected. For each instantaneous velocity, the deviations from the mean are then calculated, squared, and summed. The instantaneous shear stress is calculated by multiplying the radial and axial deviations at each data point; these stresses are then summed and averaged to determine mean shear at the test location. Root-mean-square velocity deviations are calculated for each component, then combined and divided into the average shear to establish the local velocity correlation. Three-sigma limits for the velocities are

calculated and the summing and averaging loops are then repeated if filtering is to be applied. Filtered output velocity files and Reynolds stress files are created for any further analysis and the mean values are output to the console, with an automatic screen dump to a local printer typically used for permanent record purposes.

Routines to calculate and plot probability density functions for Doppler frequency, velocity, and shear stress were all constructed as independent programs, but their similarities are so great that only the velocity version (GRAPHV.FOR) will be discussed and included in Appendix A. The histogram plotting routine runs interactively, with the console operator choosing the components to be analyzed and scales to be used for plotting. Burner test parameters are read from the input data file and the reference velocity calculated. The velocities are then read and assigned to one of 64 bins between the specified plotting limits, with both the number of samples in each bin and the total number of samples tracked until all data have been read. The percentage of the data falling within the plot limits and the size of the largest bin are calculated for scaling and reference purposes. After the numerical calculations are completed, actual plotting is accomplished by a graphics routine written in ReGIS, a language compatible with both the GIGI system console and LA-50 graphics printer. After the plot is complete, the operator is offered a list of

options including rescaling, changing the parameter being analyzed, or selecting a new data set.

Temporal plots for velocity, shear, and TBD are provided by other interactive ReGIS routines; again, only the velocity version (TIMPLT.FOR) will be specifically addressed. This program is similar in operation to the PDF routine, with the operator specifying the parameters and scales to be used in the graphical output. After scaling, the data points are read sequentially and plotting started when the specified plot start time is encountered. Graphical output continues until the plot stop time entered previously by the operator is reached. A title block is written and the rescaling option offered as before.

The final item of software to be discussed is the vector plot routine used to display the flowfield and help visually correlate the data taken throughout the spatial test matrix, as opposed to the previously discussed programs which analyze information at specific, individual locations. This HPGL plotting package was already in existence on the laboratory's Integrated Solutions IS-68K minicomputer and required only minor modifications to produce the graphical output seen in the results section. A listing of this program is included in Appendix A.

CHAPTER VI
RESULTS AND DISCUSSION

With the LDV optical and electronic systems assembled and the relevant software written, it was necessary to evaluate the application of the instrumentation system to reacting flows with high soot loadings and to obtain data sufficient to determine velocity statistics throughout the flowfield. These efforts were conducted concurrently. As the results were difficult to anticipate, entire flowfields were mapped for each fuel condition then evaluated for internal consistency, with analysis for any observed data irregularities reserved for a later period. This provided the opportunity to eliminate nonproblem test conditions from the evaluation of soot effects on the data acquisition. Table 1 shows relevant test conditions for the flowfield mapping.

TABLE 1. FUEL CONDITIONS FOR FLOWFIELD MAPPING

Fuel	Fuel Rate cc/s	Nitrogen Rate cc/s	Velocity m/s	A/F Ratio
Propene	4.1	0.0	2.8	6000
Propene	62.2	0.0	42.1	400
Propene	142.2	0.0	96.5	180
Isobutene	24.2	0.0	16.3	800
None	0.0	0.0	0.0	
None	0.0	93.3	63.2	400
Propene	46.7	31.0	52.6	370
Butene	23.3	46.6	47.3	400
Butene	31.1	31.0	42.0	400

Treatment of Data

Mean velocities and turbulence levels were monitored and reviewed as testing progressed. Post-test examination of velocity-time plots revealed some unexpected spikes in the data, predominantly in the nonseparated region of the flowfield and in the axial component (Figure 9). An investigation revealed that these characteristics were not a real phenomenon as they could be eliminated during data acquisition by lowering the processor gains and changing the frequency shift settings, with an associated decrease in data rate, as seen in Figure 10. The erroneous signals were concluded to be caused by particles scattering light from areas other than the actual probe volume, which then mixed with light from other sources (such as flare from the transmitting lenses) to produce a Doppler-type signal. These erroneous signals would be weaker than valid measurements unless caused by unusually large particles, which would be expected only in the areas of the flowfield dominated by the annular flow. To eliminate the contribution of this noise from the data which had already been stored, a filtering technique was incorporated into the statistical package as described in Chapter V, and the effect of this filtering investigated.

During influence testing for data filtering, the effect of TBD weighting was also evaluated. Mean velocities, turbulent fluctuations, Reynolds stress ($-\overline{uv}$) and the correlation coefficient $-\overline{uv}/u'v'$ were treated. As the

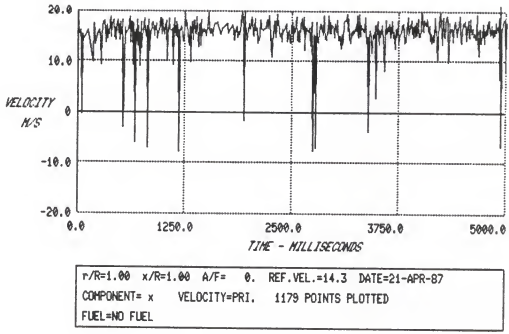

Figure 9. Axial velocity as a function of time at high processor gain, showing erroneous data points.

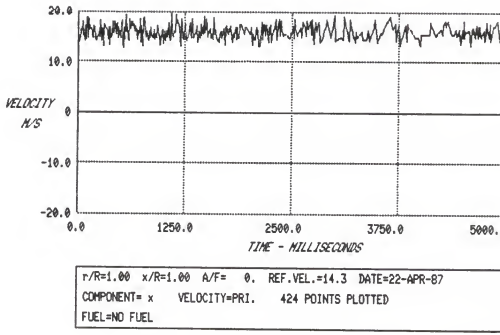

Figure 10. Axial velocity as a function of time at lower processor gain, showing elimination of faulty data.

erroneous spikes were generally single-particle events of very short duration, the effect of their removal by three-sigma filtering was expected to be more apparent on particle averages than time-weighted averages. Greater effects were also anticipated on the turbulence correlations than on the mean velocities.

The propene (propylene) data at the air/fuel ratio of 6000 was chosen as the test case. Deviations between results obtained using different combinations of filtering and weighting were calculated for the parameters of interest and averaged over all 45 locations in the spatial matrix. Three-sigma filtering rejected an average of 6 velocity data points of 256 at each location, with a maximum rejection of 14 of 256 at a point in the annular-flow-dominated area. The largest changes, as expected, were observed between unweighted, unfiltered data and the same input data sets with filtering and TBD weighting.

For the mean velocities, the average differences between statistics obtained using results from unweighted, unfiltered data and weighted, filtered data were 0.12 m/s for the radial component and 0.23 m/s for the axial, both within the expected accuracy range of the data. A comparison of other data treatment combinations showed these differences to be due primarily to TBD weighting in the radial component (where the erroneous data was not evident), and to filtering in the axial component.

The effects of weighting and filtering were expectedly larger on the calculation of turbulent fluctuations, with average differences of 0.16 m/s radial and 0.61 m/s axial observed between unfiltered, unweighted data and filtered, weighted data. The larger of these values is well outside the expected accuracy range of the data. The major contributor was filtering for both components, with the effect of TBD weighting alone not significantly outside the anticipated accuracy band. Turbulent correlations, in the forms of Reynolds shear and correlation coefficient, also showed sensitivities to data manipulation. The expected accuracies were 0.20 $(m/s)^2$ and 0.07, respectively. Observed differences were 0.35 $(m/s)^2$ and 0.07. Three-sigma filtering and TBD weighting were about equally influential in the observed differences for both parameters.

As a result of these comparisons, choices were made for the data treatments to be applied to the remaining data herein presented. All mean velocities are TBD weighted, in accord with the recommendations of the 1985 bias committee recommendations detailed in Chapter III, but have not been filtered. The individual turbulence components shown later in Figures 25 and 26 are likewise TBD weighted and are calculated from three-sigma filtered velocity files. The effects of filtering are within the expected accuracy of the data in the separated region of the flow but are larger outside this area where the majority of the anomalous data points were observed in the velocity-time plots. The

Reynolds shear is filtered but not weighted, as the bias committee specifically advised against applying temporal corrections to cross-correlated parameters due to a lack of a suitable data base, while the treatment of the correlation coefficient has something of a mixed nature as the stress in the numerator (-uv) is unweighted while the denominator ($u'v'$) is weighted. The differences between unweighted statistics for filtered and unfiltered data sets are 0.23 (m/s) for the shear and 0.04 for correlation coefficient. Velocity probability density functions are filtered but not TBD weighted.

Mean Flowfield Mapping

Vector plots for the test fuel conditions are shown in Figures 12 to 17 and 19 to 21, with the corresponding numerical velocity components in both radial and axial directions listed in Appendix B. Also included in these tables are unfiltered rms fluctuations in each component and the overall turbulence level as referenced to the annular inlet mean velocity of 14 m/s. The uncertainty in each component of the mean velocities, as obtained from a series of measurements at a fixed location and fuel rate, is approximately 0.25 m/s, corresponding to a vector length of 0.2 mm at the scale used in the figures.

The flow pattern in this type system has been postulated by Chen and Lightman (1985), Roquemore et al. (1986), and Roquemore et al. (1980), as shown in Figure 11. These flowfields are similar to those seen in several

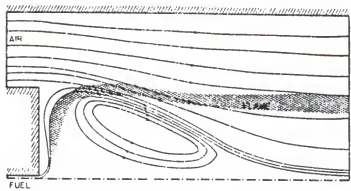

a

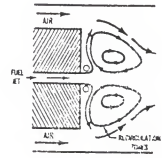

b

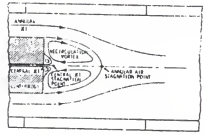

c

Figure 11. Anticipated flowfields as presented by (a) Roquemore et al. (1980); (b) Roquemore et al. (1986); (c) Chen and Lightman (1985).

photographs of separated flows as presented by Van Dyke (1982). In the current data, there are two general flow patterns evident. At low heat release rates, the pattern looks as expected, with a single recirculation vortex between the fuel nozzle and the centerbody outer radius and no significant flow across the burner centerline. This matches the referenced anticipated results. At higher heat release rates, significant crossflow is evident at the centerline and some tests seem to show large secondary flow patterns. These patterns were found to be nonrepeatable and were chosen as the basis for investigation of the limits of the data acquisition system. The flow patterns fitting the expected results are discussed first.

Figure 12 shows the flow pattern with no flow through the fuel nozzle. The recirculation pattern downstream of the centerbody face is clearly evident, with a centerline stagnation point at approximately x/R=1.8 and a circulating flow centered around a point near (x/R=0.75, r/R=0.6) in the separated zone. There is very little flow across the centerline, indicating a nearly symmetric flowfield. At the outer radius of the centerbody (r/R=1.0), the velocity approaches the annular average of 14 m/s. The mean flow has become fairly uniform by four radii downstream.

Figure 13 shows the effect of injecting nitrogen at an a/f mass ratio of 400. The centerline velocity at x/R=0.50 drops somewhat due to the influence of the fuel jet, and there is some increase in radial outflow along the

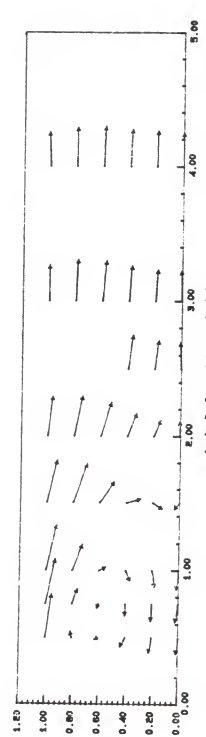

Figure 12. Velocity vector plot for no fuel jet.

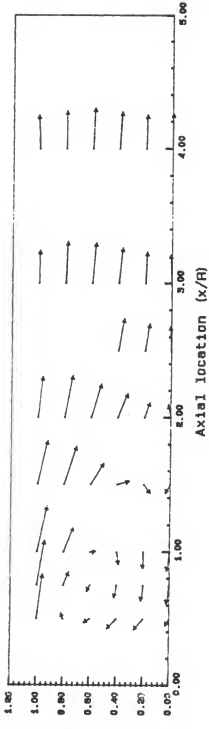

Figure 13. Velocity vector plot for nitrogen at a/f=400.

centerbody face, suggesting that the fuel jet reverses in less than 0.5 radii and flows radially outward along the face of the centerbody, to be entrained in the axially outflowing air in the shear layer near r/R=0.9.

This characteristic of the fuel jet flow corresponds to the type A pattern of Masri and Bilger (1985), although the apparatus used in the present study displayed this behavior at jet velocities as high as 47 m/s in reacting flows and 63 m/s for the nonreacting nitrogen flow, whereas the referenced results would indicate a maximum expected velocity for this pattern to be near 30 m/s. The configurations of the fuel nozzles were different, however, with theirs being a straight jet rather than the conical nozzle used for the current tests. Other than the local influences of the fuel jet near the centerbody face, differences between the two nonreacting cases are negligible, and the recirculation length in the axial direction stays constant at 1.8 radii.

Figure 14 depicts the flowfield with a propylene fuel at a/f=6000, which is about the maximum value (or lean limit) at which combustion can be maintained in this burner. Even this relatively small amount of heat release can be seen to increase radial outflow near the face, increase axial inflow throughout the recirculation zone, expand the recirculation region radially, and lengthen the recirculation axially to 2.2 radii. Due to the radial expansion, the position of the zero axial velocity surface

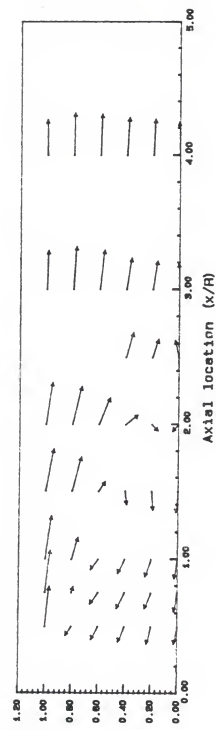

Figure 14. Velocity vector plot for propylene at a/f=6000.

has shifted. The significance of this surface, as pointed out by Switzer et al. (1986), is that it separates the gases flowing axially outward from the recirculated gases flowing axially inward, with significantly different histories for the fluid elements on either side. It can be concluded that the effect of a small amount of heat release is more significant than the fluid mechanical effect of a nonreacting fuel jet even at nearly 15 times the mass flow, for the range of conditions tested.

The vector plots at the lower heat release rates provide more insight into the effects of varying heat release rate and fuel chemistry. Isobutene at a/f=800 (Figure 15) and a 1:1 mixture of butene and nitrogen at overall a/f=400 (Figure 16) have approximately the same heat release per unit time, with the latter having twice the fuel jet mass flow. In this case, the fluid mechanical effect of the higher jet velocity can be seen in the radial outflow on and near the centerline at x/R=0.5. There is also some shift in the vectors along the shear layer, but this variation is probably within the positioning accuracy of the burner table mechanism, as the velocity gradient is very high in this region. The patterns are otherwise quite similar.

A comparison between butene/nitrogen 1:1 mix and butene/nitrogen 2:1 mix (Figure 17) shows no significant difference. Here the heat release changes by 50 percent at a fixed fuel mass flow. Both patterns are seen to be quite

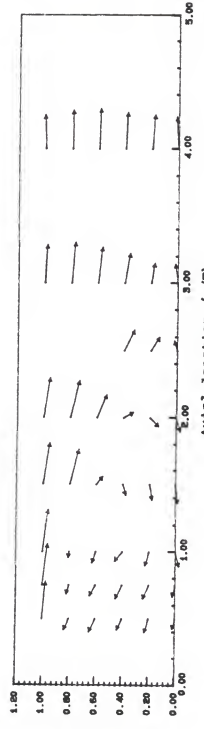

Figure 15. Velocity vector plot for isobutene at a/f=800.

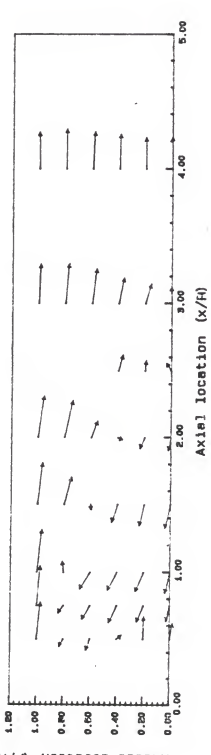

Figure 16. Velocity vector plot for butene-nitrogen 1:1 mix at a/f=400.

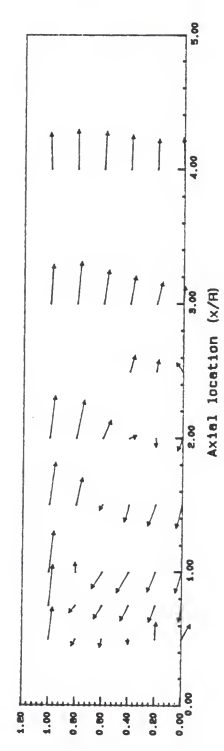

Figure 17. Velocity vector plot for butene-nitrogen 2:1 mix at a/f=400.

similar to the propylene flowfield at a/f=6000. At the higher heat release rates within this group (Figures 15-17), increased inflow (or decreased outflow) near the shear zone near r/R=0.8 indicates a slight radial expansion of the recirculation zone, but no axial change is evident as the centerline stagnation point holds constant at 2.2 radii. The general trend shows no significant change in flow pattern or recirculation zone extent despite a tenfold increase in fuel flow. It is again observed that fuel jet flow rate is not a strong driver of flowfield pattern within the range tested. It also seems that the effect of heat release is most dramatic at very low fuel rates, with increasing fuel flow not being significant to the structure of the recirculation zone. The specific fuel chemistry, as expected, shows no influence on the flowfield.

The axial velocities measured by Switzer et al. (1986) can be directly compared to the data of this investigation. Figure 18 shows the radial distribution of axial velocity at approximately one centerbody radius downstream of the face. The agreement is good except along the centerline. Here, the current study shows axial inflow, with the recirculation pattern dominating the fuel jet, while the referenced work shows the fuel jet dominating the centerline, resulting in axial outflow. This may be ascribed to the higher jet velocities and differing fuel nozzle characteristics in the burner used by Switzer et al., and differences in the strengths of the recirculating patterns because of

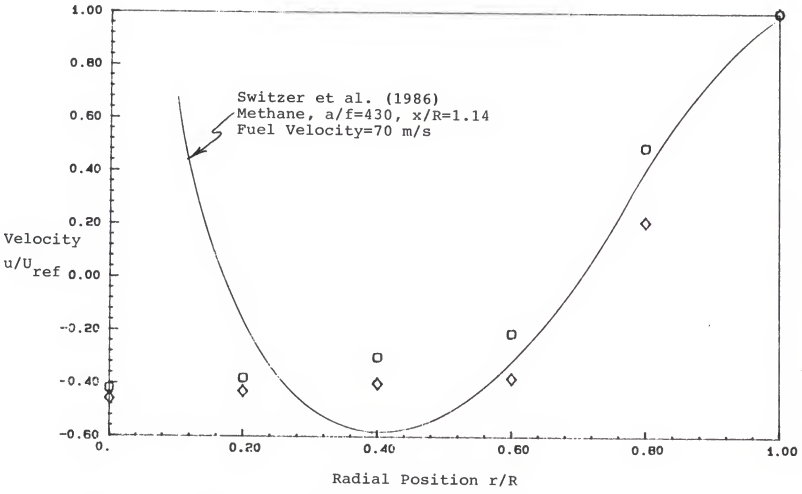

Figure 18. Radial profile of axial velocity at axial position x/R=1.00.
○ Propene, a/f=6000, fuel velocity = 2.8 m/s
◇ Butene/nitrogen 1:1 mix, a/f=400 fuel velocity = 47.3 m/s

downstream flow configuration differences. The possibility of differing statistics due to different seeding methods and biasing treatments cannot be discounted.

Soot Interference Studies

The previously mentioned anomalous flowfield patterns provided the starting point for another series of tests designed to help determine the effect of soot particles on the LDV data acquisition. Figures 19 to 21 represent these apparently erroneous flowfields. Follow-up testing under similar conditions along the full centerbody diameter revealed poor repeatability and nonsymmetric flow patterns. As the flame appeared symmetric to the eye and no physical argument for an abrupt change in flow pattern was evident, these results were felt to be erroneous.

An evaluation of the testing sequence, dates, and conditions showed that the differentiation between these two categories of results correlated to reactant flow only, with the lower air/reactant ratios always producing the anomalous results. Fluid mechanical effects were not felt to be responsible for the observed trends as the nonreacting nitrogen jet pattern is well behaved at the higher mass flow rate and nozzle velocity already shown in Table 1. Since the fuels being tested were all known to be soot producers, the influence of this uncontrolled particulate material on the LDV data was investigated.

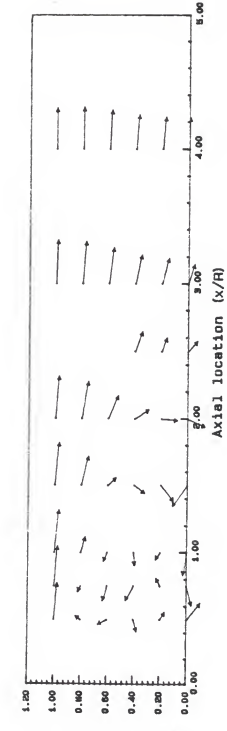

Figure 19. Velocity vector plot for propylene at a/f=400.

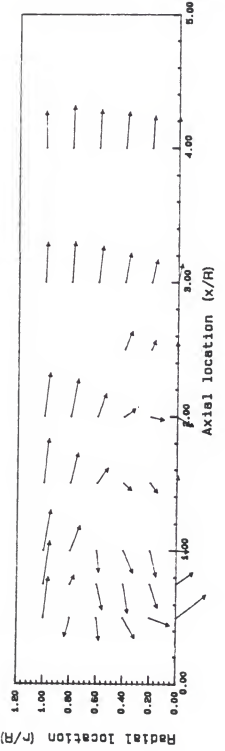

Figure 20. Velocity vector plot for propylene at a/f=180.

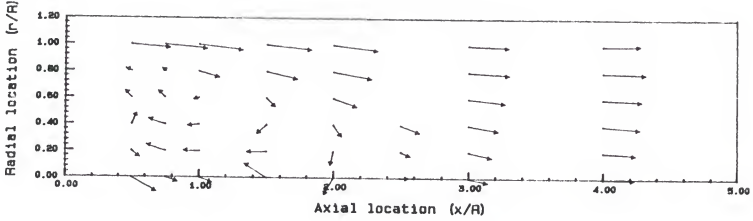

Figure 21. Velocity vector plot for propylene-nitrogen 2.26:1 mix at a/f=370.

Three mechanisms for soot interference were postulated: obscuration of the probe volume by particulates between the measuring region and the receiving optics; overloading of the probe volume by large numbers of particles; and lowering of the signal-to-noise ratio by particle luminosity. The expected effects of these three mechanisms were consistent with an earlier observation that the LDV data rate decreased noticeably in the reaction region of the more heavily sooting flames. Since the problems were anticipated to be most serious in regions of high soot concentration, a soot mapping exercise was conducted.

For soot mapping purposes, the seeder was disconnected and the processor settings were changed to provide a greater sensitivity to the natural particles. Two Doppler cycles were counted in the multiple measurement per burst mode, with no data validation. The resulting count rate was felt to be indicative of the relative local soot loading. Although the spatial resolution was not fine enough to produce reliable contour plots, the results were in general agreement with those generated by the associated soot profiling studies being conducted as part of the overall investigation. The highest concentrations were in a region extending radially between the burner centerline and $r/R=0.80$, with an axial extent from $x/R=0.75$ to $x/R=1.5$. Obscuration, overloading, and luminosity testing was carried out in this area.

Table 2 shows the results of the luminosity tests. LDV data were taken in the annular region on the optics side of the burner, with the luminous flame in the background of the viewing area of the receiving optics. The processor and photomultiplier gains were held constant for all tests, with the photomultiplier gain set near the maximum current limit for the most luminous flame condition (propene). It can be seen that increasing luminosity decreases the data rate substantially, with an even larger effect expected if the gain settings had been increased for the less luminous conditions. No obvious effect on measured mean velocity is evident in this nonseparated flow region.

TABLE 2. LUMINOSITY EVALUATION AT A/F = 800.

Fuel	Rate Hz	V m/s	U m/s
Nitrogen	1400	-0.92	12.07
Natural gas	700	-0.88	12.05
Propene	250	-0.81	12.57

Table 3 shows the combined effect of luminosity and obscuration from data taken in the annular region behind the flame. Here, with the reacting region between the probe volume and optics, there are still no marked deviations in mean velocity. The trend in data rate is quite similar to that for the luminosity tests.

Table 4 shows the result of increasing propene flow at a fixed location within the reaction zone. The rate and velocities are steady down to an air/fuel ratio of 3000, then variations are introduced at richer mixtures. With the

TABLE 3. OBSCURATION AND LUMINOSITY EVALUATION AT A/F = 800.

Fuel	Rate Hz	V m/s	U m/s
Nitrogen	1200	-0.92	12.87
Natural gas	700	-1.08	12.74
Propene	250	-0.87	12.43

seeder off, oscilloscope observations of the filtered photomultiplier outputs revealed a noticeable change around a/f=2000. Above this value, no Doppler bursts were visible and there was no data count. With richer mixtures, large clusters of particulates were visible on the scope and LDV data rates approached 10 percent of the seeded values shown in the table. Examination of the oscilloscope traces showed that each burst was composed of a large number of overlapping and interfering Doppler-type signals, indicative of dense pockets of soot intermittently passing through the probe volume.

TABLE 4. PARAMETERS WITHIN PROPENE FLAME

Air/fuel	Rate Hz	V m/s	U m/s
5000	160	2.00	-3.94
4000	150	2.00	-4.23
3000	210	1.95	-3.92
2000	100	1.82	-3.48
1000	110	0.45	-4.37
800	90	0.80	-5.37
400	90	0.37	-5.19

Figures 22 and 23 show TBD plotted against run time for two of the seeded tests of Table 4. The intermittency is evident, with the assumption that the areas of high TBD

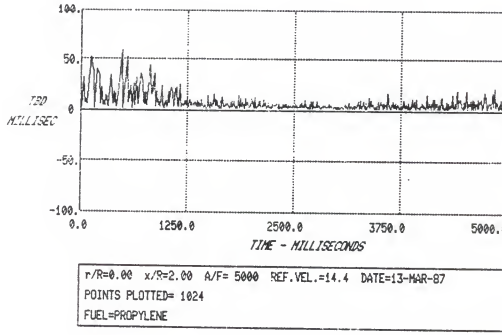

Figure 22. Time between data points as a function of run time for lean mixture.

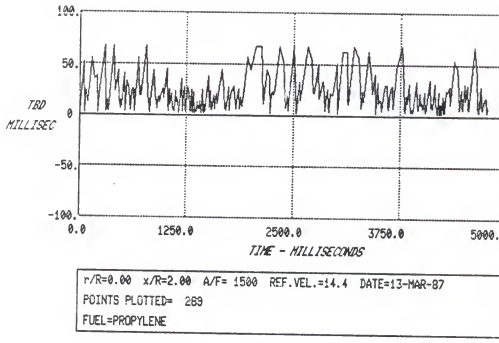

Figure 23. Time between data points as a function of run time for rich mixture.

coincide with passing clouds of soot. The corresponding velocity-time plot for Figure 23 is shown in Figure 24. Although the data rate slows dramatically in the soot passage areas, obviously erroneous velocity data is not apparent.

As a result of this intermittent interference, the effects of obscuration and luminosity are not really separable. If normal data acquisition is disrupted during passage of a soot cloud, this disruption would be expected to have the same influence on the data whether caused by luminosity (which was demonstrated) or obscuration (which was not independently observed). In this set of experiments, windowing of the data by obscuration and luminosity apparently outweighed the increased particulate density associated with the soot and preferentially conditioned the sampling to periods when soot was not present in the vicinity of the LDV system line of sight. It is quite likely that the opposite effect could be observed under circumstances with different photomultiplier gains, processor settings, soot loading, and relative contributions of the three mechanisms being considered.

Turbulent Fluctuations

An evaluation of the turbulent fluctuation levels was conducted for the cases of no fuel jet, the nonreacting nitrogen fuel jet, and the propene-fueled results at a/f=6000. These results can be compared to the limited data

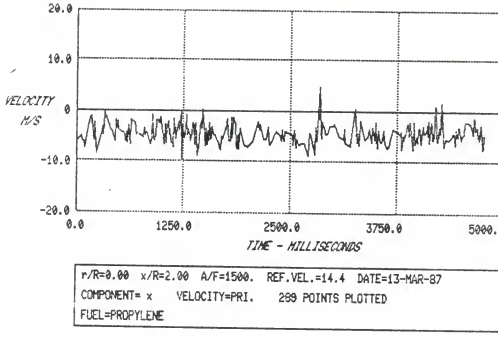

Figure 24. Axial velocity as a function of run time for rich mixture.

from similar, centerbody-type experiments and also to typical premixed studies. The rms averaged fluctuations are accurate to approximately 0.15 m/s, are TBD weighted, and have been calculated from three-sigma-weighted velocity files.

Figure 25 depicts the rms deviation in the radial velocity component (v´) for these cases. The data from the nitrogen test and the test with no fuel jet match within the experimental accuracy at 42 of the 45 points in the spatial matrix, so only the nitrogen and propene results are plotted. The points for the propene flame have been connected to serve as a reference line for the other data. For the two cases, little influence of the fuel jet or reaction is seen, as the curves for the different fuel conditions match closely. Independent of the fuel effects, other general trends are apparent. The turbulent velocities in the recirculating region are higher than in the mainstream, and are higher near the centerline at large x/R than in the areas closer to the burner face. This means that the turbulent fluctuations present in the annular flow region increase in the separated portion of the flow as it turns and begins flowing radially and axially inward. This level then diminishes as the flow travels down along the centerline and then radially outward along the face of the centerbody. There is no indication that the reaction greatly affects the radial turbulent component within the recirculation zone.

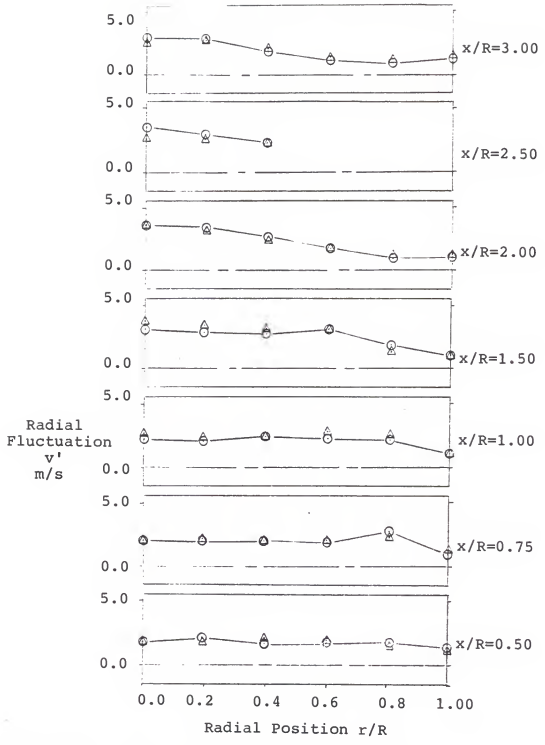

Figure 25. Radial profiles of radial turbulence at seven axial locations.
⊙ Propene, a/f=6000
△ Nitrogen, a/f=400

Figure 26 shows different trends for the axial fluctuations (u'). The fluctuations are still somewhat higher in the recirculation region than in the inlet flow, but the presence of reaction can be seen to increase the turbulence in the flow immediately downstream of the flame front even at this lean condition. This additional contribution to the fluctuations diminishes rapidly, however, with no indication of the reaction influence seen by axial position x/R=3.0. At the position nearest the fuel nozzle exit, the fluctuations correlate well with the fuel jet flow rate, with the highest turbulence for the nitrogen jet at a/f=400 and the lowest for the no-fuel condition.

Switzer et al. (1986) obtained axial statistics in a centerbody burner similar to that used in this study and also showed a fluctuation increase near the flame front, and axial turbulence levels on the order of 20 percent relative to the annular inlet velocity. This magnitude agrees closely with the present work.

In the nonreacting, separated flow in a disk wake, Durao and Whitelaw (1978) observed that, near the centerline stagnation point, the radial fluctuations were as much as 100 percent higher than the axial fluctuations. A comparison between Figures 25 and 26 shows a similar trend seen at x/R=1.50 and x/R=2.00 in both reacting and nonreacting cases, although the increase of the radial over the axial turbulence is more on the order of 75 percent. An examination of the referenced radial profiles showed an

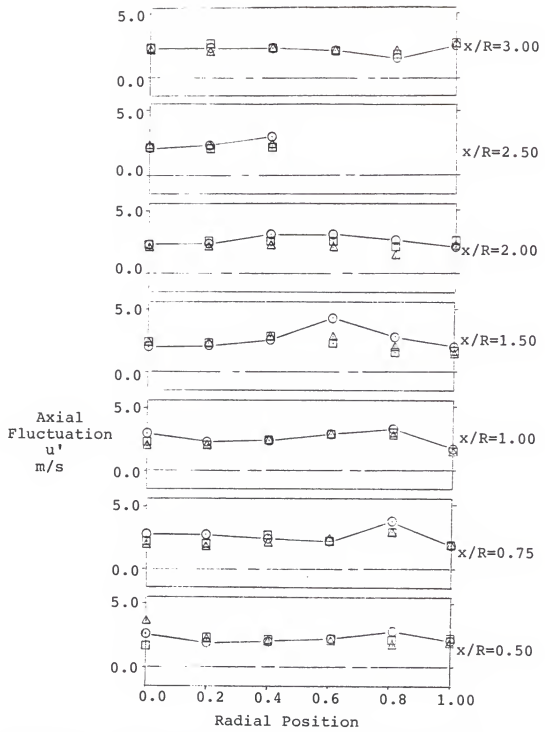

Figure 26. Radial profiles of axial turbulence at seven axial locations.
⊙ Propene, a/f=6000
△ Nitrogen, a/f=400
□ No fuel jet

increase in axial fluctuations with increasing radius, whereas the present results show a more constant turbulence, with a peak near the annular/recirculated mixing layer. Radial fluctuations were constant in the referenced work, while a radially decreasing trend is seen in Figure 25. The substantially nonisotropic nature of the turbulence in the separated region is inconsistent with k-e modeling (Leder, 1985) and must be considered when closure models are applied.

The observation that the axial turbulence is influenced more heavily by the reaction is consistent with the results of Moreau and Boutier (1976) in premixed flames in a duct. Cheng and Ng (1983) observed sharp increases in both fluctuating components in the reaction zone in a rod-stabilized, premixed flame; Yoshida (1980) saw no major change in turbulence at the flame front in a Bunsen flame. The major source of discrepancy in these studies is the specific geometry tested. The characteristics of the flame front that would be expected to alter the observed fluctuations include wrinkling, intermittency, steadiness, and the angle between the flame front and the instantaneous velocity vector. Generally, the reaction can be expected to accelerate the flow due to expansion, and the component of velocity more nearly normal to the flame front would be expected to show the higher fluctuations. Conclusions from differing test geometries must be interpreted with this consideration.

Turbulence Correlations

The most apparent effect of the reaction is seen in the shear stress distribution. Figure 27 shows that the Reynolds shear ($-\overline{uv}$) is generally slightly negative along the centerline. The stress then trends to the positive in the recirculating zone, but shows a marked increase in the vicinity of the reaction front, which also coincides with the high velocity gradient region where the outer radius of the recirculating pattern merges with the annular flow.

This increase in shear then dissipates downstream in a manner similar to the axial fluctuation. It can also be seen that the shear stress decreases as the flow turns and starts back down in the recirculating part of the flow, indicating a nonrandom correlation originating in the high mean velocity gradient region of the flow (with a higher Reynolds stress seen in the reacting case) and decaying as the flow recirculates. This decay occurs faster in the reacting case than in the nonreacting flowfields.

It should also be noted that although the low shear zones observed at x/R=0.50, 0.75, and 1.00 generally correspond to areas of low velocity gradient, the turbulence levels in these regions are substantial. Areas of zero shear do not generally correspond to areas of zero turbulent kinetic energy. These facts are not consistent with eddy viscosity modeling schemes (Durao and Whitelaw, 1978). Concerning general trends in the relations, the data for no fuel jet generally match the nonreacting nitrogen fuel jet

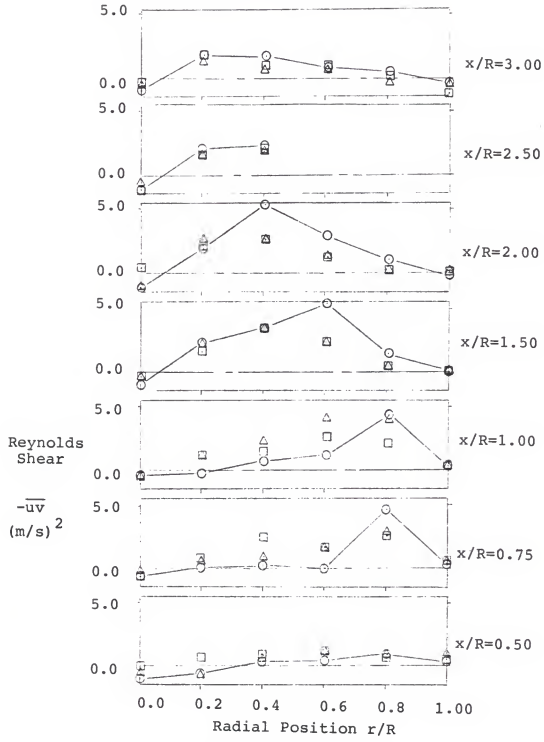

Figure 27. Radial profiles of Reynolds shear stress at seven axial locations.
⊙ Propene, a/f=6000
△ Nitrogen, a/f=400
⊡ No fuel jet

data more closely than the reacting case, again indicating the predominance of energy release effects over purely fluid mechanical influences.

The maximum shear is approximately 2.5 percent of the squared inlet velocity, which compares closely with the nonreacting results of Leder (1985) behind a flat plate with a splitter, and is an order of magnitude lower than Leder's value behind the same plate without a splitter in the separated flow region. Moreau and Boutier observed no significant shear stress in their evaluation, Yoshida noted a slight increase in shear through the reacting region, and Cheng and Ng saw a sharp increase, all of these in premixed, reacting systems. The geometry arguments which apply to the interpretation of the individual turbulent components also apply to the cross-correlations. Durao and Whitelaw show low shears near the centerline, then positive in the recirculation zone, and negative downstream. This shows some agreement, although the referenced data shows an earlier transition to negative values and much larger areas of negative shear.

Other evidence of the extent of correlation between the velocity fluctuations is indicated in Figure 28. The correlation coefficient $-\overline{uv}/(u'v')$ is seen to have a fairly low magnitude along the centerline and in the unseparated regions which are dominated by undisturbed flow from the annulus. This is indicative of generally random, or uncorrelated, turbulence, as also reflected by the low shear

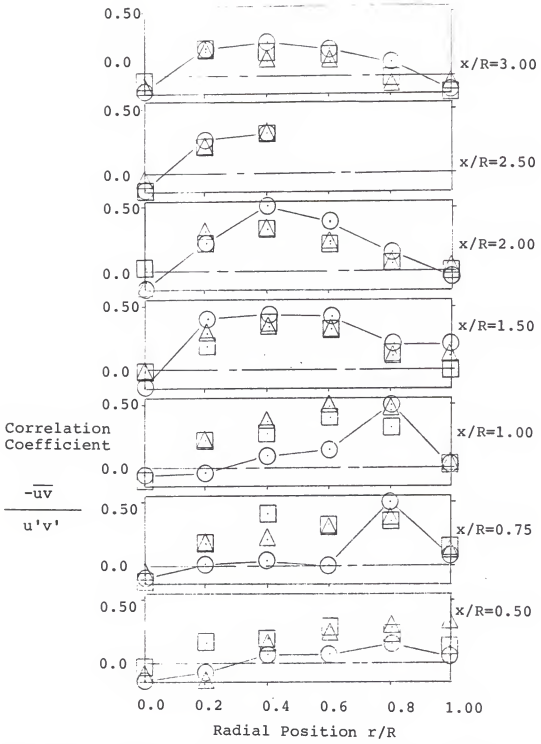

Figure 28. Radial profiles of correlation coefficient at seven axial locations. Symbol size represents uncertainty.
⊙ Propene, a/f=6000
△ Nitrogen, a/f=400
⊡ No fuel jet

values in these areas. Within the recirculation zone, the coefficient trends to higher values, indicating some correlation to the turbulent fluctuations.

Although the effect of the reaction on this parameter is not strongly defined, there is some indication that combustion may increase the correlation near the flame front and in the immediate downstream regions, but some nonreacting flow regions show correlations nearly as high as the maximum value of 0.5 observed in the reacting case. The uncertainty level for the correlation coefficient is relatively high due to accumulation of errors in the three terms required for its calculation, making strong arguments from this presentation of the data difficult to make.

The indicated increase in correlation near the reaction zone may be partially a result of flame front intermittency, where motion of the flame front would influence the flow in a manner exhibiting high correlation, but more akin to unsteady flow than to small-scale turbulence. An inspection of time-dependent shear in the high correlation area near the flame front (Figure 29, which actually shows the velocity cross-correlation, or negative of shear) indicates a fairly random nature, with no obvious periodicity that might be associated with flame front motion. The PDF for this shear also shows no bimodal behavior (Figure 30). The observed correlation in this region cannot be entirely attributed to the presence of the reaction, as the

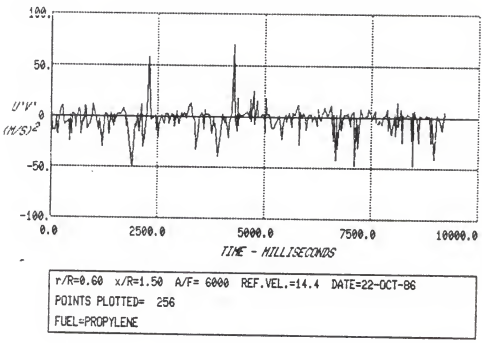

Figure 29. Velocity cross-correlation near flame front as a function of run time.

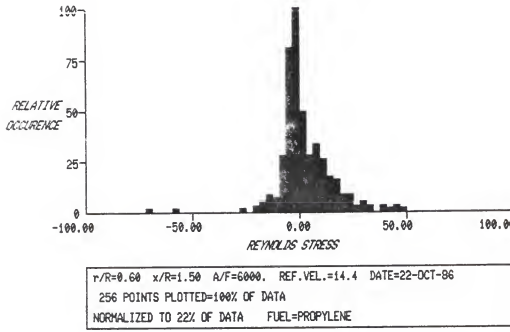

Figure 30. Probability distribution for Reynolds shear near flame front.

nonreacting cases show somewhat the same trend, although to a lesser degree.

The maximum correlation observed is not indicative of highly correlated fluctuations. Cheng and Ng measured values as high as 0.75 near the flame front in a rod stabilized, premixed flame, with the correlation coefficient reaching above 0.95 along the centerline of the wake. A recalculation of Yoshida's data produces correlation coefficients ranging from 0.28 to -0.20, with the highest value seen just downstream of the flame front of the Bunsen burner. The extent of correlation must also be interpreted considering the limits imposed by the correlation window in the data interface. The 1.2 msec processor coincidence time in effect for these experiments may randomize turbulence correlations occurring over shorter time scales, so the results presented should only be seen as indicative of trends in large-scale, low-frequency fluctuations. If the radius of the centerbody is taken as the relevant scale length, a reference velocity of 14 m/s corresponds to a characteristic flow frequency of approximately 500 Hz, implying that the coincidence time used should identify any large-scale fluctuations present.

Velocity Probability Density Functions

Typical velocity PDFs for propene at a/f=6000 are shown in Figures 31 through 36. It can be seen that the general form is that of a roughly Gaussian distribution, with no

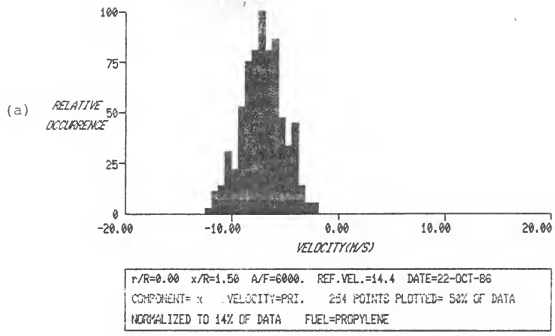

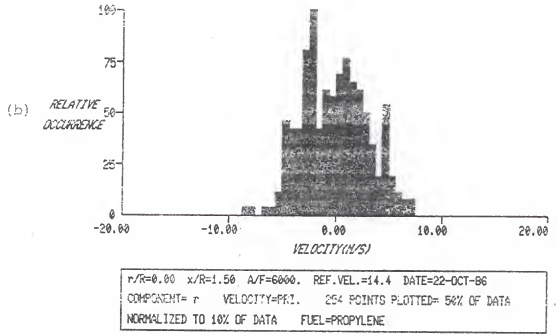

Figure 31. Velocity probability density functions at 1.50 radii downstream of centerbody face and r/R=0.00 for a) axial component and b) radial component.

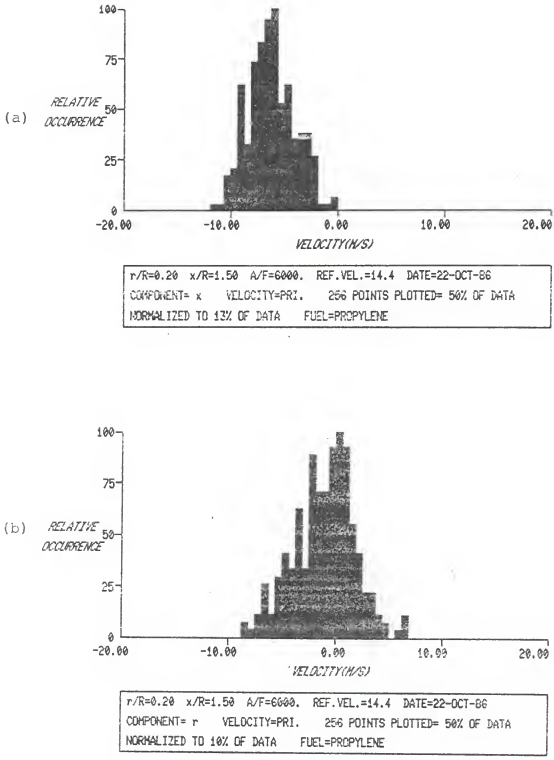

Figure 32. Velocity probability density functions at 1.50 radii downstream of centerbody face and r/R=0.20 for a) axial component and b) radial component.

(a)

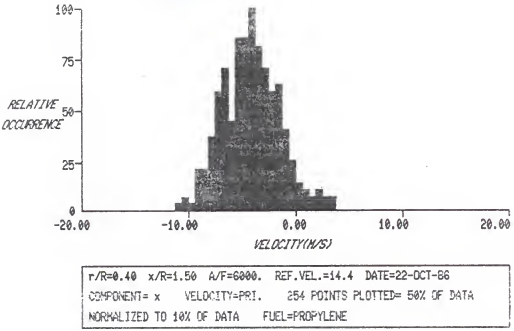

(b)

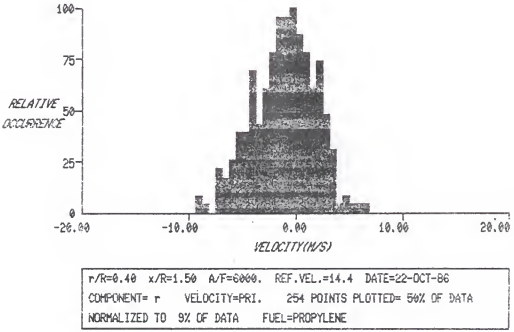

Figure 33. Velocity probability density functions at 1.50 radii downstream of centerbody face and r/R=0.40 for a) axial component and b) radial component.

(a)

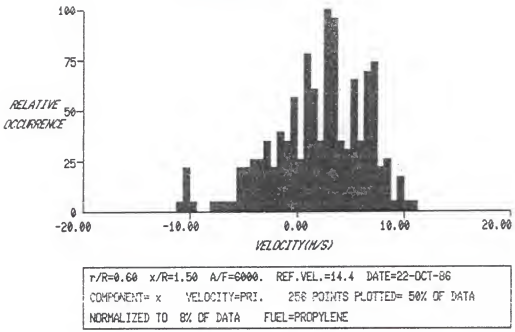

(b)

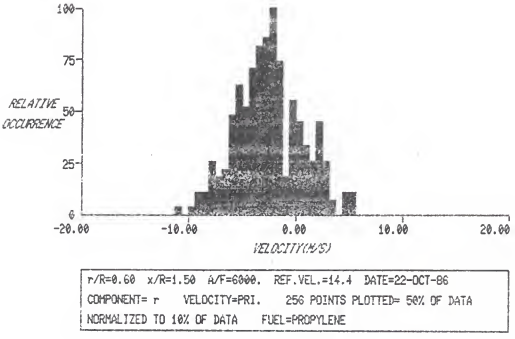

Figure 34. Velocity probability density functions at 1.50 radii downstream of centerbody face and r/R=0.60 for a) axial component and b) radial component.

(a)

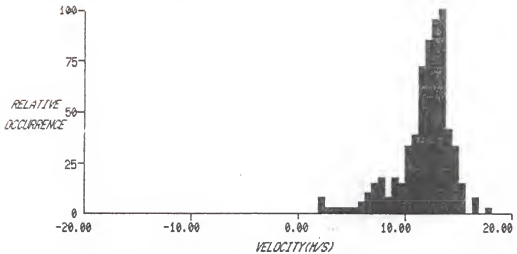

r/R=0.80 x/R=1.50 A/F=6000. REF.VEL.=14.4 DATE=22-OCT-86
COMPONENT= x VELOCITY=PRI. 247 POINTS PLOTTED= 50% OF DATA
NORMALIZED TO 15% OF DATA FUEL=PROPYLENE

(b)

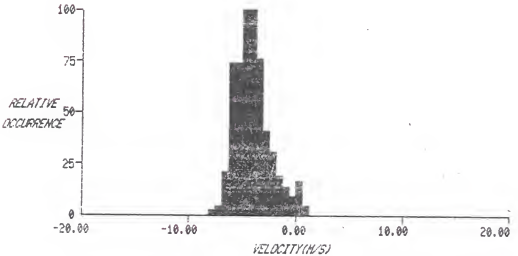

r/R=0.80 x/R=1.50 A/F=6000. REF.VEL.=14.4 DATE=22-OCT-86
COMPONENT= r VELOCITY=PRI. 247 POINTS PLOTTED= 50% OF DATA
NORMALIZED TO 17% OF DATA FUEL=PROPYLENE

Figure 35. Velocity probability density functions at 1.50 radii downstream of centerbody face and r/R=0.80 for a) axial component and b) radial component.

(a)

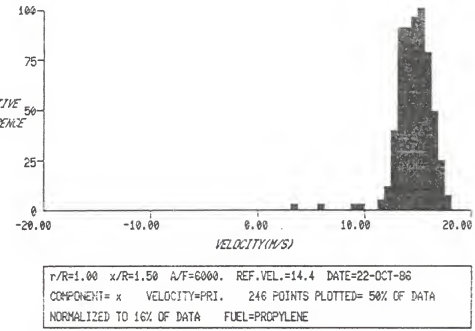

(b)

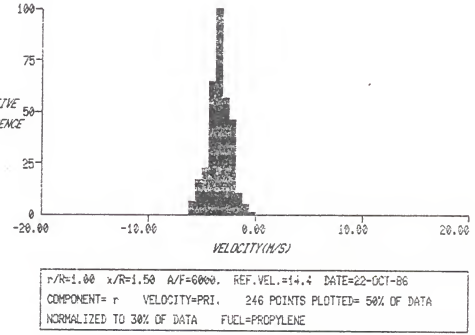

Figure 36. Velocity probability density functions at 1.50 radii downstream of centerbody face and r/R=1.00 for a) axial component and b) radial component.

apparent bimodality evident. (The small-scale structure seen in the distributions is due to the relatively small number of data points (256) being fit into 64 bins for these histograms. This limits the resolution of this type data presentation.)

The distributions are expectedly broader in areas of higher turbulence, and the axial components are generally broader than the radial near the reaction zone, consistent with the turbulence level plots. Similarly, the radial distributions are broader near the centerline stagnation point. The absence of bimodal distribution evidence, even in the regions of high shear and high correlation function, indicates no predominant frequency in any large-scale motion that may exist.

Some previous researchers have observed bimodality and attributed it to true unsteadiness (Durst et al., 1972), acoustic coupling with the exhaust duct (El Banhawy et al., 1983), or seeding abnormalities (Zimmerman, 1985). Gouldin et al. (1985), for example, observed low frequency oscillations (25 to 100 Hz) in swirling, reacting flows in a confined, coaxial jet system. These oscillations were not present in nonreacting tests and were attributed to periodic oscillations in the position of the reaction zone, driven by a coupling of mixing mechanisms with combustion-induced changes in the flowfield. No evidence for any of these phenomena is observed in the cases under study here. A

complete set of velocity PDFs throughout the flowfield for propylene at a/f=6000 are included as Appendix C.

Summary

The mean flowfield results qualitatively match the anticipated pattern. The fuel jet is stagnated early and flows radially outward along the face of the centerbody, where it mixes with the air in the recirculating vortex and begins reacting. For the range of fuel flows tested, the fluid mechanical effect of the centerline fuel jet is not a major contributor to the flow pattern. The effect of heat release is most influential when comparing nonreacting flows to flows with low heat release. Additional fuel flow does not alter the mean flowfield significantly.

Data obtained at high flows of sooting was affected adversely by the presence of the soot particles. Although the individual contributions of soot luminosity, probe volume overloading, and obscuration of the probe area were not separately identifiable, the intermittent nature of the soot arrival is evident and can be expected to bias the results in this type combustor. TBD-weighted mean velocities and fluctuations did not significantly differ from particle averages.

The turbulence in the separated region is nonisotropic and generally of a skewed Gaussian distribution. Average shear is relatively low, with an increase near the flame front in reacting flows. The shear PDFs are also much

broader in this region. Inspection of the data shows no bimodal relationships and no indication of large-scale periodicity.

CHAPTER VII
CONCLUSIONS AND RECOMMENDATIONS

Conclusions

A state-of-the-art, two-component, laser Doppler anemometer has been constructed, interfaced, and calibrated. Flexible data acquisition and analysis software has been written for this system, providing a wide range of computational options, including data storage, retrieval, filtering, weighting, statistical analysis, and plotting as a function of time or location. The hardware and software have been evaluated and applied to the acquisition of data in a difficult environment. This proven system now provides a facility with a sophisticated present and future capability for high-level fluid mechanical research.

The separated, reacting flowfield in the wake of a centerbody diffusion burner was mapped using this LDV system. The influence of differing statistical treatments of the acquired data was investigated. Three-sigma filtering of the velocity data sets was found to significantly affect only the calculation of axial velocity fluctuations in regions of the flow dominated by the annular air stream where erroneous data points were observed on velocity-time traces. TBD-weighted mean velocities and turbulence

fluctuations did not significantly vary from particle-weighted averages.

Data acquisition at high fuel flows was adversely affected by the presence of soot particles, although the individual contributions of soot luminosity, probe volume overloading and obscuration of the probe area were not separately identifiable. The intermittent nature of the soot arrival was evident and has the potential to bias the sampling in combustors of this type. In regions of relatively steady flow, such as the nonseparated annular area, this intermittency may have only a minor effect on mean velocity calculations, but in the unsteady wake region where the reaction is occurring, high soot loadings may significantly bias the data by preferentially rejecting those regions of the flow containing pockets of soot. This problem may be correctable with specialized operating parameters for the instrumentation system, such as polarization filtering, stricter verification limits, seeding modifications, and amplitude filtering.

Utilizing this fully-characterized hardware, software, and analysis system, mean flow patterns for nine different fuel conditions were evaluated and compared to qualitative predictions by other researchers, with good agreement. The fuel flow stagnates quickly downstream of the nozzle and flows radially outward along the centerbody face, where it continually mixes with the recirculating vortex gases and begins reacting. Reaction in this area is impeded, however,

by the cold surface of the centerbody face, as evidenced by a rapid soot buildup even when operating on natural gas. As a result, there is a possibility that the mixture in the shear zone, where the bulk of the reaction seems to occur, may be more closely approximated as premixed. Premixed results from other studies may be more relevant to this particular situation than coaxial jets or dump combustors where the flowfield/reaction zones are substantially different.

For the range of fuel flows tested, the fluid mechanical effect of the centerline fuel jet was found to be not a significant contributor to the overall flow pattern. Likewise, fuel chemistry did not influence the mean flowfield. The effect of heat release was found to be most significant when comparing nonreacting flows to flows with low heat release; the addition of fuel beyond the minimum required to sustain combustion did not substantially alter the mean flowfield.

The turbulence in the separated region was found to be nonisotropic and to generally display skewed Gaussian distributions. The presence of reaction has no significant influence on radial turbulence, but increases the axial level near the reaction region. Near the centerline stagnation point, the radial fluctuations are 75 percent greater than the axial fluctuations in both reacting and nonreacting cases. The average Reynolds shear is relatively

low, with an increase near the flame front in reacting flows.

Velocity-time plots, velocity PDF's, shear-time plots, and shear PDF's show no bimodal relationships and no indication of large-scale periodicity. The only evidence of nonrandom fluctuations is the increase in Reynolds shear and correlation coefficient near the flame front in reacting cases, but this correlation is not exceptionally large and may be due primarily to motion of the flame front. The nonisotropic nature of the turbulence, and the observed occurrence of zero shear in regions of nonzero turbulent kinetic energy, are generally inconsistent with eddy viscosity and k-e turbulence models.

A fully-developed instrumentation system has been used to verify the separated flow pattern, and to establish the mean velocities, turbulent fluctuations, turbulent correlations, and velocity probability density functions in a realistic, reacting environment. The data base necessary for evaluation of soot measurements and the development of enhanced modeling techniques in reacting flows in geometries applicable to gas turbine combustors is now available.

Recommendations for Further Study

As the fuel chemistry has been determined to be insignificant to the flowfield development and fuel rate is not a strong driver within the range of interest tested in this work, further testing should be confined to a single chemistry and a single, intermediate air-fuel ratio.

Additionally, a denser spatial matrix should be chosen to provide better spatial resolution of the observed properties of the flow. More data points should be recorded at each position to provide better statistical bases and to generate smoother probability density functions. The influence of varying annular air flow rates should also be investigated.

Unless a specific gas turbine type fuel nozzle is required for consistency with associated testing or to meet contract specifications, future investigations should utilize a straight cylindrical fuel exit geometry to make the results more directly comparable to related information in the literature.

Some expansions to the current instrumentation system could be incorporated to provide for correlated temperature measurement. This would provide the capability to generate density-velocity correlations necessary for momentum transport studies, and would also allow conditional sampling to be applied to the velocity data. Correlated velocity-temperature data would be very useful near the reaction region, enabling the researcher to determine the instantaneous location of the flame front and separate flame-front fluctuations from other unsteadiness in the flow. Improved analyses of the turbulent fluctuations and stresses in this region would follow.

Another modification that would prove useful is the installation of specialized signal processors to allow for velocity spectral analyses of the low rate, discrete data

generated by this type system. This would allow Fourier transform methods to be applied to the velocity data and would provide more information relevant to the identification of periodicity of any large-scale motion that may exist in the wake flow. Such processors are currently under development and should be available in the near future.

APPENDIX A
COMPUTER PROGRAMS

```
C   ROUTINE IMA.FOR
C   DATA TABULATION AND DISPLAY ROUTINE FOR TSI 1998 DATA PROCESSOR
C   MARCH 26, 1986
C
C
        DIMENSION JBUF(1200),JBUFC(14),FBUFC(14)
        EXTERNAL GTDMA,C1998
        INTEGER ERROR
        EQUIVALENCE (JBUFC,FBUFC)
C   INPUT SETUP DATA
1       WRITE(7,2)
2       FORMAT(//' THIS PROGRAM CONTPOLS DATA ACQUISITION',/,
     & ' FOR 256 DATA POINTS AND PERMITS OUTPUT',/,
     & ' TO SCREEN OR DISK FILE.',///)
C  FIX OPTION AND TYPE
        IOPTN=2
        ITYPE=1980
23      WRITE(7,25)
25      FORMAT(/,' ENTER THE NUMBER OF COUNTERS/DATA PT:',/,
     & '   RANDOM MODE = 1',/,'   COINCIDENCE MODE = NO. OF COUNTERS')
        READ(7,30)INUMB
30      FORMAT(I1)
        IF(INUMB.LT.1.OR.INUMB.GT.4)GO TO 23
C   CORRECT NUMBER OF CYCLES FOR MISTRANSFER FROM 1990 (HARDWARE PROBLEM)
        WRITE(7,21)
21      FORMAT(/,' ENTER NUMBER OF CYCLES COUNTED')
        READ(7,22)NCYCLC
22      FORMAT(I3)
C  INPUT BURNER TEST PARAMETERS
        WRITE(7,26)
26      FORMAT(/,' DO YOU WISH TO STORE TEST PARAMETERS? ( <Y> OR <N> )')
        READ(7,27)ITQ
27      FORMAT(A1)
        IF(ITQ.EQ.'N')GO TO 31
275     WRITE(7,28)
28      FORMAT(/,' INPUT CENTERLINE COORDINATES (X,Y),',
     & ' AIRFLOW (CFM), SHIFT@ (MHZ), & SHIFT1')
        READ(7,281,ERR=275) CX,CY,SCFM,SHF0,SHF1
281     FORMAT(5F)
        WRITE(7,29)
29      FORMAT(/,' ENTER FUEL TYPE (12 CHARACTERS MAX)')
        READ(7,24)IF1,IF2,IF3,IF4,IF5,IF6
        WRITE(7,299)
299     FORMAT(/,' ENTER DATE (DD-MMM-YY)')
        READ(7,24)ID1,ID2,ID3,ID4,ID5
24      FORMAT(6A2)
285     WRITE(7,288)
288     FORMAT(/,' ENTER TEST COORDINATES (X,Y), ELEVATION (mm), PHI')
        READ(7,289,ERR=285)TX,TY,ZZ,PHI
289     FORMAT(4F)
C   CONVERT TRANSLATION TABLE COORDINATES TO MILLIMETERS
        XX=(TX-CX)/1000.
        YY=(TY-CY)/1000.
C   NON-DIMENSIONALIZE BY CENTERBODY DIAMETER
        XR=XX/28.56
        YR=YY/28.56
        ZR=ZZ/28.56
31      CONTINUE
C  CALL DMA DRIVER ROUTINE. THIS ROUTINE LOADS A MAX OF 32K WORDS
C  INTO ARRAY JBUF.
C
```

```
      ERROR=0
32    WRITE(7,1223)
1223  FORMAT(' ENTERING DMA DRIVER ROUTINE',/)
      CALL GTDMA(JBUF,1280,ERROR)
      WRITE(7,1222)
1222  FORMAT(' SUCCESSFUL RETURN FROM DMA DRIVER ROUTINE',/)
      IF(ERROR.EQ.1)GO TO 230
33    WRITE(7,1224)
1224  FORMAT(' OUTPUT TO SCREEN  ==> 7',/,
     &  ' OUTPUT TO DISK ==> 2',/,' DUMP ==> D',/,' ?')
      READ(7,1225,ERR=230)LP
1225  FORMAT(I1)
      IF(LP.EQ.2)WRITE(7,34)
34    FORMAT(' FILE NAME?',/)
      IF(LP.EQ.2)CALL ASSIGN(2,'DUMMY',-1)
      IF(ITQ.EQ.'N')WRITE(LP,41)
41    FORMAT(//)
      IF(ITQ.EQ.'N')GO TO 35
      WRITE(LP,42)
42    FORMAT('   XR       YR       ZR    PHI    SCFM      SHF0'
     &  ,'   SHF1    FUEL      DATE  ')
      WRITE(LP,43)XR,YR,ZR,PHI,SCFM,SHF0,SHF1,
     &  IF1,IF2,IF3,IF4,IF5,IF6,ID1,ID2,ID3,ID4,ID5
43    FORMAT(3F8.3,F8.4,3F8.2,1X,6A2,1X,5A2)
35    WRITE(LP,40)
40    FORMAT('  ADDR / FREQ(MHZ) / N-CYCLE /     TIME     /',
     &' MODE / SYNC / TBD(MICROSEC)')
C
52    IWORDS=(INUMB*2)+1
60    IMAX=((512/INUMB)*IWORDS)
      IPOINT=0
C
      DO 225 II=1,IMAX,IWORDS
            CALL C1980(JBUF(II),JBUFC,IOPTN,INUMB,ITYPE)
            IPOINT=IPOINT+1
            I=1
            DO 150 JJ=1,INUMB
77                K=(I+5)/2
                  NCYCLE=JBUFC(I)
                  IADD=JBUFC(I+1)
                  IRC=JBUFC(I+2)
                  ISYNC=JBUFC(I+3)
                  I=I+6
80                TIME=FBUFC(K)
C     CORRECT TIME FOR 1990 PROCESSOR MIXED WITH 1980 SYSTEM
                  IF(IADD.EQ.0)TIME=TIME/2.0
                  IF(TIME.LT.1.0)TIME=1.0
C           CORRECT NO. OF CYCLES HERE FOR HARDWARE MALFUNCTION
                  NCYCLE=NCYCLC
                  FREQ=NCYCLE/TIME*1000.0
C           CHECK FOR GARBAGE DATA DUE TO 1938J MALFUNCTION
                  IF(IADD.GT.1.AND.LP.EQ.2)GO TO 999
                  IF(JJ.EQ.INUMB)GO TO 150
85                WRITE(LP,86)IADD,FREQ,NCYCLE,TIME,IRC,ISYNC
86                FORMAT(2X,I2,2X,'/',1X,F9.5,1X,'/',3X,I3,3X,
     &                 '/',F11.1,3X,'/',1X,I2,3X,'/',1X,I2,3X,'/')
150           CONTINUE
```

```
C
                TBD=FBUFC(K+1)
C   GENERATE DATA POINT NUMBER IN PLACE OF SYNC
                ISORN=IPOINT
                IF(ISYNC.EQ.1)ISORN=ISYNC
                WRITE(LP,180)IADD,FREQ,NCYCLE,TIME,IRC,ISORN,TBD
180             FORMAT(2X,I2,2X,'/',1X,F9.5,1X,'/',3X,I3,3X,'/',
     &          F11.1,3X,'/',1X,I2,3X,'/',1X,I4,1X,'/',F10.1)
225     CONTINUE
C
        GO TO 228
999     WRITE(7,990)
990     FORMAT(' INCORRECT DATA DETECTED')
228     REWIND LP
        IF(LP.EQ.2)CALL CLOSE(2)
230     WRITE(7,235)
235     FORMAT('$ <P>rinter,<N>ew data,<R>eenter,<M>enu,<S>tore- ')
        READ(7,250)INEXT
250     FORMAT(1A1)
        IF(LP.EQ.6)CALL CLOSE(6)
        IF(INEXT.EQ.'P')GO TO 260
        IF(INEXT.EQ.'N')GO TO 285
        IF(INEXT.EQ.'R')GO TO 1
        IF(INEXT.EQ.'M')GO TO 300
        IF(INEXT.EQ.'S')GO TO 33
        GO TO 230
260     LP=6
        OPEN(UNIT=6,CARRIAGECONTROL='FORTRAN')
        GO TO 35
300     CALL CLOSE(2)
        END
```

EXAMPLE FREQUENCY OUTPUT FILE FROM ROUTINE DMA.FOR

XR	YR	ZR	PHI	SCFM	SHF0	SHF1	FUEL	DATE
1.000	0.000	2.000	0.0280	76.50	-10.00	10.00	PROPYLENE	17-MAR-87
ADDR	FREQ(MHZ)	N-CYCLE		TIME	MODE	SYNC	TSD(MICROSEC)	
1	10.58201	8		756.0	0	0		
0	18.47575	8		433.0	0	1	262080.0	
1	10.95830	8		730.0	0	0		
0	17.69912	8		452.0	0	2	1216.0	
1	10.72386	8		746.0	0	0		
0	19.13876	8		418.0	0	3	1088.0	
1	11.20448	8		714.0	0	0		
0	18.09955	8		442.0	0	4	6016.0	
1	10.75269	8		744.0	0	0		
0	18.22324	8		439.0	0	5	3904.0	
1	11.14206	8		718.0	0	0		
0	18.18182	8		440.0	0	6	8192.0	
1	10.25641	8		780.0	0	0		
0	17.42919	8		459.0	0	7	640.0	
1	10.92896	8		732.0	0	0		
0	17.81737	8		449.0	0	8	18880.0	
1	11.17318	8		716.0	0	0		
0	18.64802	8		429.0	0	9	12800.0	
1	11.36364	8		704.0	0	0		
0	18.60465	8		430.0	0	10	3968.0	
1	10.72386	8		746.0	0	0		
0	19.60784	8		408.0	0	11	896.0	
1	10.92896	8		732.0	0	0		
0	17.85714	8		448.0	0	12	4608.0	
1	10.28278	8		778.0	0	0		
0	18.69159	8		428.0	0	13	5504.0	
1	11.23596	8		712.0	0	0		
0	16.73640	8		478.0	0	14	3600.0	
1	10.41667	8		768.0	0	0		
0	15.44402	8		518.0	0	15	15104.0	
1	11.56069	8		692.0	0	0		
0	17.85714	8		448.0	0	16	256.0	
1	11.04972	8		724.0	0	0		
0	13.32367	8		414.0	0	17	45312.0	
1	10.55409	8		758.0	0	0		
0	18.08465	8		430.0	0	18	832.0	
1	10.89918	8		734.0	0	0		
0	17.54386	8		456.0	0	19	3968.0	
1	10.63830	8		752.0	0	0		
0	19.00238	8		421.0	0	20	5952.0	

```
C     ROUTINE MASCON.FOR
C     FREQUENCY TO VELOCITY CONVERSION ROUTINE
C     FOR SEQUENCE OF FILES, FOR UNATTENDED CONVERSIONS
          DIMENSION IIN(10),IOUT(10)
          WRITE(7,20)
20        FORMAT(' THIS ROUTINE READS LIST OF INPUT AND OUTPUT',/,
     & ' FILE NAMES FROM DISK, CALCULATES VELOCITIES FOR EACH POINT,',/,
     & ' AND WRITES OUTPUT TO NEW DISK FILES.',///,
     & ' ENTER NAME OF FILE CONTAINING I/O FILE NAMES',/)
          CALL ASSIGN(4,'DUMMY',-1)
          WRITE(7,222)
222       FORMAT(/,' DO YOU WANT AUTOTRANSFER TO SERIAL PORT?',/)
          READ(7,226)KTRANS
226       FORMAT(A1)
          IF(KTRANS.EQ.'Y')CALL ASSIGN(6,'LS:')
C     READ DIRECTORY OF INPUT AND OUTPUT FILES
C     AND REPEAT IN LOOP TO END OF PROGRAM
          DO 1000 KK=1,100
21        READ(4,800,END=1010)(IIN(J),J=1,10),(IOUT(J),J=1,10)
800       FORMAT(10A2,T25,10A2)
          WRITE(7,801)(IIN(J),J=1,10),(IOUT(J),J=1,10)
801       FORMAT(1X,10A2,T17,10A2,/)
          OPEN(UNIT=2,NAME=IIN,TYPE='OLD',READONLY)
          READ(2,24,ERR=750)JXX,XR,YR,ZR,PHI,SCFM,SHF0,SHF1,
     &  IF1,IF2,IF3,IF4,IF5,IF6,ID1,ID2,ID3,ID4,ID5
24        FORMAT(T4,A1,/,3F8.3,F8.4,3F8.2,1X,6A2,1X,5A2)
          IF(JXX.EQ.'X')GO TO 100
750       WRITE(7,26)IIN
26        FORMAT(/,' ERROR IN FILE ',A8)
          CLOSE(UNIT=2)
          GO TO 21
100       OPEN(UNIT=3,NAME=IOUT,TYPE='NEW')
C
C     SKIP TITLE LINE IN DATA FILE
          READ(2,28)JUNK
28        FORMAT(A1)
          WRITE(3,110)
          IF(KTRANS.EQ.'Y')WRITE(6,110)
110       FORMAT('   X/R      Y/R      Z/R   PHI    SCFM      SHF0'
     &  ,'   SHF1    FUEL      DATE ')
          WRITE(3,112)XR,YR,ZR,PHI,SCFM,SHF0,SHF1,
     &  IF1,IF2,IF3,IF4,IF5,IF6,ID1,ID2,ID3,ID4,ID5
          IF(KTRANS.EQ.'Y')WRITE(6,112)XX,YY,ZZ,PHI,SCFM,SHF0,SHF1,
     &  IF1,IF2,IF3,IF4,IF5,IF6,ID1,ID2,ID3,ID4,ID5
112       FORMAT(3F8.3,F8.4,3F8.2,1X,6A2,1X,5A2)
          WRITE(3,114)
          IF(KTRANS.EQ.'Y')WRITE(6,114)
114       FORMAT('  ADDR /   FREQ(MHZ)  / VELOCITY1 / VELOCITY2 /   TBD  '
     &  ,'  /   RUN TIME   /')
          RTIME=0.0
C
C     LOOP READS SINGLE DATA POINT, CALCULATES VELOCITIES,
C     AND OUTPUTS TO DISK FILE
          DO 200 I=1,4096
                READ(2,122,END=220)JADD,FREQ,TBD
122             FORMAT(T4,I1,T8,F10.2,T60,F10.2)
```

```
C
C       DEFINE FRINGE SPACING
                IF(JADD.EQ.0)SPC=1.82
                IF(JADD.EQ.1)SPC=1.89
C       VFZ=VELOCITY FOR ZERO FREQUENCY; VSZ=VELOCITY IF SHIFT IS ZERO
                VFZ0=SPC*ABS(SHF0)
                VFZ1=SPC*ABS(SHF1)
                VSZ=SPC*FREQ
C       DEFINE TWO VELOCITIES FOR EACH COMPONENT, WITH VA BEING THE
C       PREFERRED RANGE OF OPERATION AND VB BEING ALSO POSSIBLE.
C       VELOCITIES IN THE SAME DIRECTION AS POSITIVE SHIFT ARE DEFINED
C       AS POSITIVE.  CALCULATE RUNNING TIME
C
                VFZ=VFZ0
                IF(JADD.EQ.1)VFZ=VFZ1
                VA=VFZ-VSZ
                VB=VFZ+VSZ
                IF(JADD.EQ.0.AND.SHF0.LT.0)VA=-VA
                IF(JADD.EQ.0.AND.SHF0.LT.0)VB=-VB
                IF(JADD.EQ.1.AND.SHF1.LT.0)VA=-VA
                IF(JADD.EQ.1.AND.SHF1.LT.0)VB=-VB
                IF(I.GT.2)RTIME=RTIME+TBD
                WRITE(3,132)JADD,FREQ,VA,VB,TBD,RTIME
                IF(KTRANS.EQ.'Y')WRITE(6,132)JADD,FREQ,VA,VB,TBD,RTIME
132             FORMAT(T4,I1,T8,4F12.4,F15.2)
200     CONTINUE
220     CONTINUE
C   CONVRT RUNTIME TO MILLISEC
        RTIME=RTIME/1000.
        WRITE(7,333)RTIME
333     FORMAT(' MAX RUN TIME (MILLISEC)=',F12.3)
        CLOSE(UNIT=2)
        CLOSE(UNIT=3)
        WRITE(7,990)(IIN(J),J=1,10),(IOUT(J),J=1,10)
990     FORMAT(' CONVERTED ',10A2,' TO ',10A2,/)
1000    CONTINUE
1010    CLOSE(UNIT=4)
        CALL CLOSE(6)
        END
```

EXAMPLE VELOCITY FILE, OUTPUT FROM ROUTINE MASCON.FOR

X/R	Y/R	Z/R	PHI	SCFM	SHF0	SHF1	FUEL	DATE
1.000	0.000	2.000	0.0030	76.50	-10.00	10.00	PROPYLENE	22-OCT-86
ADDR /	FREQ(MHZ)	/ VELOCITY1	/ VELOCITY2 /	TBD	/	RUN TIME	/	
1	11.0003	-2.0418	39.8418	0.0000		0.00		
0	18.6047	15.6605	-52.0605	65520.0000		0.00		
1	13.1147	-5.8869	43.6869	0.0000		0.00		
0	17.3160	13.3152	-49.7152	5696.0000		5696.00		
1	11.4286	-2.7000	40.5000	0.0000		5696.00		
0	18.7793	15.9784	-52.3784	14448.0000		20144.00		
1	11.1111	-2.1000	39.9000	0.0000		20144.00		
0	18.1818	14.8909	-51.2909	14528.0000		34672.00		
1	11.5942	-3.0130	40.8130	0.0000		34672.00		
0	19.5599	17.3990	-53.7990	21632.0000		56304.00		
1	11.2045	-2.2765	40.0765	0.0000		56304.00		
0	19.2308	16.8000	-53.2000	31968.0000		88272.00		
1	11.4613	-2.7619	40.5619	0.0000		88272.00		
0	17.8971	14.3727	-50.7727	55216.0000		143488.00		
1	10.6992	-1.6995	39.4995	0.0000		143488.00		
0	19.6560	17.5740	-53.9740	44608.0000		188096.00		
1	11.5607	-2.9497	40.7497	0.0000		188096.00		
0	17.8174	14.2276	-50.6276	2176.0000		190272.00		
1	10.5820	-1.1000	38.9000	0.0000		190272.00		
0	18.7793	15.9784	-52.3784	9088.0000		199360.00		
1	10.8108	-1.5324	39.3324	0.0000		199360.00		
0	19.8511	17.9290	-54.3290	2272.0000		201632.00		
1	10.4167	-0.7875	38.5875	0.0000		201632.00		
0	17.1674	13.0446	-49.4446	848.0000		202480.00		
1	11.1732	-2.2173	40.0173	0.0000		202480.00		
0	17.7384	14.0838	-50.4838	6480.0000		208960.00		
1	10.8401	-1.5878	39.3878	0.0000		208960.00		
0	18.9125	16.2208	-52.6208	34720.0000		243680.00		
1	11.2994	-2.4559	40.2559	0.0000		243680.00		
0	19.4175	17.1398	-53.5398	3440.0000		247120.00		
1	11.2360	-2.3360	40.1360	0.0000		247120.00		
0	17.3913	13.4522	-49.8522	32096.0000		279216.00		
1	10.5820	-1.1000	38.9000	0.0000		279216.00		
0	17.9775	14.5191	-50.9191	65520.0000		344736.00		
1	11.0803	-2.0418	39.8418	0.0000		344736.00		
0	17.6991	14.0124	-50.4124	24768.0000		369504.00		
1	12.0120	-3.8027	41.8027	0.0000		369504.00		
0	18.4757	15.4259	-51.8259	7584.0000		377088.00		
1	11.7647	-3.3353	41.1353	0.0000		377088.00		
0	14.8148	8.7630	-45.1630	3680.0000		380768.00		

```
C
C   ROUTINE MASTAT.FOR
C
C   VELOCITY STATISTICS ROUTINE CALCULATES MEANS AND DEVIATIONS WITH TBD
C   WEIGHTING AS AN OPTION.  THIS VERSION READS INPUT DATA FILE NAMES
C   FROM A SEPARATE FILE, CALCULATES MEAN VELOCITIES, DEVIATIONS, AND
C   REYNOLDS STRESSES.  FILTERING OF THE INPUT DATA AT 3 SIGMA LIMITS
C   IS ALSO AVAILABLE, WITH OUTPUT TO A NEW FILTERED FILE.
C   WRITTEN BY LARRY ROE, APRIL 1987.
C
C   VARIABLE CODE: FIRST LETTER <V>elocity, <A>verage, <T>urbulence
C      SECOND LETTER  A=PRIMARY VALUE, B=SECONDARY VALUE
C      THIRD CHARACTER - PROCESSOR ADDRESS, 0 FOR VERTICAL, 1 FOR HORIZ.
C
       DIMENSION VA0(2048),VA1(2048),TBD(2048)
       DIMENSION IIN(10),IOUT(10),IFOUT(10)
       REAL LLIM0,LLIM1
       OPEN(UNIT=33,NAME='DM0:STATS.OUT',TYPE='NEW')
       WRITE(7,25)
25     FORMAT(' THIS VERSION CALCULATES PRIMARY VELOCITIES ONLY.',/,
     & ' ENTER FILE NAME FOR INPUT DATA SETS',/)
       CALL ASSIGN(10,'DUMMY',-1)
       WRITE(7,26)
26     FORMAT(' ENTER FILE NAME FOR OUTPUT REYNOLDS STRESS DATA SETS',/)
       CALL ASSIGN(11,'DUMMY',-1)
C   QUERY FOR 3 SIGMA FILTERING OF INPUT DATA
       WRITE(7,27)
27     FORMAT(' DO YOU WANT 3 SIGMA FILTERING OF DATA?')
       READ(7,28)ISIG
28     FORMAT(A1)
       IF(ISIG.NE.'Y')GO TO 33
       WRITE(7,22)
22     FORMAT(' ENTER FILE NAME FOR FILTERED OUTPUT VEL DATA SETS',/)
       CALL ASSIGN(12,'DUMMY',-1)
C   QUERY FOR TBD WEIGHTING
33     WRITE(7,30)
30     FORMAT(' DO YOU WANT TBD WEIGHTING OF ALL PARAMETERS?')
       READ(7,28)ITBD
C   READ FILE NAMES, PROCESS DATA, CLOSE FILES, AND LOOP
       DO 1000 KK=1,100
       READ(10,800,END=1010)(IIN(J),J=1,10)
800    FORMAT(T25,10A2)
       READ(11,801,END=1010)(IOUT(J),J=1,10)
801    FORMAT(10A2)
       OPEN(UNIT=13,NAME=IIN,TYPE='OLD',READONLY)
       OPEN(UNIT=14,NAME=IOUT,TYPE='NEW')
C   SKIP FIRST LINE OF DATA FILE, REENTER IF NOT FOUND
       READ(13,162,ERR=750)JXX
162    FORMAT(A1)
C   READ TEST PARAMETERS
       READ(13,164)XR,YR,ZR,PHI,SCFM,SHF0,SHF1,
     &  IF1,IF2,IF3,IF4,IF5,IF6,ID1,ID2,ID3,ID4,ID5
       WRITE(14,164)XR,YR,ZR,PHI,SCFM,SHF0,SHF1,
     &  IF1,IF2,IF3,IF4,IF5,IF6,ID1,ID2,ID3,ID4,ID5
164    FORMAT(3F8.3,F8.4,3F8.2,1X,6A2,1X,5A2)
       READ(13,166)JUNK
166    FORMAT(A1)
168    SUM=0.0
```

```
C   CALCULATE REFERENCE VELOCITY FROM SCFM
        RV=0.1878*SCFM
        IF(RV.EQ.0.0)RV=0.001
C   SET PARAMETER TO TRACK MAX TBD VALUE TO CHECK FOR CLOCK OVERFLOW
        TBDMAX=0.0
C   WRITE FILE NAME
        WRITE(7,990)(IIN(J),J=1,10)
990     FORMAT(T3,10A2,/)
C
C   LOOP READS DATA POINTS, STORES IN FOUR ARRAYS
        DO 375 JJ=1,2048
                READ(13,163,END=376)JADD1,VA1(JJ),VB1
                READ(13,163,END=376)JADD0,VA0(JJ),VB0,TBD(JJ),RTIME
163             FORMAT(T4,I1,T20,3F12.4,F15.2)
                IF(TBD(JJ).GT.TBDMAX.AND.JJ.GT.1)TBDMAX=TBD(JJ)
                N=JJ
                IF(JADD1.NE.1.OR.JADD0.NE.0)GO TO 749
375     CONTINUE
376     CONTINUE
C   SET TBD FOR FIRST POINT EQUAL TO AVERAGE TBD
        TBD(1)=RTIME/N
C   CALCULATE AVERAGE DATA RATE IN HZ
        RATE=1000000./TBD(1)
C   SET UP FILTERING LIMITS FOR FIRST PASS
        HLIM1=1.0E+06
        HLIM0=1.0E+06
        LLIM1=-1.0E+06
        LLIM0=-1.0E+06
C   SUM VELOCITIES AND RUNTIME
388     SUM1=0.0
        RTIME=0.0
        SUM0=0.0
        JR=0
        DO 410 I=1,N
                IF(VA1(I).GT.HLIM1.OR.VA1(I).LT.LLIM1)GO TO 409
                IF(VA0(I).GT.HLIM0.OR.VA0(I).LT.LLIM0)GO TO 409
                RTIME=RTIME+TBD(I)
                JR=JR+1
                IF(ITBD.NE.'Y')SUM1=SUM1+VA1(I)
                IF(ITBD.NE.'Y')SUM0=SUM0+VA0(I)
                IF(ITBD.EQ.'Y')SUM1=SUM1+VA1(I)*TBD(I)
                IF(ITBD.EQ.'Y')SUM0=SUM0+VA0(I)*TBD(I)
409             CONTINUE
410     CONTINUE
C   CALCULATE AVERAGES
        AVC0=SUM0/JR
        AVC1=SUM1/JR
        IF(ITBD.EQ.'Y')AVC0=SUM0/RTIME
        IF(ITBD.EQ.'Y')AVC1=SUM1/RTIME
C   CALCULATE DEVIATIONS AND SUM
        SUMRE=0.0
        SUM0=0.0
        SUM1=0.0
        RTIME=0.0
        DO 420 I=1,N
                IF(VA1(I).GT.HLIM1.OR.VA1(I).LT.LLIM1)GO TO 420
                IF(VA0(I).GT.HLIM0.OR.VA0(I).LT.LLIM0)GO TO 420
                DEV1=AVC1-VA1(I)
                DEV0=AVC0-VA0(I)
                RTIME=RTIME+TBD(I)
                REN=DEV1*DEV0
```

```
                WRITE(14,44)REN,TBD(I)
44              FORMAT(2F20.5)
                IF(ITBD.NE.'Y')SUM1=SUM1+DEV1*DEV1
                IF(ITBD.NE.'Y')SUM0=SUM0+DEV0*DEV0
                IF(ITBD.NE.'Y')SUMRE=SUMRE+REN
                IF(ITBD.EQ.'Y')SUM1=SUM1+DEV1*DEV1*TBD(I)
                IF(ITBD.EQ.'Y')SUM0=SUM0+DEV0*DEV0*TBD(I)
                IF(ITBD.EQ.'Y')SUMRE=SUMRE+REN*TBD(I)
420     CONTINUE
C
C   DEVIATION=SQRT OF AVERAGE OF SQUARED DEVIATIONS FROM MEAN
        T1=SQRT((SUM1)/JR)
        T0=SQRT((SUM0)/JR)
        STRES=-SUMRE/JR
        IF(ITBD.EQ.'Y')T1=SQRT((SUM1)/RTIME)
        IF(ITBD.EQ.'Y')T0=SQRT((SUM0)/RTIME)
        IF(ITBD.EQ.'Y')STRES=-SUMRE/RTIME
C   RERUN STATISTICS ONCE IF FILTERING
        IF(ISIG.NE.'Y')GO TO 422
        IF(HLIM1.NE.1.0E+06)GO TO 422
        HLIM1=AVG1+3.0*T1
        LLIM1=AVG1-3.0*T1
        HLIM0=AVG0+3.0*T0
        LLIM0=AVG0-3.0*T0
        GO TO 388
C   CALCULATE CORRELATION COEFFICIENT
422     CC=STRES/T1/T0
        WRITE (7,20)
20      FORMAT('    XMEAN     XDEV    ZMEAN',
     &  '      ZDEV   STRESS  CORRELL  RATE     MAX TBD     POINTS')
        WRITE(7,560)AVG1,T1,AVG0,T0,STRES,CC,RATE,TBDMAX,N,JR
        WRITE(33,560)AVG1,T1,AVG0,T0,STRES,CC,RATE,TBDMAX,N,JR
560     FORMAT(7F9.3,F12.0,2I5/)
        IF(ISIG.NE.'Y')GO TO 750
C   READ AND WRITE OUT NEW FILTERED DATA FILE HERE
        READ(12,802)(IFOUT(J),J=1,10)
802     FORMAT(T50,10A2)
        OPEN(UNIT=15,NAME=IFOUT,TYPE='NEW')
        WRITE(15,473)
473     FORMAT('   r/R       y/R       x/R   PHI    SCFM     SHF0'
     &  ,'   SHF1    FUEL        DATE ')
        WRITE(15,164)XR,YR,ZR,PHI,SCFM,SHF0,SHF1,
     &  IF1,IF2,IF3,IF4,IF5,IF6,ID1,ID2,ID3,ID4,ID5
        WRITE(15,733)
733     FORMAT('  ADDR /   FREQ(MHZ)  / VELOCITY1 / VELOCITY2 /   TBD '
     &  ,'  /   RUN TIME   /')
        RTIME=0.0
        DO 700 I=1,N
                IF(VA1(I).GT.HLIM1.OR.VA1(I).LT.LLIM1)GO TO 709
                IF(VA0(I).GT.HLIM0.OR.VA0(I).LT.LLIM0)GO TO 709
                RTIME=RTIME+TBD(I)
                WRITE(15,163)JADD1,VA1(I),VB1
                WRITE(15,163)JADD0,VA0(I),VB0,TBD(I),RTIME
709             CONTINUE
700     CONTINUE
```

```
      GO TO 750
749   WRITE(7,165)
165   FORMAT(' OUT OF SEQUENCE DATA SET')
750   CLOSE(UNIT=14)
      IF(ISIG.EQ.'Y')CLOSE(UNIT=15)
      CLOSE(UNIT=13)
1000  CONTINUE
1010  CONTINUE
      CLOSE(UNIT=10)
      CLOSE(UNIT=33)
      CLOSE(UNIT=11)
      IF(ISIG.EQ.'Y')CLOSE(UNIT=12)
      STOP
      END
```

```
C
C   ROUTINE GRAPHV.FOR
C   GRAPHICS SUBROUTINE USING TSI VERSION 02.5 BIN SYSTEM
C   MAJOR MODIFICATIONS AND REGIS ROUTINES ADDED BY LARRY ROE
C   THIS VERSION NORMALIZES BINS TO MAX BIN TO GO FULL SCALE ON PLOTS
        SUBROUTINE GRAPHV
        DIMENSION BIN(64),IBIN(65),LOUT(64),TERM(8)
        DOUBLE PRECISION IV,ICOMP
        WRITE (7,20)
20      FORMAT(' THIS ROUTINE PLOTS A HISTOGRAM FROM DATA ON DISK ',//)
22      WRITE(7,25)
25      FORMAT(' ENTER FILE NAME',/)
        CALL ASSIGN(2,'DUMMY',-1)
        WRITE(7,130)
130     FORMAT(/,' ENTER THE PROCESSOR ADDRESS -  0, 1, OR 2 FOR BOTH')
        READ(7,135)IADD
135     FORMAT(I1)
145     CONTINUE
C   SKIP FIRST LINE OF DATA FILE, REENTER IF NOT FOUND
        READ(2,162,ERR=750)JXX
162     FORMAT(A1)
        WRITE(7,150)
150     FORMAT(/,' ENTER THE UPPER LIMIT IN M/S')
        READ(7,155)FMAX
155     FORMAT(F10.2)
        WRITE(7,160)
160     FORMAT(/,' ENTER THE LOWER LIMIT IN M/S')
        READ(7,165)FMIN
165     FORMAT(F10.2)
C   INITIALIZE BINS TO ZERO
195     DO 200 J=0,64
        IBIN(J)=0
200     CONTINUE
C   SET UP BIN CONSTANT
        CONST=64/(FMAX-FMIN)
C   READ TEST PARAMETERS AND CHECK THAT THIS IS A VELOCITY FILE
        READ(2,164)XR,YR,ZR,PHI,SCFM,SHF0,SHF1,
     &  IF1,IF2,IF3,IF4,IF5,IF6,ID1,ID2,ID3,ID4,ID5
164     FORMAT(3F8.3,F8.4,3F8.2,1X,6A2,1X,5A2)
        READ(2,166)ISVEL
166     FORMAT(T25,A1)
        IF(ISVEL.EQ.'V')GO TO 168
        WRITE(7,167)
167     FORMAT(/,' NOT A VELOCITY FILE')
        CALL CLOSE (2)
        GO TO 22
168     IOUT=0
        IMAX=0
        ISAMP=0
C   CALCULATE REFERENCE VELOCITY FROM SCFM
        RV=0.1878*SCFM
C   PLOT PRIMARY OR SECONDARY VELOCITY CALCULATION, OR BOTH
        WRITE(7,171)
171     FORMAT(/,' ENTER <P> FOR PRIMARY VELOCITY VALUE'./.
     &  ' ENTER <S> FOR SECONDARY VELOCITY VALUE',/.
     &  ' ENTER <B> FOR BOTH COMPONENTS TOGETHER',/)
        READ(7,172)IPORS
172     FORMAT(A1)
```

```
C
C   LOOP READS DATA POINTS, SORTS BY COUNTER NUMBER AND VELOCITY
      DO 375 JJ=1,4096
               READ(2,163,END=376)JADD,VA,VB
163            FORMAT(T4,I1,T20,2F12.4)
               ISPL=JJ
               IF(IADD.EQ.2)GO TO 270
               IF(JADD.EQ.IADD)GO TO 270
               GO TO 375
270            CONTINUE
               FREQ=VA
               IF(IPORS.EQ.'S')FREQ=VB
               IF(FREQ.LT.FMIN.OR.FREQ.GT.FMAX)GO TO 374
               ISAMP=ISAMP+1
C   L = BIN NUMBER 1 TO 64
               L=INT(CONST*(FREQ-FMIN))
               IF(L.EQ.0)L=1
               IBIN(L)=IBIN(L)+1
               IF(IBIN(L).GT.IMAX)IMAX=IBIN(L)
374            CONTINUE
               IF(IPORS.NE.'B')GO TO 375
               FREQ=VB
               IF(FREQ.LT.FMIN.OR.FREQ.GT.FMAX)GO TO 375
               ISAMP=ISAMP+1
C   L = BIN NUMBER 1 TO 64
               L=INT(CONST*(FREQ-FMIN))
               IF(L.EQ.0)L=1
               IBIN(L)=IBIN(L)+1
               IF(IBIN(L).GT.IMAX)IMAX=IBIN(L)
375    CONTINUE
376    NORM=IMAX
C   IF NO SAMPLES WITHIN RANGE, WRITE WARNING AND RESCALE
      IF(ISAMP.GT.0)GO TO 377
      WRITE(7,3765)
3765   FORMAT(/,' NO DATA WITHIN THIS RANGE, RESCALE REQUIRED')
      GO TO 750
C   ISPC=PERCENTAGE OF DATA POINTS ACTUALLY PLOTTED
377    ISPC=INT((FLOAT(ISAMP)/FLOAT(ISPL))*100.)
C   JNRM=PERCENTAGE OF DATA POINTS REPRESENTED BY 100% ON HISTOGRAM
      JNRM=INT((FLOAT(IMAX)/FLOAT(ISAMP))*100.)
      IF(NORM.LT.1)NORM=1
C
C   BEGINNING OF REGIS PLOT ROUTINE
1000   DO 1020 I=1,64
      IBIN(I)=INT(FLOAT(IBIN(I))/FLOAT(NORM)*300.0)
1020   CONTINUE
      N=7
```

```
C
C   SET UP AXES
        WRITE(7,1120)
1120    FORMAT(' !S(E)W(R,I7,P1.N0,A0,S0')
        WRITE(7,1140)
1140    FORMAT(' !P[20,138]T(D0)(S1)(D0)(I-20)"RELATIVE"
     &  P[10,168]T"OCCURRENCE" ')
        WRITE(7,1130)
1130    FORMAT(' !P[125,8]V[,+300]V[+640]P[386,348]T(D0)(S1)(D0)
     &  (I-20) "VELOCITY(M/S)" ')
        WRITE(7,1150)
1150    FORMAT(' !P[105,300]T(S1)(I0)"0"P[95,225]T"25"P[95,150]
     &  T"50"P[95,75]T"75"P[85,0]T"100" ')
        A=FMIN
        E=FMAX
        IDIV=4.00
        B=(FMAX-FMIN)/IDIV+FMIN
        C=(FMAX-FMIN)*2.0/IDIV+FMIN
        D=(FMAX-FMIN)*3.0/IDIV+FMIN
        WRITE(7,1160)A,B,C,D,E
1160    FORMAT(' !P[-138,320]T(S1)"',3F18.2,2F17.2'"')
C   PUT TICK MARKS ON AXES
        WRITE(7,1170)
1170    FORMAT(' !P[125,8]V[-10]P[,+75]V[+10]P[,+75]V[-10]
     &  P[,+75]V[+10]P[+160,+75]V[,+10]P[+160]V[,-10]
     &  P[+160]V[,+10]P[+160]V[,-10]')
        WRITE(7,1175)
1175    FORMAT(' !P[125,308]W(S1)')
        DO 1100 I=1,64
                NN=IBIN(I-1)-IBIN(I)
                IF(NV.LT.0)WRITE(7,1040)NV
1040            FORMAT(' !V[,',I4,']V[+10]')
                IF(NV.GE.0)WRITE(7,1041)NV
1041            FORMAT(' !V[,+',I4,']V[+10]')
1100    CONTINUE
C
C  SET UP TEST INFO BLOCK
                PHI=6000.0
        WRITE(7,1200)
1200    FORMAT(' !P[125,388]W(S0)V[+640]V[,+90]V[-640]V[,-90]')
        WRITE(7,1210)XR,ZR,PHI,RV,ID1,ID2,ID3,ID4,ID5
1210    FORMAT(' !P[125,393]T" r/R=',F4.2,'  x/R=',F4.2,
     &  '  A/F=',F5.0,'  REF.VEL.=',F4.1,'  DATE=',5A2,'"')
        ICOMP='BOTH'
        IV='BOTH'
        IF(IADD.EQ.1)ICOMP='  '
        IF(IADD.EQ.0)ICOMP='  '
        IF(IPORS.EQ.'P')IV='PRI.'
        IF(IPORS.EQ.'S')IV='SEC.'
        WRITE(7,1220)ICOMP,IV,ISAMP,ISPC
1220    FORMAT(' !P[125,423]T" COMPONENT=',A4,'  VELOCITY=',A4,3X,
     &  I4,' POINTS PLOTTED=',I3,'% OF DATA"')
        WRITE(7,1230)JNRM,IF1,IF2,IF3,IF4,IF5,IF6
1230    FORMAT(' !P[125,453]T" NORMALIZED TO',
     &  I3,'% OF DATA     FUEL=',6A2,'"')
        READ(7,780)INJUNK
C   END OF REGIS PLOT ROUTINE
```

```
C
750     REWIND 2
        WRITE(7,775)
775     FORMAT(1X,'<A>ddress, <N>ew data, <R>eenter, <S>cale, ',
     &  '<M>enu -',$)
        READ(5,780)IN
780     FORMAT(1A1)
        IF(IN.EQ.'A')GO TO 790
        IF(IN.EQ.'N')GO TO 870
        IF(IN.EQ.'S')GO TO 845
        IF(IN.EQ.'R')GO TO 870
        GO TO 900
790     WRITE(7,795)
795     FORMAT(///,' ENTER NEW ADDRESS -',$)
        READ(5,796)IADD
796     FORMAT(I1)
        GO TO 145
845     CONTINUE
        GO TO 145
870     CALL CLOSE(2)
        GO TO 22
900     CALL CLOSE(2)
        RETURN
        END
```

```
C
C   ROUTINE TIMPLT.FOR
C   REGIS ROUTINE FOR TEMPORAL PLOTS
C   WRITTEN BY LARRY ROE, APRIL, 1986
C   THIS ROUTINE PLOTS VELOCITY VERSUS TIME, USING TBD INFO
        SUBROUTINE TIMPLT
        DOUBLE PRECISION ICOMP,IV
        WRITE (7,20)
20      FORMAT(' THIS ROUTINE PLOTS V VERSUS T FROM DATA ON DISK ',//)
22      WRITE(7,25)
25      FORMAT(' ENTER FILE NAME',/)
        CALL ASSIGN(2,'DUMMY',-1)
        WRITE(7,130)
130     FORMAT(/,' ENTER THE PROCESSOR ADDRESS -  0, 1, OR 2 FOR BOTH')
        READ(7,135)IADD
135     FORMAT(I1)
145     CONTINUE
C   SKIP TITLE LINE IN DATA FILE
        READ(2,162,ERR=750)JXX
162     FORMAT(A1)
        WRITE(7,150)
150     FORMAT(/,' ENTER THE MAX VELOCITY IN M/S')
        READ(7,155)VMAX
155     FORMAT(F10.2)
        WRITE(7,158)
158     FORMAT(/,' ENTER THE STARTING PLOT TIME IN MILLISECONDS')
        READ(7,155)TMINL
        WRITE(7,159)
159     FORMAT(/,' ENTER THE TERMINAL PLOT TIME IN MILLISECONDS')
        READ(7,155)TMAXL
C   SET UP PLOT SCALE AND CONVERT TIMES TO MICROSECONDS
        TMAX=TMAXL*1000.
        TMIN=TMINL*1000.
        XI=(TMAX-TMIN)/640.0
        YI=2.0*VMAX/300.0
C   READ TEST PARAMETERS AND CHECK THAT THIS IS A VELOCITY FILE
        READ(2,164)XR,YR,ZR,PHI,SCFM,SHF0,SHF1,
     &  IF1,IF2,IF3,IF4,IF5,IF6,ID1,ID2,ID3,ID4,ID5
164     FORMAT(3F8.3,F8.4,3F8.2,1X,6A2,1X,5A2)
        READ(2,166)ISVEL
166     FORMAT(T25,A1)
        IF(ISVEL.EQ.'V')GO TO 168
        WRITE(7,167)
167     FORMAT(/,' NOT A VELOCITY FILE')
        CALL CLOSE (2)
        GO TO 22
C   PLOT PRIMARY OR SECONDARY VELOCITY CALCULATION
168     WRITE(7,171)
169     WRITE(7,171)
171     FORMAT(/,' ENTER <P> FOR PRIMARY VELOCITY VALUE',/,
     &  ' ENTER <S> FOR SECONDARY VELOCITY VALUE',/)
        READ(7,172)IPORS
172     FORMAT(A1)
C   CALCULATE REFERENCE VELOCITY
        RV=0.1878*SCFM
C
C   SET UP AXES
        WRITE(7,1120)
1120    FORMAT(' !S(E)W(V,I7;P1,N0,A0,S0')
        WRITE(7,1140)
```

```
C
C   SCALES AND TITLES
1140    FORMAT(' !P[20,138]T(D0)(S1)(D0)(I-20)"VELOCITY"
     &  P[46,168]T"M/S"')
        WRITE(7,1130)
1130    FORMAT(' !P[386,348]T(D0)(S1)(D0)
     &  (I-20) "TIME - MILLISECONDS" ')
        A=-VMAX
        B=-VMAX/2.0
        C=VMAX/2.0
        D=VMAX
        WRITE(7,1150)A,B,C,D
1150    FORMAT(' !P[70,300]T(S1)(I0)"',F5.1,'"P[70,225]T"',
     &  F5.1,'"P[105,150]T"0"P[70,75]T"',F5.1,'"P[70,0]T"',F5.1,'"')
        A=TMINL
        E=TMAXL
        IDIV=4.00
        B=(TMAXL-TMINL)/IDIV+TMINL
        C=(TMAXL-TMINL)*2.0/IDIV+TMINL
        D=(TMAXL-TMINL)*3.0/IDIV+TMINL
        WRITE(7,1160)A,B,C,D,E
1160    FORMAT(' !P[-140,320]T(S1)"',3F18.1,2F17.1'"')
C   GRID LINES
        WRITE(7,1170)
1170    FORMAT(' !P[125,8]W(P4)V[+640]V[,+300]V[-640]V(W(P1))[,-300]
     &  P[,+75]V[+640]P[,+75]V(W(P1))[-640]P[,+75]V[+640]')
        WRITE(7,1171)
1171    FORMAT(' !P[285,8]V[,+300]P[+160]V[,-300]P[+160]V[,+300]')
        WRITE(7,1175)
1175    FORMAT(' !P[125,154]W(S0,P1)')
        N0=0
        TIME=0.0
        KK=0
        LL=0
374     CONTINUE
C
C   LOOP READS DATA POINTS, SORTS, AND  PLOTS
        DO 375 JJ=1,2048
                READ(2,163,END=376)JADD1,VA1,VB1,TBD1
                READ(2,163,END=376)JADD0,VA0,VB0,TBD0
163             FORMAT(T4,I1,T20,3F12.4)
                ISPL1=JJ
                IF(IADD.EQ.JADD1)GO TO 270
                JADD=JADD0
                V=VA0
                IF(IPORS.EQ.'S')V=VB0
                GO TO 280
270             CONTINUE
                JADD=JADD1
                V=VA1
                IF(IPORS.EQ.'S')V=VB1
280             CONTINUE
                TBD=TBD0
                IF(TBD1.GT.TBD0)TBD=TBD1
                IF(JJ.EQ.1)TBD=0.0
                TIME=TIME+TBD
```

```
C
C       SKIP DATA POINTS BEFORE START TIME OR AFTER STOP TIME
                IF(TIME.LT.TMIN)GO TO 375
                IF(TIME.GT.TMAX)GO TO 376
                KK=KK+1
C       SCALE AND PLOT VALUES
                NV=INT(V/YI)
                NY=N0-NV
                NX=INT(TBD/XI)
                IF(NX.EQ.0)NX=1
C       ESTABLISH OFFSET FOR FIRST DATA POINT
                IF(KK.GT.1)GO TO 286
                NX=INT((TIME-TMIN)/XI)
                IF(NY.LT.0)WRITE(7,282)NX,NY
282             FORMAT(' !PI+',I3,',',I4,'I')
                IF(NY.GE.0)WRITE(7,284)NX,NY
284             FORMAT(' !PI+',I3,',+',I4,'I')
                GO TO 300
C       PLOT REMAINING POINTS
286             CONTINUE
                IF(NY.LT.0)WRITE(7,288)NX,NY
288             FORMAT(' !VI+',I3,',',I4,'I')
                IF(NY.GE.0)WRITE(7,290)NX,NY
290             FORMAT(' !VI+',I3,',+',I4,'I')
300             N0=NV
375     CONTINUE
376     CONTINUE
C
C   RESET AND REPLOT IF PLOTTING BOTH COMPONENTS TOGETHER
C
        IF(IADD.NE.2)GO TO 2376
        REWIND 2
        READ(2,2350)K1,K2,K3
2350    FORMAT(A1,/,A1,/,A1)
        N0=0
        TIME=0.0
        LL=0
        WRITE(7,1175)
        DO 2375 JJ=1,2048
                READ(2,163,END=2376)JADD1,VA1,VB1,TBD1
                READ(2,163,END=2376)JADD0,VA0,VB0,TBD0
                JADD=JADD1
                V=VA1
                IF(IPORS.EQ.'S')V=VB1
                TBD=TBD0
                IF(TBD1.GT.TBD0)TBD=TBD1
                IF(JJ.EQ.1)TBD=0.0
                TIME=TIME+TBD
                IF(TIME.LT.TMIN)GO TO 2375
                IF(TIME.GT.TMAX)GO TO 2376
                LL=LL+1
                NV=INT(V/YI)
                NY=N0-NV
                NX=INT(TBD/XI)
                IF(NX.EQ.0)NX=1
                IF(LL.GT.1)GO TO 2860
                NX=INT((TIME-TMIN)/XI)
                IF(NY.LT.0)WRITE(7,2820)NX,NY
```

```
C
2820            FORMAT(' !PI+',I3,',',I4,'I')
                IF(NY.GE.0)WRITE(7,2840)NX,NY
2840            FORMAT(' !PI+',I3,',+',I4,'I')
                GO TO 3000
2860            CONTINUE
                IF(NY.LT.0)WRITE(7,2880)NX,NY
2880            FORMAT(' !V(W(P11100111))I+',I3,',',I4,'I')
                IF(NY.GE.0)WRITE(7,2900)NX,NY
2900            FORMAT(' !V(W(P11100111))I+',I3,',+',I4,'I')
3000            N0=NV
2375    CONTINUE
2376    CONTINUE
C
C  SET UP TEST INFO BLOCK
        WRITE(7,1200)
1200    FORMAT(' !PI125,383W(S0,P1\V(+640)V(,+90)V(-640)V(,-90)I')
        WRITE(7,1210)XR,ZR,PHI,RV,ID1,ID2,ID3,ID4,ID5
1210    FORMAT(' !PI125,393T" r/R=',F4.2,'  x/R=',F4.2,
     &  '  A/F=',F5.0,'  REF.VEL.=',F4.1,'  DATE=',5A2,'"')
        ICOMP='BOTH'
        IV='BOTH'
        IF(IADD.EQ.1)ICOMP=' r  '
        IF(IADD.EQ.0)ICOMP=' x  '
        IF(IPORS.EQ.'P')IV='PRI.'
        IF(IPORS.EQ.'S')IV='SEC.'
        ISAMP=KK+LL
        WRITE(7,1220)ICOMP,IV,ISAMP
1220    FORMAT(' !PI125,423T" COMPONENT=',A4,'  VELOCITY=',A4,3X,
     &  I4,' POINTS PLOTTED"')
        WRITE(7,1230)IF1,IF2,IF3,IF4,IF5,IF6
1230    FORMAT(' !PI125,453T" FUEL=',6A2,'"')
749     READ(7,780)INJUNK
C   END OF REPLOT
C
C
750     REWIND 2
        WRITE(7,775)
775     FORMAT(1X,'<A>ddress, <N>ew data, <R>eenter, <S>cale, <M>enu -',$)
        READ(5,780)IN
780     FORMAT(1A1)
        IF(IN.EQ.'A')GO TO 790
        IF(IN.EQ.'N')GO TO 870
        IF(IN.EQ.'S')GO TO 845
        IF(IN.EQ.'R')GO TO 870
        GO TO 900
790     WRITE(7,795)
795     FORMAT(///,' ENTER NEW ADDRESS -',$)
        READ(5,796)IADD
796     FORMAT(I1)
        GO TO 145
845     CONTINUE
        GO TO 145
870     CALL CLOSE(2)
        GO TO 22
900     CALL CLOSE(2)
        RETURN
        END
```

APPENDIX B
VELOCITY TABLES

VELOCITY DATA FOR NO FUEL JET.

x/R	r/R	U m/s	V m/s	Turbulence %
0.5	0.0	-4.70	0.51	12.72
0.5	0.2	-4.37	0.70	13.73
0.5	0.4	-2.30	1.24	14.85
0.5	0.6	-0.14	0.45	14.31
0.5	0.8	1.20	0.31	13.45
0.5	1.0	14.87	-2.09	17.68
0.75	0.0	-5.46	0.82	14.40
0.75	0.2	-5.02	0.16	14.62
0.75	0.4	-3.10	0.00	17.15
0.75	0.6	-0.46	0.18	16.07
0.75	0.8	4.43	-1.55	19.04
0.75	1.0	15.53	-3.18	16.96
1.0	0.0	-5.86	0.56	15.72
1.0	0.2	-5.03	-0.86	16.75
1.0	0.4	-2.89	-1.26	17.15
1.0	0.6	0.79	-1.62	18.13
1.0	0.8	8.62	-3.24	19.51
1.0	1.0	15.62	-3.58	13.02
1.5	0.0	-1.45	1.22	21.61
1.5	0.2	-1.59	-2.60	22.39
1.5	0.4	1.23	-4.37	21.38
1.5	0.6	6.94	-4.76	19.67
1.5	0.8	13.60	-4.71	14.74
1.5	1.0	14.70	-3.45	14.19
2.0	0.0	4.39	0.21	21.01
2.0	0.2	4.98	-2.15	21.39
2.0	0.4	7.42	-3.02	20.05
2.0	0.6	11.38	-3.51	16.98
2.0	0.8	13.68	-2.80	13.80
2.0	1.0	13.47	-1.63	15.68
2.5	0.0	8.63	0.40	18.52
2.5	0.2	9.34	-1.21	19.31
2.5	0.4	11.24	-1.53	15.65
3.0	0.0	10.26	0.28	20.46
3.0	0.2	10.62	-0.65	20.91
3.0	0.4	12.01	-0.90	16.35
3.0	0.6	13.78	-1.25	16.65
3.0	0.8	14.23	-0.61	16.65
3.0	1.0	12.23	0.07	18.24
4.0	0.0	11.43	0.00	15.52
4.0	0.2	12.08	-0.28	17.29
4.0	0.4	12.66	-0.56	19.87
4.0	0.6	13.72	-0.46	17.83
4.0	0.8	13.36	-0.06	15.59
4.0	1.0	11.55	0.51	19.13

VELOCITY DATA FOR NITROGEN AT A/F = 400.

x/R	r/R	U m/s	V m/s	Turbulence %
0.5	0.0	-1.42	0.89	19.38
0.5	0.2	-3.13	2.66	15.53
0.5	0.4	-2.78	2.68	15.70
0.5	0.6	-0.78	1.25	14.85
0.5	0.8	1.11	0.44	13.23
0.5	1.0	15.38	-2.04	14.16
0.75	0.0	-5.58	0.87	13.95
0.75	0.2	-4.55	0.55	14.02
0.75	0.4	-3.42	0.62	15.53
0.75	0.6	-1.21	0.63	16.47
0.75	0.8	3.80	-1.63	19.59
0.75	1.0	15.50	-2.70	12.12
1.0	0.0	-5.87	0.81	15.92
1.0	0.2	-5.09	0.05	16.45
1.0	0.4	-3.52	-0.63	18.04
1.0	0.6	0.12	-1.04	20.26
1.0	0.8	8.07	-3.27	20.90
1.0	1.0	15.74	-3.46	14.46
1.5	0.0	-2.14	1.18	20.62
1.5	0.2	-2.31	-1.79	21.40
1.5	0.4	0.94	-3.49	22.22
1.5	0.6	6.88	-4.34	20.72
1.5	0.8	13.12	-4.32	16.36
1.5	1.0	15.19	-3.49	11.19
2.0	0.0	3.71	0.75	20.62
2.0	0.2	4.61	-1.68	20.49
2.0	0.4	7.89	-3.32	19.68
2.0	0.6	11.37	-3.45	17.10
2.0	0.8	14.46	-2.79	11.67
2.0	1.0	13.97	-1.56	15.21
2.5	0.0	7.97	0.37	18.87
2.5	0.2	8.79	-1.48	19.25
2.5	0.4	10.69	-1.96	17.21
3.0	0.0	9.56	0.38	17.81
3.0	0.2	10.45	-0.47	17.60
3.0	0.4	12.03	-1.29	16.20
3.0	0.6	13.88	-1.27	17.07
3.0	0.8	14.29	-0.70	15.73
3.0	1.0	11.04	-0.19	19.28
4.0	0.0	11.87	-0.19	16.75
4.0	0.2	11.43	-0.34	19.86
4.0	0.4	12.58	-0.85	19.67
4.0	0.6	13.92	-0.64	16.19
4.0	0.8	12.88	-0.15	19.04
4.0	1.0	11.26	0.45	17.89

VELOCITY DATA FOR PROPENE AT A/F = 6000.

x/R	r/R	U m/s	V m/s	Turbulence %
0.5	0.0	-5.25	0.99	15.82
0.5	0.2	-5.20	1.23	17.94
0.5	0.4	-4.56	1.87	14.88
0.5	0.6	-3.73	1.94	15.97
0.5	0.8	-2.32	1.62	17.55
0.5	1.0	13.52	-1.55	21.71
0.75	0.0	-5.63	1.07	18.55
0.75	0.2	-4.68	2.04	18.93
0.75	0.4	-4.67	2.50	16.98
0.75	0.6	-3.16	2.37	16.02
0.75	0.8	1.16	-0.38	21.90
0.75	1.0	14.73	-1.88	18.63
1.0	0.0	-5.99	1.02	19.12
1.0	0.2	-5.39	1.89	17.05
1.0	0.4	-4.21	2.06	17.66
1.0	0.6	-2.97	2.20	18.75
1.0	0.8	6.92	-2.09	21.81
1.0	1.0	14.77	-2.18	19.93
1.5	0.0	-6.53	0.53	18.39
1.5	0.2	-5.70	-0.52	17.45
1.5	0.4	-3.70	-0.50	19.82
1.5	0.6	2.67	-1.96	26.38
1.5	0.8	11.63	-3.15	22.49
1.5	1.0	14.59	-2.83	21.95
2.0	0.0	-1.65	1.51	21.63
2.0	0.2	-1.48	-1.49	20.16
2.0	0.4	2.86	-3.84	22.10
2.0	0.6	8.90	-3.78	21.28
2.0	0.8	12.97	-3.18	25.42
2.0	1.0	14.43	-2.24	18.58
2.5	0.0	5.21	1.28	22.19
2.5	0.2	5.61	-1.93	19.55
2.5	0.4	7.96	-2.48	19.65
3.0	0.0	8.65	0.25	19.80
3.0	0.2	9.53	-1.53	19.66
3.0	0.4	10.60	-1.74	17.78
3.0	0.6	13.49	-1.56	15.04
3.0	0.8	14.79	-1.02	16.87
3.0	1.0	13.32	-0.48	15.17
4.0	0.0	11.18	0.28	17.20
4.0	0.2	12.18	-0.59	15.76
4.0	0.4	12.82	-0.76	13.53
4.0	0.6	14.09	-0.48	15.28
4.0	0.8	14.53	-0.26	12.99
4.0	1.0	11.98	0.15	15.22

VELOCITY DATA FOR ISOBUTENE AT A/F = 800.

x/R	r/R	U m/s	V m/s	Turbulence %
0.5	0.0	-2.47	0.57	17.07
0.5	0.2	-3.84	0.98	18.96
0.5	0.4	-2.97	1.32	20.59
0.5	0.6	-3.83	1.85	16.79
0.5	0.8	-3.04	1.23	19.00
0.5	1.0	12.57	-1.21	29.69
0.75	0.0	-2.85	0.66	16.91
0.75	0.2	-3.77	1.68	17.22
0.75	0.4	-3.81	1.94	16.59
0.75	0.6	-2.82	1.66	21.06
0.75	0.8	-2.16	0.61	21.86
0.75	1.0	14.14	-1.84	22.67
1.0	0.0	-4.33	-1.20	18.28
1.0	0.2	-3.99	1.12	17.10
1.0	0.4	-2.61	2.16	18.74
1.0	0.6	-3.00	0.99	23.90
1.0	0.8	-1.04	0.11	28.07
1.0	1.0	14.39	-1.88	20.57
1.5	0.0	-5.71	-0.80	17.96
1.5	0.2	-4.49	-0.89	20.99
1.5	0.4	-2.82	-0.83	19.76
1.5	0.6	2.03	-1.71	28.16
1.5	0.8	11.93	-3.05	28.50
1.5	1.0	14.33	-2.26	18.56
2.0	0.0	-3.89	-1.33	20.40
2.0	0.2	-2.41	-2.46	20.41
2.0	0.4	1.48	-2.72	24.97
2.0	0.6	7.40	-3.24	23.46
2.0	0.8	12.51	-3.10	24.03
2.0	1.0	13.51	-2.20	25.29
2.5	0.0	2.66	0.83	24.90
2.5	0.2	4.06	-2.73	22.72
2.5	0.4	6.63	-3.44	24.07
3.0	0.0	6.11	0.85	24.74
3.0	0.2	6.40	-1.02	24.11
3.0	0.4	10.04	-1.78	21.38
3.0	0.6	12.25	-1.37	21.08
3.0	0.8	14.00	-1.21	23.61
3.0	1.0	13.10	-0.74	26.24
4.0	0.0	10.72	0.75	22.57
4.0	0.2	11.38	-0.89	20.29
4.0	0.4	12.28	-0.60	20.30
4.0	0.6	13.72	-0.45	22.54
4.0	0.8	13.15	-0.14	25.63
4.0	1.0	11.29	0.39	25.38

VELOCITY DATA FOR 1:1 BUTENE/N2 AT A/F = 400.

x/R	r/R	U m/s	V m/s	Turbulence %
0.5	0.0	4.89	-0.95	32.17
0.5	0.2	7.24	-0.30	31.71
0.5	0.4	0.88	-1.15	16.56
0.5	0.6	-2.96	0.97	14.68
0.5	0.8	-1.67	0.94	10.49
0.5	1.0	12.45	-1.37	23.59
0.75	0.0	-4.48	1.05	19.07
0.75	0.2	-4.85	2.04	19.65
0.75	0.4	-5.15	2.47	18.31
0.75	0.6	-4.05	2.44	18.15
0.75	0.8	-1.83	1.35	22.00
0.75	1.0	13.52	-1.20	19.57
1.0	0.0	-6.58	1.54	19.19
1.0	0.2	-6.11	2.62	17.61
1.0	0.4	-5.64	2.92	17.33
1.0	0.6	-5.36	3.31	16.92
1.0	0.8	2.94	0.36	29.06
1.0	1.0	14.54	-1.68	16.06
1.5	0.0	-7.40	1.80	22.82
1.5	0.2	-6.50	1.48	23.00
1.5	0.4	-5.24	1.75	21.44
1.5	0.6	-0.85	-0.10	27.21
1.5	0.8	8.99	-2.51	23.96
1.5	1.0	14.30	-1.72	21.40
2.0	0.0	-3.51	0.68	23.09
2.0	0.2	-2.88	1.27	23.85
2.0	0.4	-0.34	-0.80	25.98
2.0	0.6	4.99	-1.97	26.79
2.0	0.8	12.59	-2.83	17.48
2.0	1.0	14.32	-2.08	18.79
2.5	0.0	2.05	1.35	23.53
2.5	0.2	2.75	-0.28	24.92
2.5	0.4	4.83	-1.40	23.61
3.0	0.0	5.07	0.21	21.22
3.0	0.2	6.15	-1.89	18.04
3.0	0.4	8.40	-1.75	17.21
3.0	0.6	11.73	-1.55	17.39
3.0	0.8	13.60	-1.25	19.37
3.0	1.0	13.43	-0.55	21.48
4.0	0.0	10.53	0.11	17.41
4.0	0.2	10.39	0.08	19.82
4.0	0.4	11.60	-0.31	18.31
4.0	0.6	12.47	-0.65	17.79
4.0	0.8	13.44	-0.19	18.96
4.0	1.0	12.29	0.12	18.03

VELOCITY DATA FOR 2:1 BUTENE/N2 AT A/F = 400.

x/R	r/R	U m/s	V m/s	Turbulence %
0.5	0.0	4.77	-2.94	32.94
0.5	0.2	5.30	-0.39	33.25
0.5	0.4	-0.57	-0.01	19.87
0.5	0.6	-1.84	0.37	13.76
0.5	0.8	-1.50	0.81	11.90
0.5	1.0	10.65	-1.37	28.73
0.75	0.0	-4.64	0.74	17.50
0.75	0.2	-4.74	1.86	17.19
0.75	0.4	-4.46	2.42	18.91
0.75	0.6	-3.82	2.42	18.73
0.75	0.8	-1.78	1.52	21.72
0.75	1.0	13.98	-1.39	21.14
1.0	0.0	-6.50	2.00	17.00
1.0	0.2	-6.26	2.56	17.54
1.0	0.4	-6.61	3.90	15.76
1.0	0.6	-5.19	3.30	17.18
1.0	0.8	2.58	0.14	28.81
1.0	1.0	14.03	-1.59	22.84
1.5	0.0	-7.22	1.90	24.04
1.5	0.2	-6.49	2.52	23.31
1.5	0.4	-5.08	1.44	24.50
1.5	0.6	-0.94	0.56	30.54
1.5	0.8	9.02	-2.11	26.47
1.5	1.0	14.74	-2.05	17.74
2.0	0.0	-3.30	1.36	24.09
2.0	0.2	-1.95	0.00	27.35
2.0	0.4	0.65	-1.59	25.34
2.0	0.6	5.59	-2.61	27.05
2.0	0.8	12.90	-2.66	17.13
2.0	1.0	14.52	-1.74	16.28
2.5	0.0	2.42	1.94	20.37
2.5	0.2	3.27	-0.52	23.77
2.5	0.4	4.91	-1.51	24.47
3.0	0.0	5.52	-0.46	18.33
3.0	0.2	7.10	-1.82	17.39
3.0	0.4	9.34	-1.68	17.26
3.0	0.6	11.51	-1.68	17.94
3.0	0.8	14.51	-1.41	14.62
3.0	1.0	13.44	-0.83	15.60
4.0	0.0	10.46	0.37	19.07
4.0	0.2	9.93	-0.35	21.97
4.0	0.4	11.40	-0.34	18.28
4.0	0.6	12.70	-0.58	17.40
4.0	0.8	13.43	0.175	18.97
4.0	1.0	12.18	0.39	18.36

VELOCITY DATA FOR 2.26:1 PROPENE/N2 AT A/F = 370.

x/R	r/R	U m/s	V m/s	Turbulence %
0.5	0.0	8.22	-4.87	35.40
0.5	0.2	2.09	-1.78	28.74
0.5	0.4	1.39	3.19	26.10
0.5	0.6	-1.55	1.78	20.47
0.5	0.8	-1.06	0.46	13.23
0.5	1.0	12.86	-1.14	21.08
0.75	0.0	3.44	-1.23	28.00
0.75	0.2	-5.71	1.96	14.66
0.75	0.4	-4.89	1.67	12.53
0.75	0.6	-1.73	1.81	22.54
0.75	0.8	-0.22	0.21	20.10
0.75	1.0	14.14	-1.37	21.72
1.0	0.0	3.79	-1.39	29.60
1.0	0.2	-4.57	0.08	18.95
1.0	0.4	-3.10	-0.38	17.16
1.0	0.6	-0.90	-0.31	17.78
1.0	0.8	6.37	-1.98	20.04
1.0	1.0	14.89	-1.77	20.86
1.5	0.0	-7.08	4.85	13.39
1.5	0.2	-6.00	-0.25	26.21
1.5	0.4	-2.77	-2.54	21.83
1.5	0.6	2.33	-2.45	22.89
1.5	0.8	10.23	-2.47	19.30
1.5	1.0	15.46	-1.60	10.38
2.0	0.0	-2.84	-5.16	13.51
2.0	0.2	-0.88	-3.88	18.06
2.0	0.4	2.30	-3.40	21.63
2.0	0.6	7.39	-2.72	19.00
2.0	0.8	12.75	-2.39	12.79
2.0	1.0	14.96	-1.85	13.40
2.5	0.0	1.74	0.17	22.11
2.5	0.2	2.44	-1.12	22.98
2.5	0.4	5.81	-2.37	22.27
3.0	0.0	5.88	-1.23	19.98
3.0	0.2	7.47	-1.74	20.10
3.0	0.4	9.87	-1.80	16.72
3.0	0.6	12.37	-1.45	16.37
3.0	0.8	13.90	-0.87	17.19
3.0	1.0	13.71	-0.55	19.90
4.0	0.0	10.33	-0.11	17.62
4.0	0.2	10.79	-0.68	21.06
4.0	0.4	12.32	-0.99	18.35
4.0	0.6	13.03	-0.60	18.04
4.0	0.8	14.53	-0.46	11.86
4.0	1.0	12.46	0.21	20.79

VELOCITY DATA FOR PROPENE AT A/F = 400.

x/R	r/R	U m/s	V m/s	Turbulence %
0.5	0.0	5.43	-4.63	32.83
0.5	0.2	1.88	-1.26	31.48
0.5	0.4	-3.33	-0.95	13.25
0.5	0.6	-1.20	2.43	18.28
0.5	0.8	0.70	0.91	13.17
0.5	1.0	12.35	-1.13	27.29
0.75	0.0	-6.00	-1.68	15.38
0.75	0.2	1.88	1.02	26.66
0.75	0.4	-4.26	2.48	16.05
0.75	0.6	-4.22	1.29	16.58
0.75	0.8	-1.04	0.50	20.97
0.75	1.0	13.67	-1.18	22.42
1.0	0.0	-7.21	1.16	17.00
1.0	0.2	-1.65	1.21	27.92
1.0	0.4	-3.61	-0.39	16.85
1.0	0.6	-2.23	0.96	17.40
1.0	0.8	4.73	-1.40	26.01
1.0	1.0	14.61	-1.52	16.18
1.5	0.0	-6.68	5.01	12.45
1.5	0.2	-4.91	-4.12	13.38
1.5	0.4	-2.27	-3.09	14.99
1.5	0.6	2.06	-2.34	20.89
1.5	0.8	9.72	-2.30	18.25
1.5	1.0	14.84	-1.44	11.34
2.0	0.0	-2.46	-5.68	12.20
2.0	0.2	-0.47	-5.01	13.79
2.0	0.4	2.78	-4.49	13.36
2.0	0.6	7.42	-3.30	16.56
2.0	0.8	12.56	-2.21	14.74
2.0	1.0	14.63	-1.36	15.56
2.5	0.0	3.02	-2.81	15.80
2.5	0.2	4.05	-1.56	22.10
2.5	0.4	6.22	-2.31	21.91
3.0	0.0	6.13	-1.90	18.43
3.0	0.2	8.36	-2.19	12.57
3.0	0.4	9.62	-2.00	18.24
3.0	0.6	12.23	-1.56	18.27
3.0	0.8	14.47	-1.19	16.07
3.0	1.0	14.94	-0.55	17.35
4.0	0.0	10.44	-0.25	19.58
4.0	0.2	10.63	-0.93	20.93
4.0	0.4	11.47	-0.89	21.70
4.0	0.6	13.23	-0.68	17.51
4.0	0.8	14.30	-0.20	18.06
4.0	1.0	13.97	0.02	19.79

VELOCITY DATA FOR PROPENE AT A/F = 180.

x/R	r/R	U m/s	V m/s	Turbulence %
0.5	0.0	8.00	-10.58	52.78
0.5	0.2	-2.44	-6.81	36.05
0.5	0.4	-6.76	-4.02	18.67
0.5	0.6	-7.38	-1.02	18.10
0.5	0.8	-6.05	1.63	20.64
0.5	1.0	13.94	-1.68	25.43
0.75	0.0	3.82	-5.63	50.23
0.75	0.2	-7.58	-2.72	31.10
0.75	0.4	-9.42	-1.71	21.84
0.75	0.6	-8.20	-2.06	23.28
0.75	0.8	2.30	-1.09	30.31
0.75	1.0	14.77	-2.15	17.40
1.0	0.0	-0.18	-3.71	51.08
1.0	0.2	-8.48	-2.19	27.36
1.0	0.4	-7.24	-3.27	23.66
1.0	0.6	-6.87	-0.74	24.58
1.0	0.8	8.33	-3.30	29.17
1.0	1.0	13.89	-2.44	24.36
1.5	0.0	1.64	-0.32	38.67
1.5	0.2	-2.53	-2.07	25.97
1.5	0.4	-1.84	-2.12	24.44
1.5	0.6	4.77	-3.37	27.04
1.5	0.8	12.24	-2.96	21.18
1.5	1.0	14.28	-1.92	20.78
2.0	0.0	2.94	-0.87	23.74
2.0	0.2	6.11	-2.94	23.58
2.0	0.4	7.69	-3.30	22.05
2.0	0.6	10.17	-2.48	21.09
2.0	0.8	12.53	-1.06	20.31
2.0	1.0	14.57	-0.41	14.68
2.5	0.0	8.45	-1.93	20.45
2.5	0.2	7.64	0.43	19.27
2.5	0.4	7.99	0.30	20.61
3.0	0.0	11.56	0.41	15.97
3.0	0.2	12.52	-1.83	17.03
3.0	0.4	12.53	-1.60	18.34
3.0	0.6	13.94	-0.76	15.37
3.0	0.8	14.95	0.02	12.74
3.0	1.0	14.50	0.74	16.93
4.0	0.0	13.88	0.33	16.60
4.0	0.2	13.75	-0.53	17.81
4.0	0.4	14.52	-1.04	15.47
4.0	0.6	14.82	-0.68	15.09
4.0	0.8	15.20	-0.07	10.67
4.0	1.0	15.08	0.49	11.62

APPENDIX C
VELOCITY PDFS

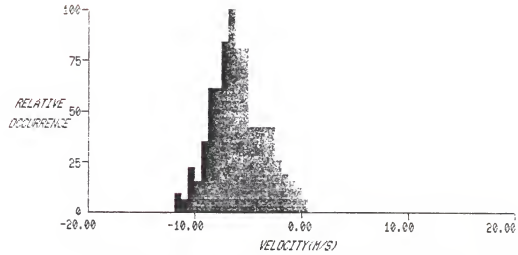

r/R=0.00 x/R=0.50 A/F=6000. REF.VEL.=14.4 DATE=22-OCT-86
COMPONENT= x VELOCITY=PRI. 250 POINTS PLOTTED= 56% OF DATA
NORMALIZED TO 12% OF DATA FUEL=PROPYLENE

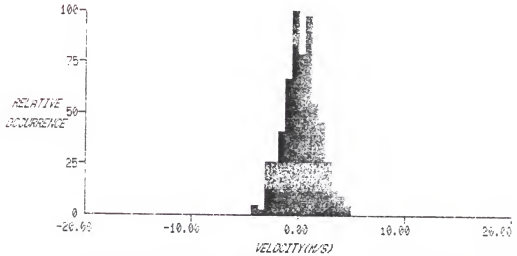

r/R=0.00 x/R=0.50 A/F=6000. REF.VEL.=14.4 DATE=22-OCT-86
COMPONENT= r VELOCITY=PRI. 250 POINTS PLOTTED= 56% OF DATA
NORMALIZED TO 16% OF DATA FUEL=PROPYLENE

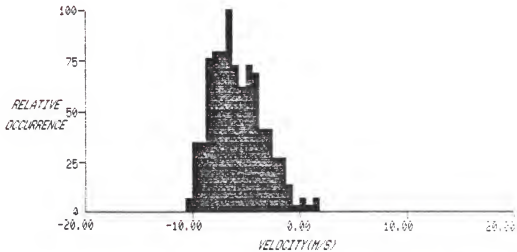

r/R=0.20 x/R=0.50 A/F=6000. REF.VEL.=14.4 DATE=22-OCT-96
COMPONENT= x VELOCITY=PRI. 249 POINTS PLOTTED= 50% OF DATA
NORMALIZED TO 11% OF DATA FUEL=PROPYLENE

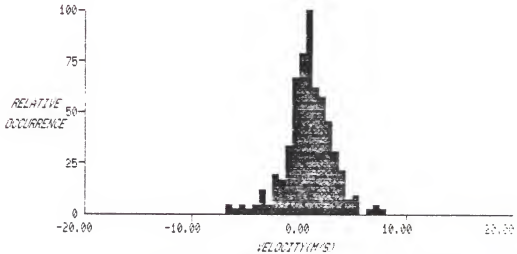

r/R=0.20 x/R=0.50 A/F=6000. REF.VEL.=14.4 DATE=22-OCT-96
COMPONENT= r VELOCITY=PRI. 249 POINTS PLOTTED= 50% OF DATA
NORMALIZED TO 16% OF DATA FUEL=PROPYLENE

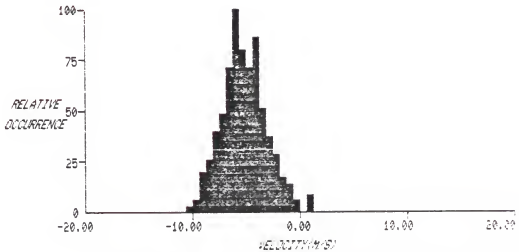

r/R=0.40 x/R=0.50 A/F=6000. REF.VEL.=14.4 DATE=22-OCT-86
COMPONENT= x VELOCITY=PRI. 250 POINTS PLOTTED= 50% OF DATA
NORMALIZED TO 14% OF DATA FUEL=PROPYLENE

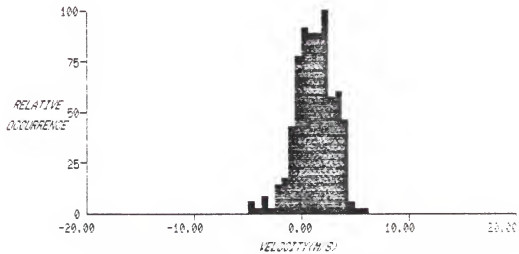

r/R=0.40 x/R=0.50 A/F=6000. REF.VEL.=14.4 DATE=22-OCT-86
COMPONENT= r VELOCITY=PRI. 250 POINTS PLOTTED= 50% OF DATA
NORMALIZED TO 14% OF DATA FUEL=PROPYLENE

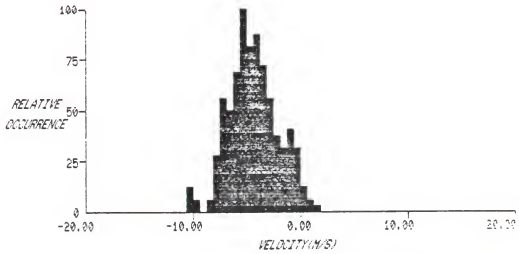

r/R=0.60 x/R=0.50 A/F=6000. REF.VEL.=14.4 DATE=22-OCT-86
COMPONENT= x VELOCITY=PRI. 252 POINTS PLOTTED= 50% OF DATA
NORMALIZED TO 12% OF DATA FUEL=PROPYLENE

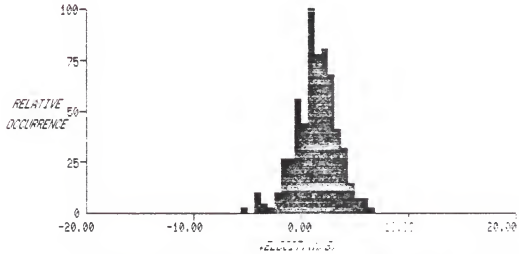

r/R=0.60 x/R=0.50 A/F=6000. REF.VEL.=14.4 DATE=22-OCT-86
COMPONENT= r VELOCITY=PRI. 252 POINTS PLOTTED= 50% OF DATA
NORMALIZED TO 16% OF DATA FUEL=PROPYLENE

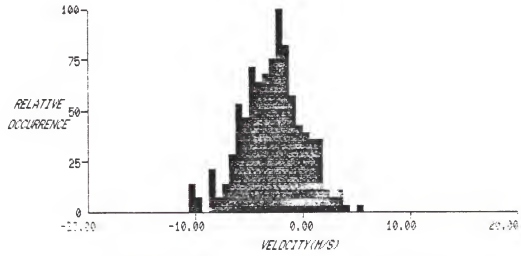

r/R=0.80 x/R=0.50 A/F=6000. REF.VEL.=14.4 DATE=22-OCT-86
COMPONENT= x VELOCITY=PRI. 252 POINTS PLOTTED= 50% OF DATA
NORMALIZED TO 11% OF DATA FUEL=PROPYLENE

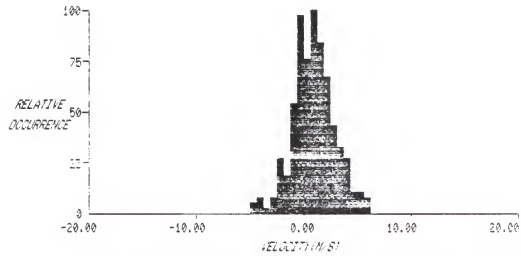

r/R=0.80 x/R=0.50 A/F=6000. REF.VEL.=14.4 DATE=22-OCT-86
COMPONENT= r VELOCITY=PRI. 252 POINTS PLOTTED= 50% OF DATA
NORMALIZED TO 14% OF DATA FUEL=PROPYLENE

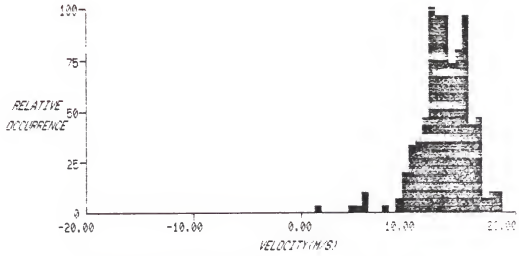

r/R=1.00 x/R=0.50 A/F=6000. REF.VEL.=14.4 DATE=22-OCT-86
COMPONENT= x VELOCITY=PRI. 248 POINTS PLOTTED= 50% OF DATA
NORMALIZED TO 12% OF DATA FUEL=PROPYLENE

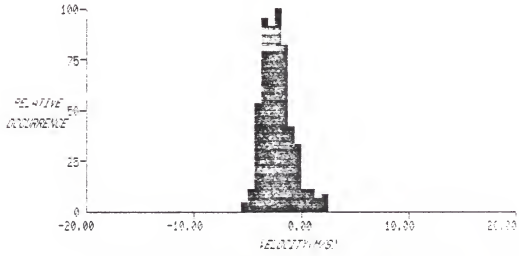

r/R=1.00 x/R=0.50 A/F=6000. REF.VEL.=14.4 DATE=22-OCT-86
COMPONENT= r VELOCITY=PRI. 248 POINTS PLOTTED= 50% OF DATA
NORMALIZED TO 18% OF DATA FUEL=PROPYLENE

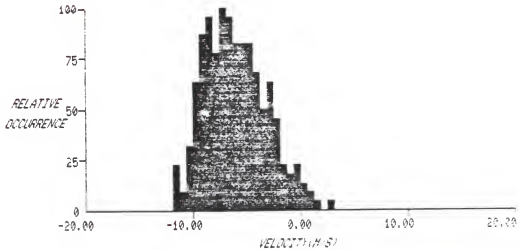

r/R=0.00 x/R=0.75 A/F=6000. REF.VEL.=14.4 DATE=22-OCT-86
COMPONENT= x VELOCITY=PRI. 253 POINTS PLOTTED= 50% OF DATA
NORMALIZED TO 8% OF DATA FUEL=PROPYLENE

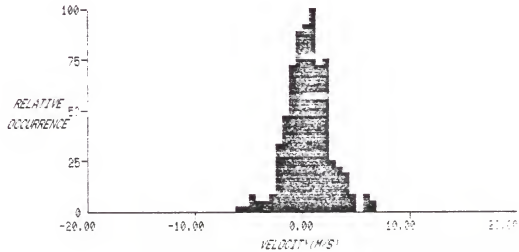

r/R=0.00 x/R=0.75 A/F=6000. REF.VEL.=14.4 DATE=22-OCT-86
COMPONENT= r VELOCITY=PRI. 253 POINTS PLOTTED= 50% OF DATA
NORMALIZED TO 14% OF DATA FUEL=PROPYLENE

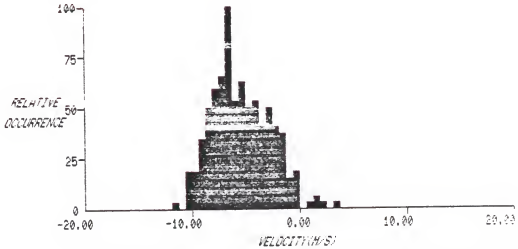

r/R=0.20 x/R=0.75 A/F=6000. REF.VEL.=14.4 DATE=22-OCT-86
COMPONENT= x VELOCITY=PRI. 252 POINTS PLOTTED= 50% OF DATA
NORMALIZED TO 12% OF DATA FUEL=PROPYLENE

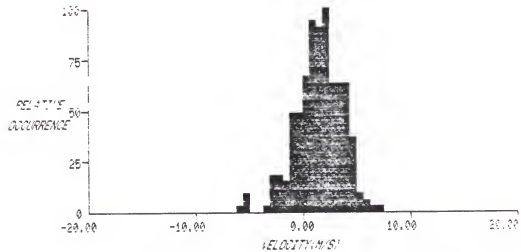

r/R=0.20 x/R=0.75 A/F=6000. REF.VEL.=14.4 DATE=22-OCT-86
COMPONENT= r VELOCITY=PRI. 252 POINTS PLOTTED= 50% OF DATA
NORMALIZED TO 13% OF DATA FUEL=PROPYLENE

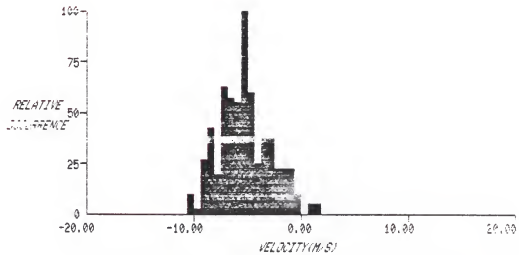

r/R=0.40 x/R=0.75 A/F=6000. REF.VEL.=14.4 DATE=22-OCT-88
COMPONENT= x VELOCITY=PRI. 250 POINTS PLOTTED= 50% OF DATA
NORMALIZED TO 16% OF DATA FUEL=PROPYLENE

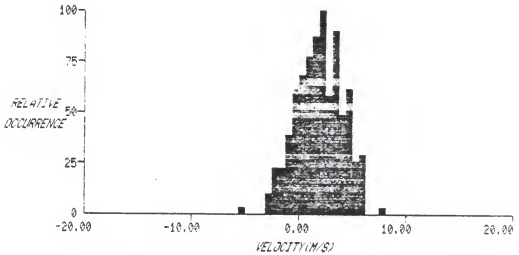

r/R=0.40 x/R=0.75 A/F=6000. REF.VEL.=14.4 DATE=22-OCT-88
COMPONENT= x VELOCITY=PRI. 250 POINTS PLOTTED= 50% OF DATA
NORMALIZED TO 12% OF DATA FUEL=PROPYLENE

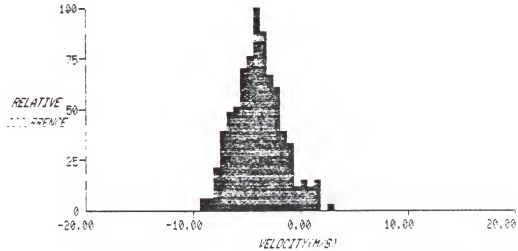

r/R=0.60 x/R=0.75 A/F=6000. REF.VEL.=14.4 DATE=22-OCT-86
COMPONENT= x VELOCITY=PRI. 252 POINTS PLOTTED= 50% OF DATA
NORMALIZED TO 12% OF DATA FUEL=PROPYLENE

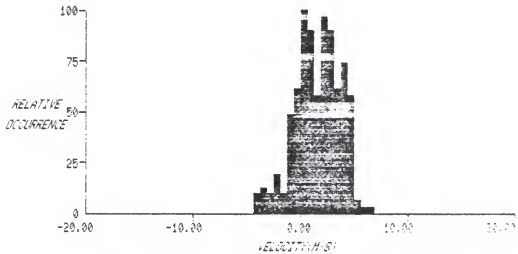

r/R=0.60 x/R=0.75 A/F=6000. REF.VEL.=14.4 DATE=22-OCT-86
COMPONENT= r VELOCITY=PRI. 252 POINTS PLOTTED= 50% OF DATA
NORMALIZED TO 12% OF DATA FUEL=PROPYLENE

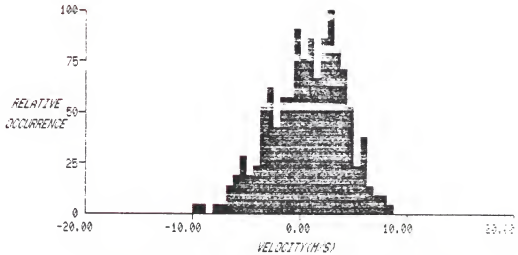

r/R=0.80 x/R=0.75 A/F=6000. REF.VEL.=14.4 DATE=22-OCT-86
COMPONENT= x VELOCITY=PRI. 253 POINTS PLOTTED= 50% OF DATA
NORMALIZED TO 8% OF DATA FUEL=PROPYLENE

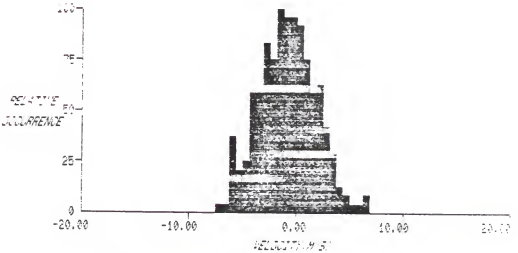

r/R=0.80 x/R=0.75 A/F=6000. REF.VEL.=14.4 DATE=22-OCT-86
COMPONENT= r VELOCITY=PRI. 257 POINTS PLOTTED= 50% OF DATA
NORMALIZED TO 9% OF DATA FUEL=PROPYLENE

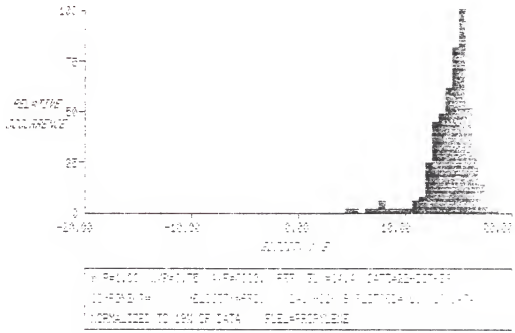

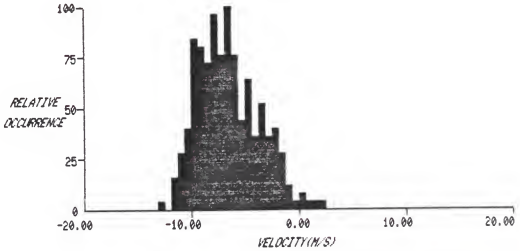

r/R=0.00 x/R=1.00 A/F=6000. REF.VEL.=14.4 DATE=22-OCT-86
COMPONENT= x VELOCITY=PRI. 252 POINTS PLOTTED= 50% OF DATA
NORMALIZED TO 9% OF DATA FUEL=PROPYLENE

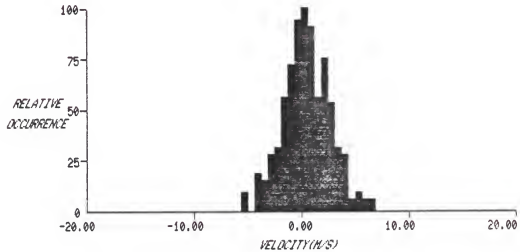

r/R=0.00 x/R=1.00 A/F=6000. REF.VEL.=14.4 DATE=22-OCT-86
COMPONENT= r VELOCITY=PRI. 252 POINTS PLOTTED= 50% OF DATA
NORMALIZED TO 12% OF DATA FUEL=PROPYLENE

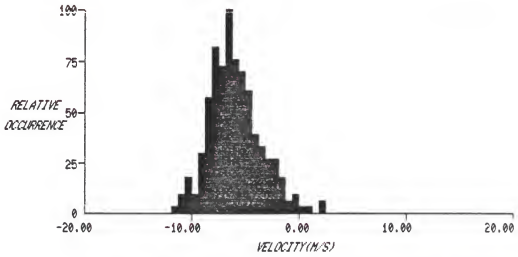

r/R=0.20 x/R=1.00 A/F=6000. REF.VEL.=14.4 DATE=22-OCT-86
COMPONENT= x VELOCITY=PRI. 251 POINTS PLOTTED= 50% OF DATA
NORMALIZED TO 13% OF DATA FUEL=PROPYLENE

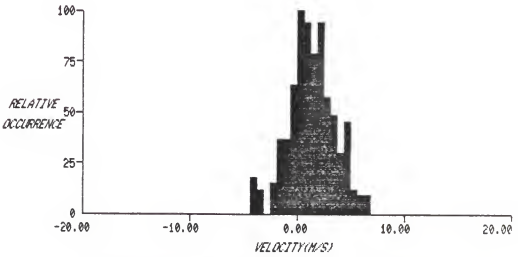

r/R=0.20 x/R=1.00 A/F=6000. REF.VEL.=14.4 DATE=22-OCT-86
COMPONENT= r VELOCITY=PRI. 251 POINTS PLOTTED= 50% OF DATA
NORMALIZED TO 13% OF DATA FUEL=PROPYLENE

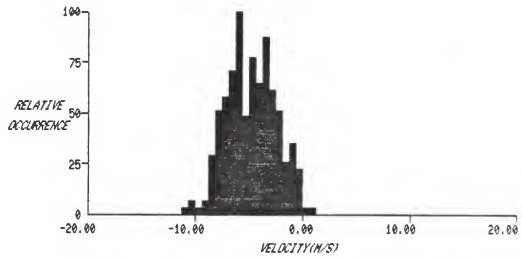

r/R=0.40 x/R=1.00 A/F=6000. REF.VEL.=14.4 DATE=22-OCT-86
COMPONENT= x VELOCITY=PRI. 251 POINTS PLOTTED= 50% OF DATA
NORMALIZED TO 12% OF DATA FUEL=PROPYLENE

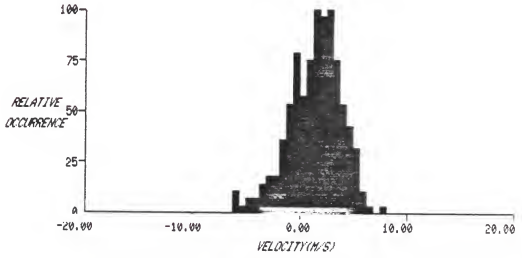

r/R=0.40 x/R=1.00 A/F=6000. REF.VEL.=14.4 DATE=22-OCT-86
COMPONENT= r VELOCITY=PRI. 251 POINTS PLOTTED= 50% OF DATA
NORMALIZED TO 11% OF DATA FUEL=PROPYLENE

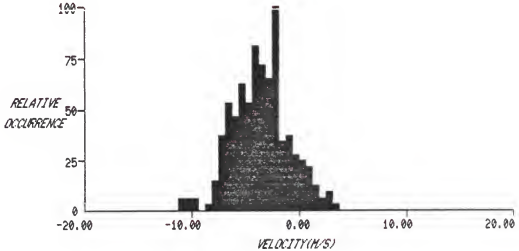

r/R=0.60 x/R=1.00 A/F=6000. REF.VEL.=14.4 DATE=22-OCT-86
COMPONENT= x VELOCITY=PRI. 252 POINTS PLOTTED= 50% OF DATA
NORMALIZED TO 12% OF DATA FUEL=PROPYLENE

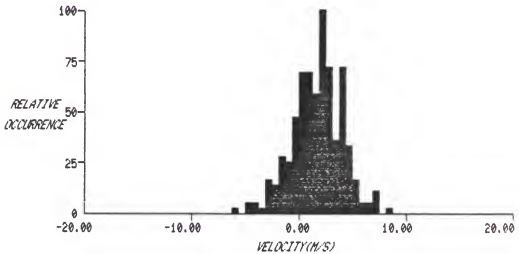

r/R=0.60 x/R=1.00 A/F=6000. REF.VEL.=14.4 DATE=22-OCT-86
COMPONENT= r VELOCITY=PRI. 252 POINTS PLOTTED= 50% OF DATA
NORMALIZED TO 14% OF DATA FUEL=PROPYLENE

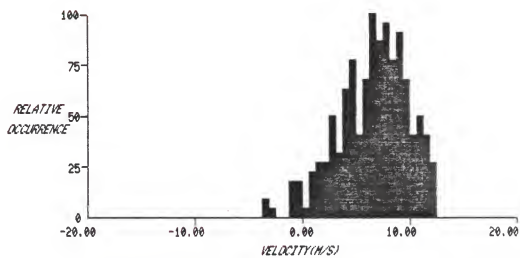

r/R=0.80 x/R=1.00 A/F=6000. REF.VEL.=14.4 DATE=22-OCT-86
COMPONENT= x VELOCITY=PRI. 251 POINTS PLOTTED= 50% OF DATA
NORMALIZED TO 8% OF DATA FUEL=PROPYLENE

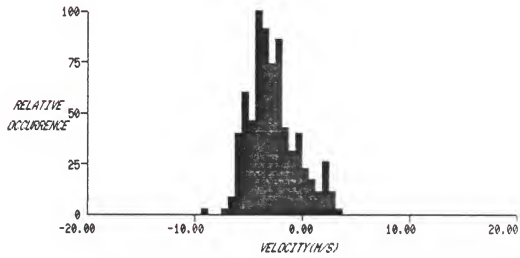

r/R=0.80 x/R=1.00 A/F=6000. REF.VEL.=14.4 DATE=22-OCT-86
COMPONENT= r VELOCITY=PRI. 251 POINTS PLOTTED= 50% OF DATA
NORMALIZED TO 13% OF DATA FUEL=PROPYLENE

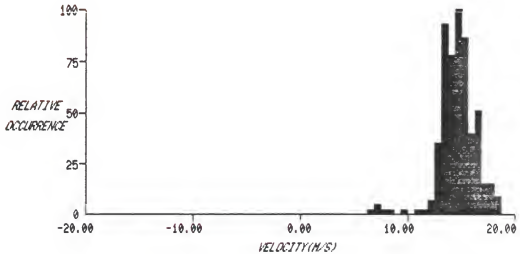

r/R=1.00 x/R=1.00 A/F=6000. REF.[illegible] DATE=22-OCT-86
COMPONENT= x VELOCITY=PRI. 247 POINTS PLOTTED= 50% OF DATA
NORMALIZED TO 18% OF DATA FUEL=PROPYLENE

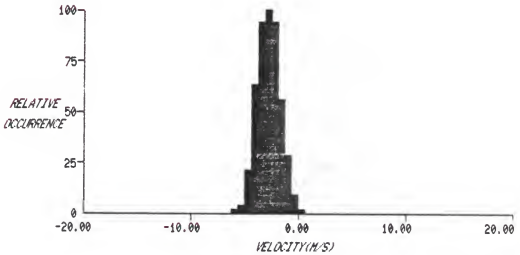

r/R=1.00 x/R=1.00 A/F=6000. REF.VEL.=14.4 DATE=22-OCT-86
COMPONENT= r VELOCITY=PRI. 247 POINTS PLOTTED= 50% OF DATA
NORMALIZED TO 21% OF DATA FUEL=PROPYLENE

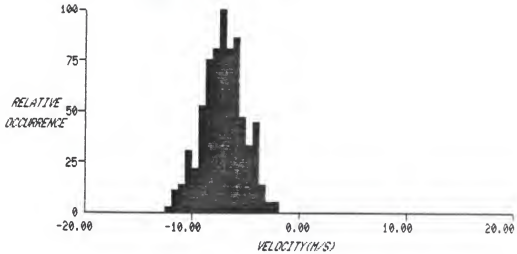

r/R=0.00 x/R=1.50 A/F=6000. REF.VEL.=14.4 DATE=22-OCT-86
COMPONENT= x VELOCITY=PRI. 254 POINTS PLOTTED= 50% OF DATA
NORMALIZED TO 14% OF DATA FUEL=PROPYLENE

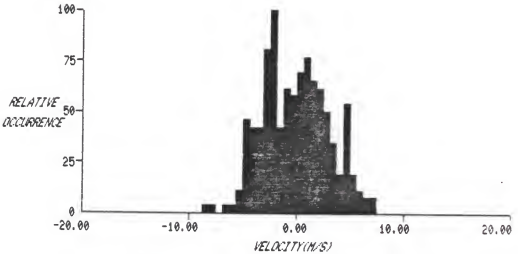

r/R=0.00 x/R=1.50 A/F=6000. REF.VEL.=14.4 DATE=22-OCT-86
COMPONENT= r VELOCITY=PRI. 254 POINTS PLOTTED= 50% OF DATA
NORMALIZED TO 10% OF DATA FUEL=PROPYLENE

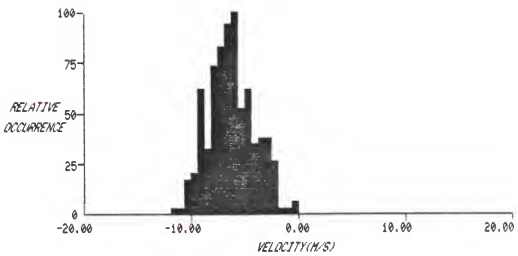

r/R=0.20 x/R=1.50 A/F=6000. REF.VEL.=14.4 DATE=22-OCT-86
COMPONENT= x VELOCITY=PRI. 256 POINTS PLOTTED= 50% OF DATA
NORMALIZED TO 13% OF DATA FUEL=PROPYLENE

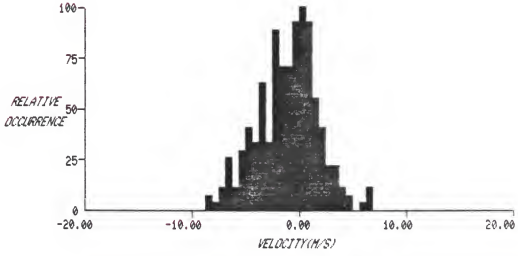

r/R=0.20 x/R=1.50 A/F=6000. REF.VEL.=14.4 DATE=22-OCT-86
COMPONENT= r VELOCITY=PRI. 256 POINTS PLOTTED= 50% OF DATA
NORMALIZED TO 10% OF DATA FUEL=PROPYLENE

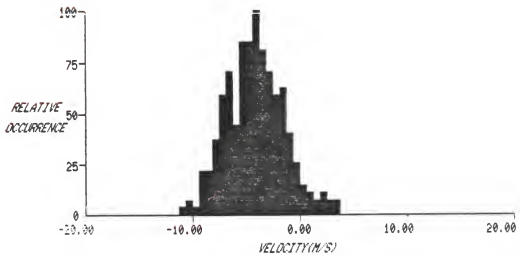

r/R=0.40 x/R=1.50 A/F=6000. REF.VEL.=14.4 DATE=22-OCT-86
COMPONENT= x VELOCITY=PRI. 254 POINTS PLOTTED= 50% OF DATA
NORMALIZED TO 10% OF DATA FUEL=PROPYLENE

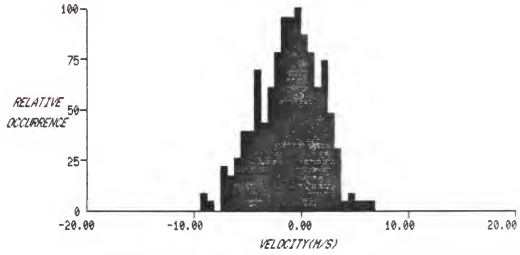

r/R=0.40 x/R=1.50 A/F=6000. REF.VEL.=14.4 DATE=22-OCT-86
COMPONENT= r VELOCITY=PRI. 254 POINTS PLOTTED= 50% OF DATA
NORMALIZED TO 9% OF DATA FUEL=PROPYLENE

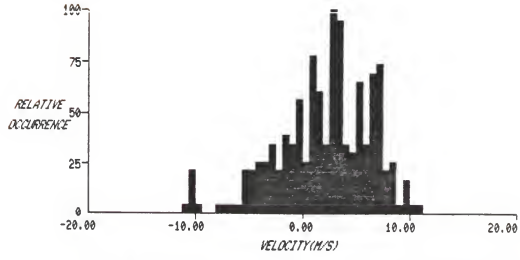

r/R=0.60 x/R=1.50 A/F=6000. REF.VEL.=14.4 DATE=22-OCT-86
COMPONENT= x VELOCITY=PRI. 256 POINTS PLOTTED= 50% OF DATA
NORMALIZED TO 8% OF DATA FUEL=PROPYLENE

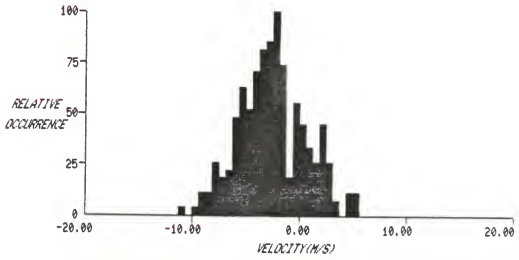

r/R=0.60 x/R=1.50 A/F=6000. REF.VEL.=14.4 DATE=22-OCT-86
COMPONENT= r VELOCITY=PRI. 256 POINTS PLOTTED= 50% OF DATA
NORMALIZED TO 10% OF DATA FUEL=PROPYLENE

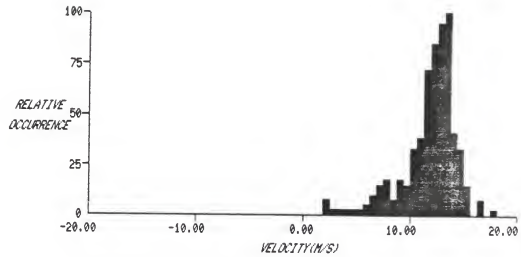

r/R=0.80 x/R=1.50 A/F=6000. REF.VEL.=14.4 DATE=22-OCT-86
COMPONENT= x VELOCITY=PRI. 247 POINTS PLOTTED= 50% OF DATA
NORMALIZED TO 15% OF DATA FUEL=PROPYLENE

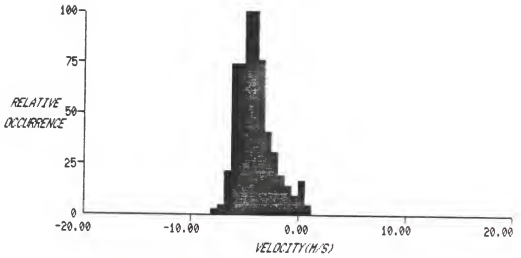

r/R=0.80 x/R=1.50 A/F=6000. REF.VEL.=14.4 DATE=22-OCT-86
COMPONENT= r VELOCITY=PRI. 247 POINTS PLOTTED= 50% OF DATA
NORMALIZED TO 17% OF DATA FUEL=PROPYLENE

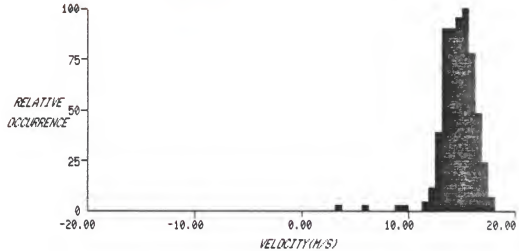

r/R=1.00 x/R=1.50 A/F=6000. REF.VEL.=14.4 DATE=22-OCT-86
COMPONENT= x VELOCITY=PRI. 246 POINTS PLOTTED= 50% OF DATA
NORMALIZED TO 16% OF DATA FUEL=PROPYLENE

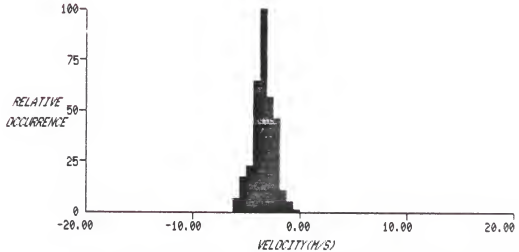

r/R=1.00 x/R=1.50 A/F=6000. REF.VEL.=14.4 DATE=22-OCT-86
COMPONENT= r VELOCITY=PRI. 246 POINTS PLOTTED= 50% OF DATA
NORMALIZED TO 30% OF DATA FUEL=PROPYLENE

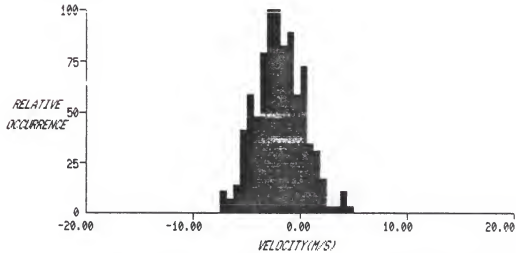

r/R=0.00 x/R=2.00 A/F=6000. REF.VEL.=14.4 DATE=22-OCT-86
COMPONENT= x VELOCITY=PRI. 251 POINTS PLOTTED= 50% OF DATA
NORMALIZED TO 11% OF DATA FUEL=PROPYLENE

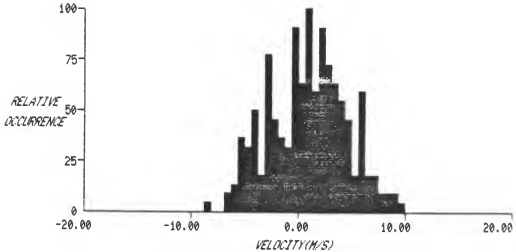

r/R=0.00 x/R=2.00 A/F=6000. REF.VEL.=14.4 DATE=22-OCT-86
COMPONENT= r VELOCITY=PRI. 251 POINTS PLOTTED= 50% OF DATA
NORMALIZED TO 8% OF DATA FUEL=PROPYLENE

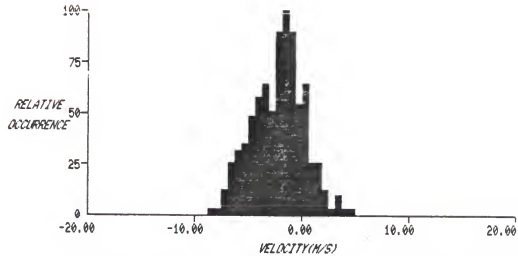

r/R=0.20 x/R=2.00 A/F=6000. REF.VEL.=14.4 DATE=22-OCT-86
COMPONENT= x VELOCITY=PRI. 254 POINTS PLOTTED= 50% OF DATA
NORMALIZED TO 12% OF DATA FUEL=PROPYLENE

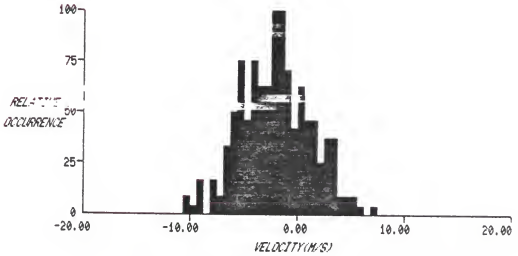

r/R=0.20 x/R=2.00 A/F=6000. REF.VEL.=14.4 DATE=22-OCT-86
COMPONENT= r VELOCITY=PRI. 254 POINTS PLOTTED= 50% OF DATA
NORMALIZED TO 9% OF DATA FUEL=PROPYLENE

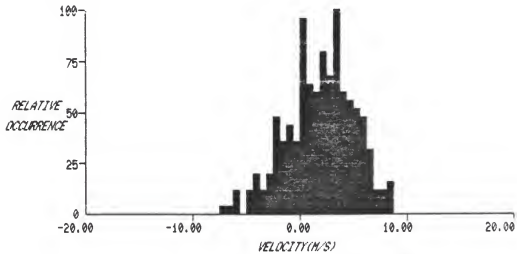

r/R=0.40 x/R=2.00 A/F=6000. REF.VEL.=14.4 DATE=22-OCT-86
COMPONENT= x VELOCITY=PRI. 251 POINTS PLOTTED= 50% OF DATA
NORMALIZED TO 9% OF DATA FUEL=PROPYLENE

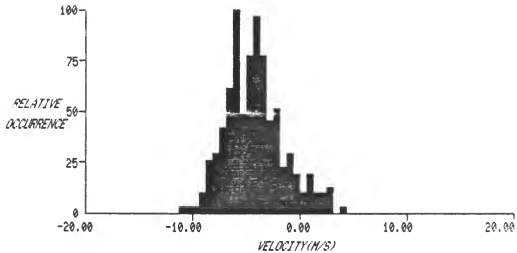

r/R=0.40 x/R=2.00 A/F=6000. REF.VEL.=14.4 DATE=22-OCT-86
COMPONENT= r VELOCITY=PRI. 251 POINTS PLOTTED= 50% OF DATA
NORMALIZED TO 12% OF DATA FUEL=PROPYLENE

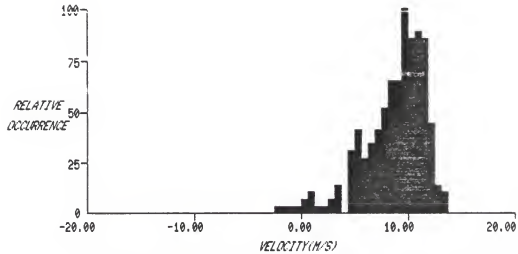

r/R=0.60 x/R=2.00 A/F=6000. REF.VEL.=14.4 DATE=22-OCT-86
COMPONENT= x VELOCITY=PRI. 246 POINTS PLOTTED= 50% OF DATA
NORMALIZED TO 11% OF DATA FUEL=PROPYLENE

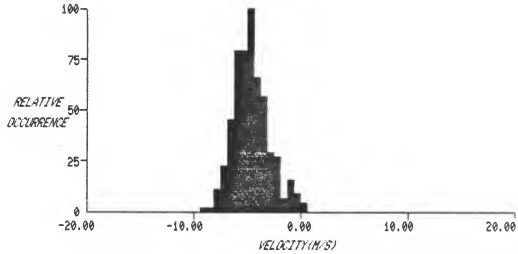

r/R=0.60 x/R=2.00 A/F=6000. REF.VEL.=14.4 DATE=22-OCT-86
COMPONENT= r VELOCITY=PRI. 246 POINTS PLOTTED= 50% OF DATA
NORMALIZED TO 17% OF DATA FUEL=PROPYLENE

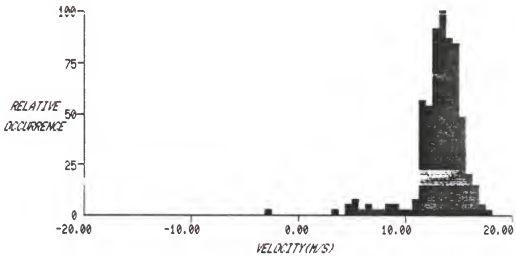

r/R=0.80 x/R=2.00 A/F=6000. REF.VEL.=14.4 DATE=22-OCT-86
COMPONENT= x VELOCITY=PRI. 242 POINTS PLOTTED= 50% OF DATA
NORMALIZED TO 16% OF DATA FUEL=PROPYLENE

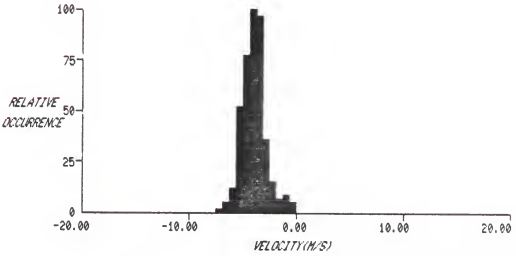

r/R=0.80 x/R=2.00 A/F=6000. REF.VEL.=14.4 DATE=22-OCT-86
COMPONENT= r VELOCITY=PRI. 242 POINTS PLOTTED= 50% OF DATA
NORMALIZED TO 23% OF DATA FUEL=PROPYLENE

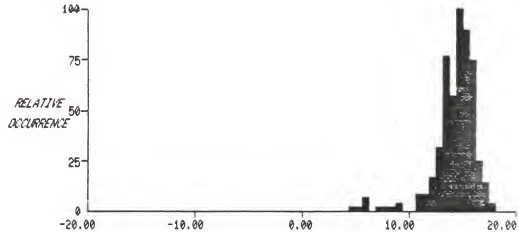

r/R=1.00 x/R=2.00 A/F=6000. REF.VEL.=14.4 DATE=22-OCT-86
COMPONENT= x VELOCITY=PRI. 249 POINTS PLOTTED= 50% OF DATA
NORMALIZED TO 18% OF DATA FUEL=PROPYLENE

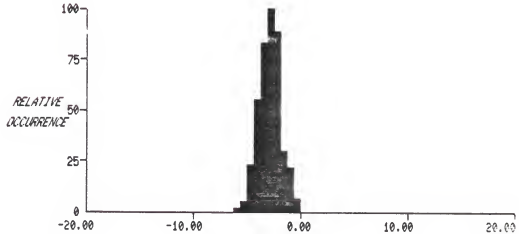

r/R=1.00 x/R=2.00 A/F=6000. REF.VEL.=14.4 DATE=22-OCT-86
COMPONENT= r VELOCITY=PRI. 249 POINTS PLOTTED= 50% OF DATA
NORMALIZED TO 24% OF DATA FUEL=PROPYLENE

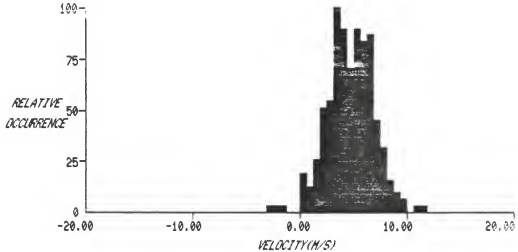

r/R=0.00 x/R=2.50 A/F=6000. REF.VEL.=14.4 DATE=24-OCT-86
COMPONENT= x VELOCITY=PRI. 252 POINTS PLOTTED= 50% OF DATA
NORMALIZED TO 12% OF DATA FUEL=PROPYLENE

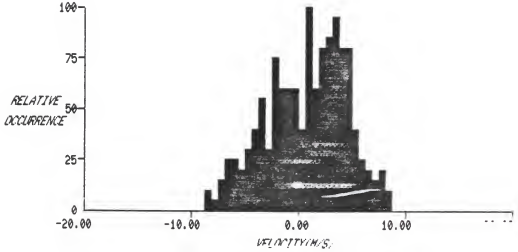

r/R=0.00 x/R=2.50 A/F=6000. REF.VEL.=14.4 DATE=24-OCT-86
COMPONENT= r VELOCITY=PRI. 252 POINTS PLOTTED= 50% OF DATA
NORMALIZED TO 7% OF DATA FUEL=PROPYLENE

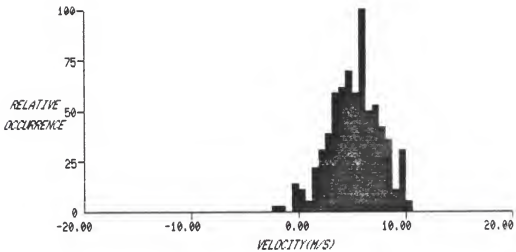

r/R=0.20 x/R=2.50 A/F=6000. REF.VEL.=14.4 DATE=24-OCT-86
COMPONENT= x VELOCITY=PRI. 253 POINTS PLOTTED= 50% OF DATA
NORMALIZED TO 14% OF DATA FUEL=PROPYLENE

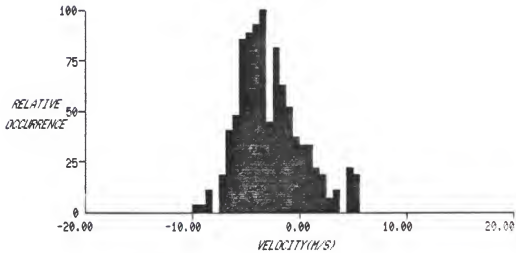

r/R=0.20 x/R=2.50 A/F=6000. REF.VEL.=14.4 DATE=24-OCT-86
COMPONENT= r VELOCITY=PRI. 253 POINTS PLOTTED= 50% OF DATA
NORMALIZED TO 10% OF DATA FUEL=PROPYLENE

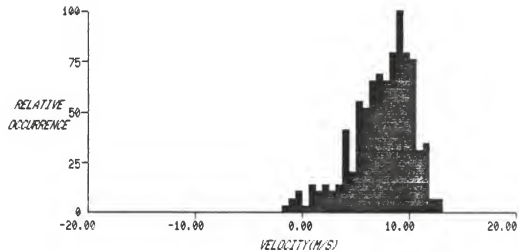

r/R=0.40 x/R=2.50 A/F=6000. REF.VEL.=14.4 DATE=24-OCT-86
COMPONENT= x VELOCITY=PRI. 252 POINTS PLOTTED= 50% OF DATA
NORMALIZED TO 11% OF DATA FUEL=PROPYLENE

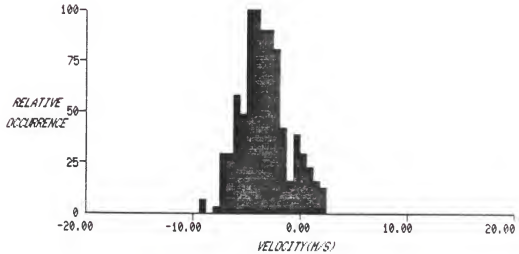

r/R=0.40 x/R=2.50 A/F=6000. REF.VEL.=14.4 DATE=24-OCT-86
COMPONENT= r VELOCITY=PRI. 252 POINTS PLOTTED= 50% OF DATA
NORMALIZED TO 12% OF DATA FUEL=PROPYLENE

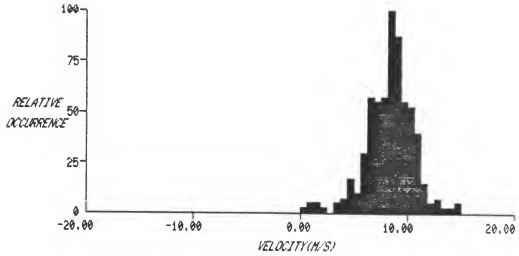

r/R=0.00 x/R=3.00 A/F=6000. REF.VEL.=14.4 DATE=24-OCT-86
COMPONENT= x VELOCITY=PRI. 251 POINTS PLOTTED= 50% OF DATA
NORMALIZED TO 15% OF DATA FUEL=PROPYLENE

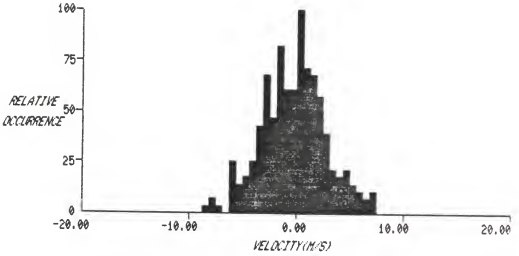

r/R=0.00 x/R=3.00 A/F=6000. REF.VEL.=14.4 DATE=24-OCT-86
COMPONENT= r VELOCITY=PRI. 251 POINTS PLOTTED= 50% OF DATA
NORMALIZED TO 11% OF DATA FUEL=PROPYLENE

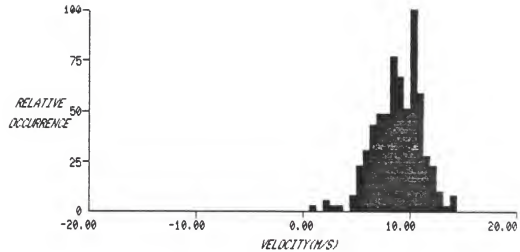

r/R=0.20 x/R=3.00 A/F=6000. REF.VEL.=14.4 DATE=24-OCT-86
COMPONENT= x VELOCITY=PRI. 250 POINTS PLOTTED= 50% OF DATA
NORMALIZED TO 15% OF DATA FUEL=PROPYLENE

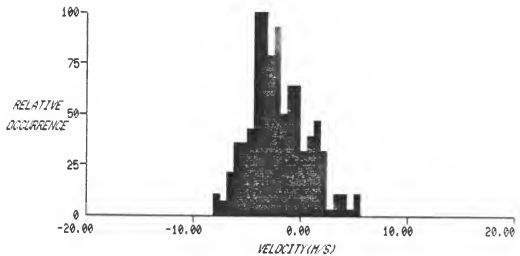

r/R=0.20 x/R=3.00 A/F=6000. REF.VEL.=14.4 DATE=24-OCT-86
COMPONENT= r VELOCITY=PRI. 250 POINTS PLOTTED= 50% OF DATA
NORMALIZED TO 11% OF DATA FUEL=PROPYLENE

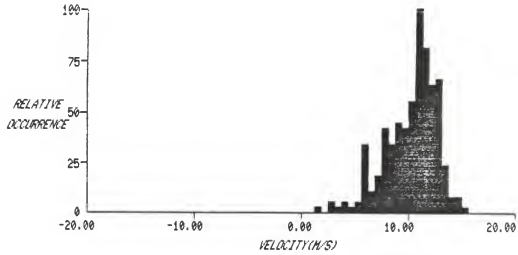

r/R=0.40 x/R=3.00 A/F=6000. REF.VEL.=14.4 DATE=24-OCT-86
COMPONENT= x VELOCITY=PRI. 250 POINTS PLOTTED= 50% OF DATA
NORMALIZED TO 15% OF DATA FUEL=PROPYLENE

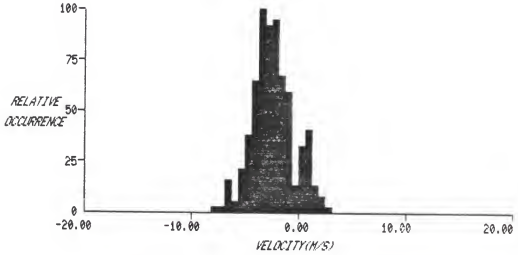

r/R=0.40 x/R=3.00 A/F=6000. REF.VEL.=14.4 DATE=24-OCT-86
COMPONENT= r VELOCITY=PRI. 250 POINTS PLOTTED= 50% OF DATA
NORMALIZED TO 14% OF DATA FUEL=PROPYLENE

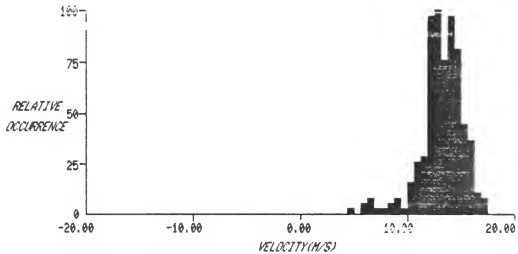

r/R=0.60 x/R=3.00 A/F=6000. REF.VEL.=14.4 DATE=24-OCT-86
COMPONENT= x VELOCITY=PRI. 251 POINTS PLOTTED= 50% OF DATA
NORMALIZED TO 15% OF DATA FUEL=PROPYLENE

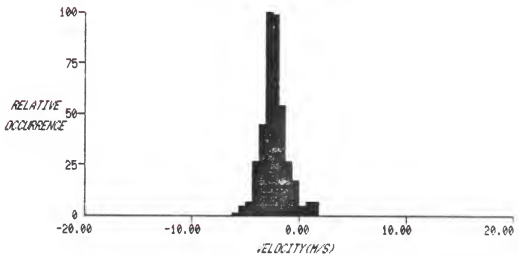

r/R=0.60 x/R=3.00 A/F=6000. REF.VEL.=14.4 DATE=24-OCT-86
COMPONENT= r VELOCITY=PRI. 251 POINTS PLOTTED= 50% OF DATA
NORMALIZED TO 25% OF DATA FUEL=PROPYLENE

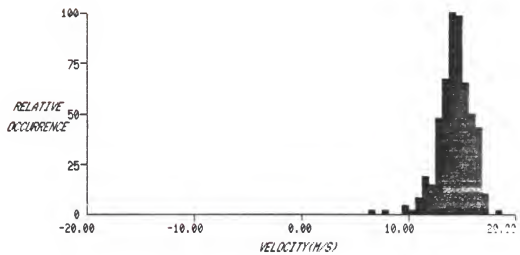

r/R=0.80 x/R=3.00 A/F=6000. REF.VEL.=14.4 DATE=24-OCT-86
COMPONENT= x VELOCITY=PRI. 248 POINTS PLOTTED= 50% OF DATA
NORMALIZED TO 18% OF DATA FUEL=PROPYLENE

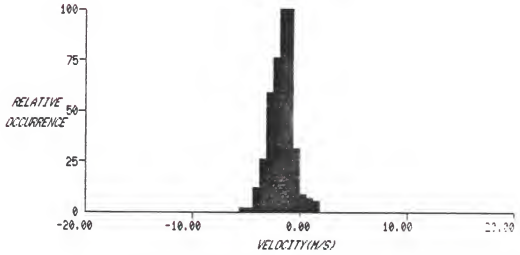

r/R=0.80 x/R=3.00 A/F=6000. REF.VEL.=14.4 DATE=24-OCT-86
COMPONENT= r VELOCITY=PRI. 248 POINTS PLOTTED= 50% OF DATA
NORMALIZED TO 23% OF DATA FUEL=PROPYLENE

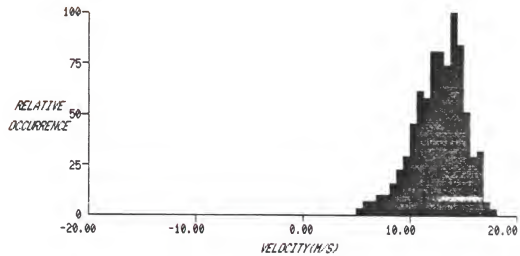

r/R=1.00 x/R=3.00 A/F=6000. REF.VEL.=14.4 DATE=24-OCT-86
COMPONENT= x VELOCITY=PRI. 251 POINTS PLOTTED= 50% OF DATA
NORMALIZED TO 12% OF DATA FUEL=PROPYLENE

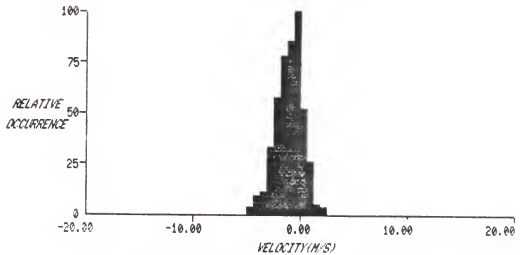

r/R=1.00 x/R=3.00 A/F=6000. REF.VEL.=14.4 DATE=24-OCT-86
COMPONENT= r VELOCITY=PRI. 251 POINTS PLOTTED= 50% OF DATA
NORMALIZED TO 21% OF DATA FUEL=PROPYLENE

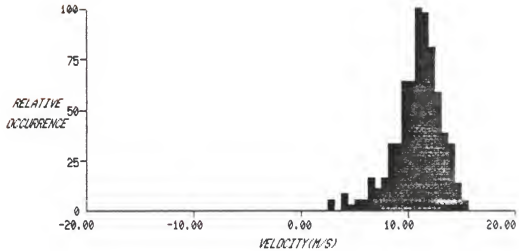

r/R=0.00 x/R=4.00 A/F=6000. REF.VEL.=14.4 DATE=24-OCT-86
COMPONENT= x VELOCITY=PRI. 250 POINTS PLOTTED= 50% OF DATA
NORMALIZED TO 14% OF DATA FUEL=PROPYLENE

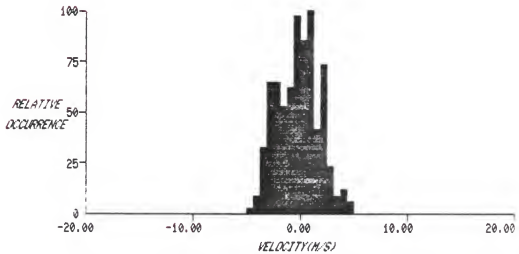

r/R=0.00 x/R=4.00 A/F=6000. REF.VEL.=14.4 DATE=24-OCT-86
COMPONENT= r VELOCITY=PRI. 250 POINTS PLOTTED= 50% OF DATA
NORMALIZED TO 13% OF DATA FUEL=PROPYLENE

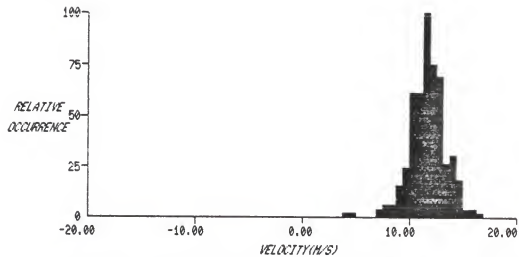

r/R=0.20 x/R=4.00 A/F=6000. REF.VEL.=14.4 DATE=24-OCT-86
COMPONENT= x VELOCITY=PRI. 252 POINTS PLOTTED= 50% OF DATA
NORMALIZED TO 19% OF DATA FUEL=PROPYLENE

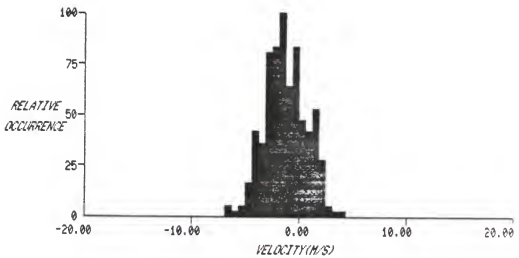

r/R=0.20 x/R=4.00 A/F=6000. REF.VEL.=14.4 DATE=24-OCT-86
COMPONENT= r VELOCITY=PRI. 252 POINTS PLOTTED= 50% OF DATA
NORMALIZED TO 14% OF DATA FUEL=PROPYLENE

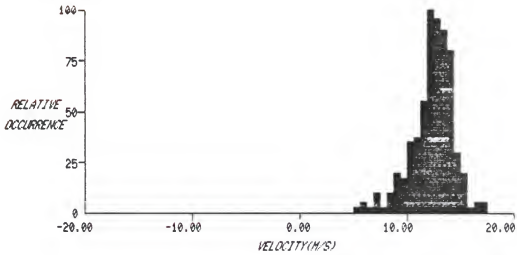

r/R=0.40 x/R=4.00 A/F=6000. REF.VEL.=14.4 DATE=24-OCT-86
COMPONENT= x VELOCITY=PRI. 250 POINTS PLOTTED= 50% OF DATA
NORMALIZED TO 16% OF DATA FUEL=PROPYLENE

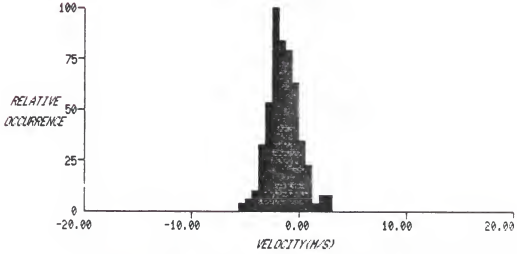

r/R=0.40 x/R=4.00 A/F=6000. REF.VEL.=14.4 DATE=24-OCT-86
COMPONENT= r VELOCITY=PRI. 250 POINTS PLOTTED= 50% OF DATA
NORMALIZED TO 19% OF DATA FUEL=PROPYLENE

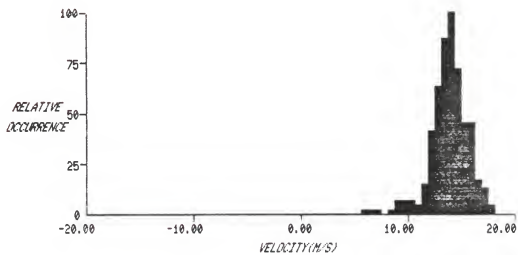

r/R=0.60 x/R=4.00 A/F=6000. REF.VEL.=14.4 DATE=24-OCT-86
COMPONENT= x VELOCITY=PRI. 247 POINTS PLOTTED= 50% OF DATA
NORMALIZED TO 18% OF DATA FUEL=PROPYLENE

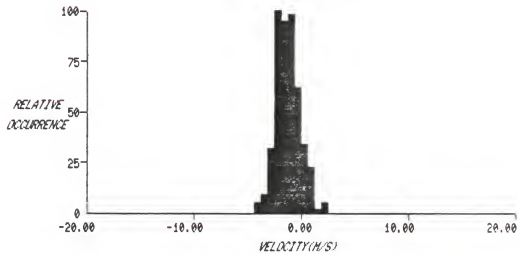

r/R=0.60 x/R=4.00 A/F=6000. REF.VEL.=14.4 DATE=24-OCT-86
COMPONENT= r VELOCITY=PRI. 247 POINTS PLOTTED= 50% OF DATA
NORMALIZED TO 21% OF DATA FUEL=PROPYLENE

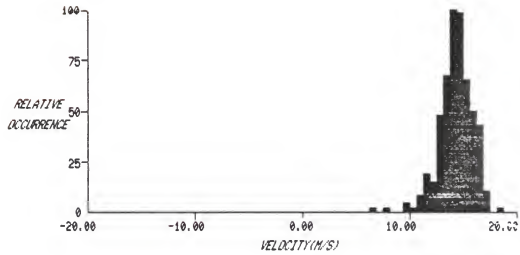

r/R=0.80 x/R=3.00 A/F=6000. REF.VEL.=14.4 DATE=24-OCT-86
COMPONENT= x VELOCITY=PRI. 248 POINTS PLOTTED= 50% OF DATA
NORMALIZED TO 18% OF DATA FUEL=PROPYLENE

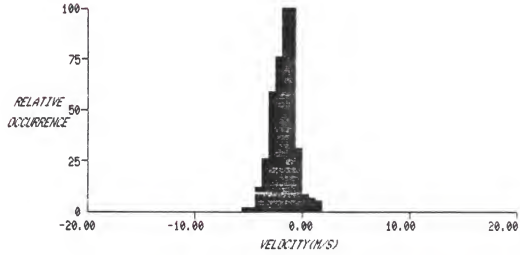

r/R=0.80 x/R=3.00 A/F=6000. REF.VEL.=14.4 DATE=24-OCT-86
COMPONENT= r VELOCITY=PRI. 248 POINTS PLOTTED= 50% OF DATA
NORMALIZED TO 23% OF DATA FUEL=PROPYLENE

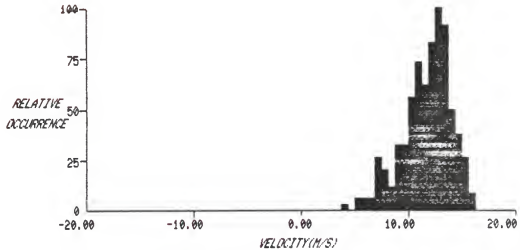

r/R=1.00 x/R=4.00 A/F=6000. REF.VEL.=14.4 DATE=24-OCT-86
COMPONENT= x VELOCITY=PRI. 249 POINTS PLOTTED= 50% OF DATA
NORMALIZED TO 13% OF DATA FUEL=PROPYLENE

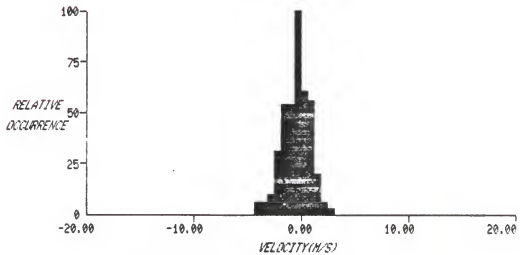

r/R=1.00 x/R=4.00 A/F=6000. REF.VEL.=14.4 DATE=24-OCT-86
COMPONENT= r VELOCITY=PRI. 249 POINTS PLOTTED= 50% OF DATA
NORMALIZED TO 24% OF DATA FUEL=PROPYLENE

REFERENCES

Adams, E. W., and J. K. Eaton, "An LDA Study of the Backward-Facing Step Flow, Including the Effects of Velocity Bias," International Symposium on Laser Anemometry, ASME, FED vol. 33, New York, pp. 255-264, 1985.

Baker, R. J., P. J. Bourke, and J. H. Whitelaw, "Application of Laser Anemometry to the Measurement of Flow Properties in Industrial Burner Flames," Fourteenth Symposium (International) on Combustion, The Combustion Institute, Pittsburgh, pp. 699-706, 1973.

Baker, R. J., P. Hutchinson, E. E. Khalil, and J. H. Whitelaw, "Measurements of Three velocity Components in a Model Furnace with and without Combustion," Fifteenth Symposium (International) on Combustion, The Combustion Institute, Pittsburgh, pp. 553-559, 1974.

Baker, R. J., P. Hutchinson, and J. H. Whitelaw, "Detailed Measurements of Flow in the Recirculation Region of an Industrial Burner by Laser Anemometry," Fourteenth Symposium (International) on Combustion, The Combustion Institute, Pittsburgh, pp. 583-588, 1973.

Ballantyne, A., and K. N. C. Bray, "Investigation into the Structure of Jet Diffusion Flames Using Time-Resolved Optical Measuring Techniques," Sixteenth Symposium (International) on Combustion, The Combustion Institute, Pittsburgh, pp. 777-787, 1976.

Barnett, D. O., and H. T. Bentley, "Statistical Bias of Individual Realization Laser Velocimeters," Proceedings of the Second International Workshop on Laser Velocimetry, Purdue University, vol. 1, pp. 428-442, 1974.

Bill, R. G., I. Namer, L. Talbot, R. K. Cheng, and F. Robben, "Flame Propagation in Grid-Induced Turbulence," Combustion and Flame, vol. 43, pp. 229-242, 1981.

Bill, R. G., and K. Tarabanis, "The Interaction of Turbulence and Premixed Combustion in the Recirculation Zone of Two-Dimensional Bluff Bodies," Proceedings of 1984 Technical Meeting, Eastern Section of the Combustion Institute, Clearwater Beach, Fla., pp. 21-24, 1984.

Bogard, D. G., and W. G. Tiederman, "Experimental Evaluation of Sampling Bias in Naturally Seeded Flows," Laser Velocimetry and Particle Sizing, Hemisphere, Washington, D. C., pp. 100-109, 1978.

Boutier, A.,"Laser Anemometry in a Highly Turbulent Supersonic Flow," Proceedings of the Second International Workshop on Laser Velocimetry, Purdue University, vol. 1, pp. 105-112, 1974.

Chen, T. H., and A. J. Lightman, "Effects of Particle Arrival Statistics on Laser Anemometer Measurements," International Symposium on Laser Anemometry, ASME, FED vol. 33, New York, pp. 231-234, 1985.

Cheng, R. K., and T. T. Ng, "Velocity Statistics in Premixed Turbulent Flames," Combustion and Flame, vol. 52, pp. 185-202, 1983.

Chigier, N. A., and K. Dvorak, "Laser Anemometer Measurements in Flames with Swirl," Fifteenth Symposium (International) on Combustion, The Combustion Institute, Pittsburgh, pp. 573-585, 1974.

Dibble, R. W., W. Kollman, and R. W. Schefer, "Conserved Scalar Fluxes Measured in a Turbulent Nonpremixed Flame by Combined Laser Doppler Velocimetry and Laser Raman Scattering," Combustion and Flame, vol. 55, pp. 307-321, 1984.

Driscoll, J. F., and D. G. Pelaccio, "Laser Velocimetry Measurements in a Gas Turbine Research Combustor," Laser Velocimetry and Particle Sizing, Hemisphere, Washington, D. C., pp. 158-165, 1978.

Driscoll, J. F., R. W. Schefer, and R. W. Dibble, "Mass Fluxes Measured in a Turbulent Nonpremixed Flame," Nineteenth Symposium (International) on Combustion, The Combustion Institute, Pittsburgh, pp. 477-485, 1982.

Durao, D. F. G., and J. H. Whitelaw, "Velocity Characteristics in the Near Wake of a Disk," Journal of Fluid Mechanics, vol. 85, part 2, pp. 369-385, 1978.

Durrett, R. P., W. H. Stevenson, and H. D. Thompson, "Radial and Axial Turbulent Flow Measurements With an LDV in an Axisymmetric Sudden Expansion Air Flow," International Symposium on Laser Anemometry, ASME, FED vol. 33, New York, pp. 127-134, 1985.

Durst, F., Informal presentation, Proceedings of the Second International Workshop on Laser Velocimetry, Purdue University, vol. 2, pp. 301-306, 1974.

Durst, F., and R. Kleine, "Velocity Measurements in Turbulent Premixed Flames by Means of Laser Doppler Anemometers," Sixth German Flame Conference, Essen, 1973.

Durst, F., A. Melling, and J. H. Whitelaw, "The Application of Optical Anemometry to Measurement in Combustion Systems," Combustion and Flame, vol. 18, pp. 197-201, 1972.

Edwards, R. V., "How Real are Particle Bias Errors?" Laser Velocimetry and Particle Sizing, Hemisphere, Washington, D. C., pp. 79-85, 1978.

El Banhawy, Y., S. Sivasegaram, and J. H. Whitelaw, "Premixed, Turbulent Combustion of a Sudden-Expansion Flow," Combustion and Flame, vol. 50, pp. 153-165, 1983.

Elliman, D. G., D. E. Fussey, and N. Hay, "Predictions and Measurements of a Turbulent, Axisymmetric Ducted Diffusion Flame," International Journal of Heat and Mass Transfer, vol. 21, pp. 1393-1402, 1978.

Fujii, S., M. Gomi, and K. Eguchi, " Cold Flow Tests of a Bluff-Body Flame Stabilizer," ASME Journal of Fluids Engineering, vol. 100, pp. 323-332, Sept. 1978.

Giel, T. V., and D. O. Barnett, "Analytical and Experimental Study of Statistical Bias in Laser Velocimetry," Laser Velocimetry and Particle Sizing, Hemisphere, Washington, D. C., pp. 86-99, 1978.

Gouldin, F. C., R. N. Halthore, and B. T. Vu, "Periodic Oscillations Observed in Swirling Flows With and Without Combustion," Twentieth Symposium (International) on Combustion, The Combustion Institute, Pittsburgh, pp. 269-276, 1985.

Gunther, R., and V. Wittmer, "The Turbulent Reaction Field in a Concentric Diffusion Flame," Eighteenth Symposium (International) on Combustion, The Combustion Institute, Pittsburgh, pp. 961-967, 1980.

Jones, W. P., and J. H. Whitelaw, "Modelling and Measurements in Turbulent Combustion," Twentieth Symposium (International) on Combustion, The Combustion Institute, Pittsburgh, pp. 233-249, 1985.

Krishnamurthy, L., "Isothermal Flowfield Predictions of Confined Coflowing Turbulent Jets in an Axisymmetric Bluff-body Near Wake," AFWAL-TR-81-2036, Air Force Wright Aeronautical Labs, 1981.

Larsen, P.S., and P. Buchhave, "Flow Measurements: Why, What, and How? Part 1.," Dantec Information No. 01, Dantec Elektronik, Skovlunde, Denmark, pp. 2-7, 1985.

Leder, A., "Physical Properties of Separated Flows Behind Two-Dimensional Bluff Bodies in Uniform Flows," International Symposium on Laser Anemometry, ASME, FED Vol. 33, New York, pp. 273-280, 1985.

Lightman, A. J., and P. D. Magill, "Velocity Measurements in Confined Dual Coaxial Jets Behind an Axisymmetric Bluff Body: Isothermal and Combusting Flows," AFWAL-TR-81-2018, Air Force Wright Aeronautical Labs, 1981.

Lightman, A. J., R. D. Richmond, L. Krishnamurthy, P. D. Magill, W. M. Roquemore, R. P. Bradley, Jr., S. Stutrud, and C. M. Reeves, "Velocity Measurements in a Bluff-Body Diffusion Flame," AIAA paper 80-1544, 1980.

Masri, A. R., and R. W. Bilger, "Turbulent Diffusion Flames of Hydrocarbon Fuels Stabilized on a Bluff Body," Twentieth Symposium (International) on Combustion, The Combustion Institute, Pittsburgh, pp. 319-326, 1985.

Mayo, W. T., "A Discussion of Limitations and Extentions of Power Spectrum Estimation with Burst-Counter LDV Systems," Proceedings of the Second International Workshop on Laser Velocimetry, vol. 1, Purdue University, pp. 90-104, 1974.

McLaughlin, D. K., and W. G. Tiederman, "Biasing Correction for Individual Realization of Laser Anemometer Measurements in Turbulent Flows," The Physics of Fluids, vol. 16, no. 12, 1973.

Mongia, H. C., R. S. Reynolds, and R. Srinivasan, "Multidimensional Gas Turbine Combustion Modeling: Applications and Limitations," AIAA Journal, vol. 24, no. 6, 1986.

Moreau, P., "Experimental Determination of Probability Density Functions within a Turbulent High Velocity Premixed Flame," Eighteenth Symposium (International) on Combustion, The Combustion Institute, Pittsburgh, pp. 993-1000, 1980.

Moreau, P., and A. Boutier, "Laser Velocimeter Measurements in a Turbulent Flame," Sixteenth Symposium (International) on Combustion, The Combustion Institute, Pittsburgh, pp. 1747-1756, 1976.

Owen, F. K., "Laser Velocimeter Measurements in Free and Confined Coaxial Jets with Recirculation," AIAA paper 75-120, 1975.

Owen, F. K., "Laser Velocimeter Measurements of the Structure of Turbulent Spray Flames," AIAA paper 77-215, 1977.

Owen, F. K., "Measurements in Combustion Systems," Laser Velocimetry and Particle Sizing, Hemisphere, Washington, D. C., pp. 123-135, 1978.

Owen, F. K., L. J. Spadaccini, and C. T. Bowman, "Pollutant Formation and Energy Release in Confined Turbulent Diffusion Flames," Sixteenth Symposium (International) on Combustion, The Combustion Institute, Pittsburgh, pp. 105-117, 1976.

Park, C. J., and L-D. Chen, "LDA Measurements of Confined Turbulent Coaxial Jets," Proceedings of 1984 Technical Meeting, Eastern Section of the Combustion Institute, Clearwater, Fla., pp. 191-194, 1984.

Polyakov, A. F., and S. A. Shindin, "Some Aspects of Measuring the Structure of Non-Isothermic Turbulence by Simultaneous Application of DISA's LDA and Hot-Wire Anemometer," DISA Information no. 28, Disa Elektronik A/S, Skovlunde, Denmark, pp. 10-14, 1983.

Pope, S. B., and J. H. Whitelaw, "The Calculation of Near-wake Flows," Journal of Fluid Mechanics, vol. 73, part 1, pp. 9-32, 1976.

Proctor, C. L., S. E. Beladi, L. A. Roe, and D. Touati, "Optical Measurement of Flame Structure and Soot Emissions," USAF contract FO8635-C-0136, Task Order 83-03, U. of Florida Combustion Laboratory, Gainesville, Fl., 1985.

Proctor, C. L., L. A. Roe, and D. Touati, "Optical Measurement of Soot Formation," USAF contract FO8635-C-0136, Task Order 86-02, U. of Florida Combustion Laboratory, Gainesville, Fl., 1987.

Ribeiro, M. M., and J. H. Whitelaw, "Statistical Characteristics of a Turbulent Jet," Journal of Fluid Mechanics, vol. 70, pp. 1-15, 1975.

Roquemore, W. M., R. P. Bradley, T. A. Jackson, S. W. Kizirnis, L. P. Goss, G. L. Switzer, D. D. Trump, B. Sarka, D. R. Ballal, A. J. Lightman, P. P. Yaney, and T. H. Chen, "Development of Laser Diagnostics For Combustion Research," 1986 Spring Technical Meeting of the Central States Section of the Combustion Institute, Cleveland, 1986.

Roquemore, W. M., R. P. Bradley, J. S. Stutrud, C. M. Reeves, and L. Krishnamurthy, "Preliminary Evaluation of a Combustor for Use in Modeling and Diagnostics Development," ASME paper 80-GT-93, 1980.

Shepherd, I. G., J. B. Moss, and K. N. C. Bray, "Turbulent Transport in a Confined Premixed Flame," Nineteenth Symposium (International) on Combustion, The Combustion Institute, Pittsburgh, pp. 423-431, 1982.

Smith, D. M., and D. M. Meadows, "Power Spectra from Random-Time Samples for Turbulence Measurements with a Laser Velocimeter," Proceedings of the Second International Workshop on Laser Velocimetry, vol. 1, Purdue University, pp. 27-46, 1974.

Smith, G. D., and T. V. Giel, "Two Component Laser Velocimeter Measurements in a Dump Combustor Flowfield," Laser Velocimetry and Particle Sizing, Hemisphere, Washington, D. C., pp. 147-157, 1978.

Starner, S. H., and R. W. Bilger, "Measurement of Scalar-Velocity Correlations in a Turbulent Diffusion Flame," Eighteenth Symposium (International) on Combustion, The Combustion Institute, Pittsburgh, pp. 921-930, 1980.

Stevenson, W. H., "Principles of Laser Velocimetry," Experimental Diagnostics in Gas Phase Combustion Systems, Progress in Aeronautics and Astronautics, AIAA, New York, vol. 53, pp. 307-336, 1977.

Stevenson, W. H., H. D. Thompson, and R. D. Gould,"Laser Velocimeter Measurements and Analysis in Turbulent Flows With Combustion, Part II," AFWAL-TR-82-2076, Air Force Wright Aeronautical Labs, 1983.

Stevenson, W. H., H. D. Thompson, and T. C. Roesler, "Direct Measurement of Laser Velocimeter Bias Errors in a Turbulent Flow," AIAA Journal, vol. 20, no. 12, pp. 1720-1723, 1982.

Switzer, G. L., L. P. Goss, D. D. Trump, C. M. Reeves, J. S. Stutrud, R. P. Bradley, and W. M. Roquemore, "CARS Measurements in the Near-Wake Region of an Axisymmetric Bluff-Body Combustor," AIAA Journal, vol. 24, no. 7, pp. 1155-1162, 1986.

Takagi, T., H. Shin, and A. Ishio, "Properties of Turbulence in Turbulent Diffusion Flames," Combustion and Flame, vol. 40, pp. 121-140, 1981.

Thompson, H. D., and W. H. Stevenson, eds., Proceedings of the Second International Workshop on Laser Velocimetry, Purdue University, pp. 221-313, 1974.

Thompson, H. D., and W. H. Stevenson, eds., Laser Velocimetry and Particle Sizing, Hemisphere, Washington, D. C., 1978.

Tiederman, W. G., "Interpretation of Laser Velocimeter Measurements in Turbulent Boundary Layers and Regions of Separation," 5th Biennial Symposium on Turbulence, Missouri, 1977.

Tishkoff, J. M., "AFOSR Sponsored Research in Airbreathing Propulsion," AFOSR Contractors Meeting on Air Breathing Combustion Dynamics Research, Scottsdale, Ariz., 1983.

Van Dyke, M. V., ed., An Album of Fluid Motion, Parabolic Press, Stanford, 1982.

Whiffen, M. C., J. C. Lau, and D. M. Smith, "Design of Laser Velocimeter Experiments for Turbulence Measurements," Laser Velocimetry and Particle Sizing, Hemisphere, Washington, D. C., pp. 197-207, 1978.

Whiffen, M. C., and D. M. Meadows, "Two Axis Single Particle Laser Velocimeter System for Turbulence Spectral Analysis," Proceedings of the Second International Workshop on Laser Velocimetry, Purdue University, vol. 1, pp. 1-15, 1974.

Yanagi, T., and Y. Mimura, "Velocity-Temperature Correlation in Premixed Flame," Eighteenth Symposium (International) on Combustion, The Combustion Institute, Pittsburgh, pp. 1031-1039, 1980.

Yeh, Y., and H. Z. Cummins, "Localized Fluid Flow Measurements with an He-Ne Laser Spectrometer," Applied Physics Letters, vol. 4, p. 176, 1964.

Yoshida, A., "An Experimental Study of Wrinkled Laminar Flame," Eighteenth Symposium (International) on Combustion, The Combustion Institute, Pittsburgh, pp. 931-939, 1980.

Zimmerman, D. R., "Laser Anemometer Measurements of the Flow from a Simulated Fuel Nozzle," International Symposium on Laser Anemometry, ASME, FED vol. 33, New York, pp. 13-18, 1985.

BIOGRAPHICAL SKETCH

Larry A. Roe was born at Fort Benning, Georgia, on January 14, 1949, to Agnes and Charles Roe. He graduated from Biloxi High School, Biloxi, Mississippi, in 1967 and received a BSME from the University of Mississippi in 1971. Mr. Roe did environmental and combustion research for Westinghouse Research Laboratories in Pittsburgh, Pennsylvania, until 1973, when he returned to the University of Mississippi, receiving a Master of Science in engineering science in 1976. The thesis subject was "Vertical Mass and Momentum Transfer Coefficients in Density Stratified Flow."

He conducted both analytical and experimental studies at Pratt and Whitney Aircraft, West Palm Beach, Florida, from 1976 to 1980 and again during 1984 and 1985. Areas of investigation included bearings, seals, turbine fabrication, turbine heat transfer, and compressor aerodynamics. He is a member of AIAA, ASME, Tau Beta Pi, and Phi Kappa Phi.

Mr. Roe is married to the former Cathy Haynie of Gulfport, Mississippi, and has two sons, Justin, age eight, and Colin, age two.

I certify that I have read this study and that in my opinion it conforms to acceptable standards of scholarly presentation and is fully adequate, in scope and quality, as a dissertation for the degree of Doctor of Philosophy.

C. L. Proctor, II, Chairman
Associate Professor of
Mechanical Engineering

I certify that I have read this study and that in my opinion it conforms to acceptable standards of scholarly presentation and is fully adequate, in scope and quality, as a dissertation for the degree of Doctor of Philosophy.

W. E. Lear, Jr.
Assistant Professor of
Mechanical Engineering

I certify that I have read this study and that in my opinion it conforms to acceptable standards of scholarly presentation and is fully adequate, in scope and quality, as a dissertation for the degree of Doctor of Philosophy.

A. E. S. Green
Graduate Research Professor
of Mechanical Engineering

I certify that I have read this study and that in my opinion it conforms to acceptable standards of scholarly presentation and is fully adequate, in scope and quality, as a dissertation for the degree of Doctor of Philosophy.

R. J. Gaither
Professor of Mechanical
Engineering

I certify that I have read this study and that in my opinion it conforms to acceptable standards of scholarly presentation and is fully adequate, in scope and quality, as a dissertation for the degree of Doctor of Philosophy.

E. R. Lindgren
Professor of Engineering Sciences

This dissertation was submitted to the Graduate Faculty of the College of Engineering and to the Graduate School and was accepted as partial fulfillment of the requirements for the degree of Doctor of Philosophy.

August 1987

Dean, College of Engineering

Dean, Graduate School